LIGHT TRANSMITTING PHOTOCATALYTIC MEMBRANE FOR CHEMICAL-FREE FOULING CONTROL IN WATER TREATMENT

A thesis submitted in fulfilment of the requirements of the degree of

Doctor of Philosophy

By

Lavern Tendayi Nyamutswa

BSc., B.Sc. (Hons), M.Sc.

Institute of Sustainable Industries and Liveable Cities (ISILC)

College of Engineering and Science

Victoria University

Melbourne, Australia

July 2020

Dedicated to my grandfather Antony, who always wanted me to be a doctor (albeit one who treats people, not water); my grandmother Margaret, whose nurturing, humour, storytelling and compassion for others is something that I wish to emulate, without success; my mother Sophia and my sister Paidamoyo, strong and loving women that didn't live long enough to realize their full potential, my aunt Longina (Sr. Michael) who was an amazing pillar of support and visionary in our family, and my brother Lloyd, who as a father figure helped me push through my undergraduate years.

ABSTRACT

Membrane filtration has revolutionised water treatment, enabling safer provision of drinking water due to its high efficiency to block human infectious pathogens commonly present in raw water sources. Accumulation of substances on membrane surfaces and pores during operation, referred to as fouling, is considered one of the biggest barriers to wider adoption of membrane technology in water treatment. Maintaining continuous low-pressure filtration requires significant amounts of chemicals to clean off the accumulated fouling substances. Chemical use comes with economic and environmental costs associated with acquisition, transportation, storage, usage and disposal of chemicals, especially in disadvantaged and remote communities. By conservative estimates, supply of household water to a remote community of 100 people using a membrane system would require continuous supply of at least 10 L of polyaluminium chloride coagulant and 4 L of sodium hypochlorite (in concentrated form) every month. The main aim of this thesis is to demonstrate a sustainable, innovative, low cost membrane solution harnessing conveniently available solar energy to offset these chemical demands. Coating membrane substrates with semiconductor photocatalysts such as titanium dioxide (TiO_2) is an effective method for mitigating fouling in membranes through induced superhydrophilicity, enabling cleaning from the available water without chemicals. TiO_2 also enables water contaminant degradation and pathogen inactivation through reactive oxygen species (ROS) facilitated advanced oxidation. Despite these well-known effects, a major challenge limiting practical adoption comes from light absorption and scattering by the turbid contaminants in the feed stream before reaching the TiO_2. This thesis proposed a novel solution to this challenge by transmitting light to the TiO_2 through cheap porous borosilicate glass substrates with between 10% and 80 % transmission in the 340-400 nm wavelength range relevant to activating commercial Degussa P25 TiO_2 photocatalyst. The concept novel membrane was produced using commercial glass substrates modified by simply dip-coating and heat sintering Degussa P25. The formed asymmetric membrane's mean pore size was measured at 0.5 µm, which classifies the membrane as a microfiltration (MF) membrane, which are utilised in the industry as a barrier to water-borne pathogens such as protozoa and bacteria, and partially to viruses. To

demonstrate the membrane's photocatalytic ability, photocatalytic reactions stimulated by a UV lamp (365 nm peak) facing the glass substrate side in an *ex-situ* setup led to a 52% degradation of methyl orange in aqueous solution, being only slightly lower than the 58% degradation when the TiO_2 active layer faced the UV light source. The membrane was then operated *in-situ* using a custom module with a quartz window and UV LED installed on the permeate side, enabling simultaneous microfiltration of model fouling solutions. Results showed significant reductions in trans-membrane pressure (TMP) rise rates directly linked to UV light application. Specifically, UV light was responsible for up to 3.0-fold reduction in total filtration resistance and up to 4.2-fold reduction in irreversible fouling indices. Testing continued on simulated indirect solar light with a real non-potable water. The membrane itself showed up to 94% turbidity removal and up to 80% total organic carbon (TOC) rejection. The sunlight was directly responsible for an 8-fold reduction in the irreversible fouling index. The significant practical findings were followed by an investigation to confirm the fundamental basis for improvement. Analysis by scanning electron microscopy (SEM) coupled with fouling modelling showed the beneficial photocatalytic fouling reduction effects during microfiltration stemmed from reduced intrusion of organic fouling material inside the TiO_2 membrane pores, as well as reduced cake layer resistance. Analysis of results and photocatalysis mechanisms from literature led to the conclusion this was due to both superhydrophilicity minimising organic attractions to the surface and photocatalytic oxidation of organics approaching the surface. The potential for advanced oxidation to participate in reacting with organic matter surfaces attracted to the membrane was confirmed from a measurable increase in the presence of hydroxyl radicals using para-chlorobenzoic acid (*p*CBA) probe experiments. The practical benefits for industry towards chemical consumption and energy reduction were also measured. For example, a 4.5-fold extension to the time needed for a clean-in-place (CIP) was realised when the membrane was operated in photocatalytic mode. A 50% reduction in filtration pump electricity demand was also calculated, which translates to a reduction in height of the feed water for a flux of 300 $L/m^2/h$ from 8.6 m to 3.7 m over a 5 hour run. Future work suggested includes using recycled glass to improve affordability and minimise glass manufacture environmental impact, as well as experimentally establishing the relationship hydroxyl radical concentration and TOC reduction. Optimisation of the glass material for enhancing light transmission

efficiency and development of porous glass monoliths like current commercial ceramic membranes for full-scale use, as well as optimisation to increase contaminant degradation are also suggested.

DECLARATION

"I, Lavern Tendayi Nyamutswa, declare that the PhD thesis with publications titled **"Light transmitting photocatalytic membrane for chemical-free fouling control in water treatment"** is no more than 100,000 words in length, including quotes and exclusive of tables, figures, appendices, bibliography, references and footnotes. This thesis contains no material that has previously been submitted, in whole or in part, for the award of any other academic degree or diploma. Except where otherwise indicated, this thesis is my own work".

[redacted]

Lavern Tendayi Nyamutswa

Institute for Sustainable Industries and Liveable Cities
(ISILC)
College of Engineering and Science
Victoria University
Melbourne, Australia
Date: 31.07.2020

ACKNOWLEDGEMENTS

My study journey has been a positive life changing experience which so many people and organizations contributed to. I am grateful to the Victoria University International Postgraduate Scholarships (VUIPRS) for affording me the opportunity to embark on this journey, funding my studies in full. I am also very grateful to my principal supervisor, Prof Mikel Duke, for taking me under his wing. Prof Duke has been a pillar of support from the beginning. I am fortunate to have had such an experienced mentor and membrane expert to guide me through my PhD journey. When I doubted myself, he was there to give encouragement and direction. Doors were opened for me through his networks and care for both my personal and professional wellbeing. Through Prof Duke's network, I also managed to visit Prof Karl Linden at the Mortenson Center in Global Engineering at the University of Colorado (CU), Boulder, where I had an incredibly rewarding and fruitful experience. Prof Linden has been an invaluable collaborator who has helped to shape the final stages of this thesis.

My associate supervisors, Dr. Dimuth Navaratna and Prof Stephen Collins were also invaluable to the completion of this thesis. They were available to give me direction in the many weekly meetings we had, and hundreds of emails that were sent out among us. I was fortunate to have a multi-disciplinary team to give me advice from their own experiences and expertise.

The executive director of the Institute for Sustainable Industries and Liveable Cities (ISILC), Prof Stephen Gray, was also an amazing leader who genuinely cares for his students and their work. I am grateful that he carefully considered all the funding requests we submitted.

I would also like to thank members of ISILC who took time off their own busy schedules to help me with my work. Dr. Bo Zhu was very helpful in developing the coating procedure for the membranes used in this project. Dr. Ikechukwu Anthony Ike guided me through my early days in the labs, showing me all the places to get the equipment and consumables that I needed. Noel Dow, Dr. Peter Sanciolo and Dr. Marlene Cran were always available to induct me on the use of analytical instruments. I also appreciate Dr. Anbharasi Vanangamudi's assistance in running my first SEM analysis. Catherine Enriquez was also a pillar of administrative

support and I will always be grateful for how she simplified the ordering process during my initial days.

I would also like to mention the technical staff, especially the lab manager Stacey Lloyd and Mary Marshall, who always went beyond their call of duty to make things so much easier in the lab. I also thank other technical staff members Chairmane DiQuattro, Min Nguyen, Joseph Pelle and Larruceo Bautista for the various roles they played to make my lab work easier. I also thank Mark Greaves at CSIRO's Microscopy, Digital Imaging and Surface Analysis Facility for the many hours he spent with me doing surface analysis of the membranes. I also thank CSIRO's Dr. Zongli Xie for giving me access to equipment for porometry measurements and Guang Yang for doing the analysis with me.

I am also grateful to Donald Ermel and Miroslav Radev in the Footscray workshop and electronics department respectively, for the time they spent machining and putting together the electronic equipment for the filtration module.

My research visit to the United States wouldn't have been a pleasant success if it were not for the ready assistance of Dr. Frank Leresche, Bryan Liu, Jasmine Gamboa, Dr. Sarah Fischer and Blair Hanson, members of the Sustainability, Energy and Environment Laboratory (SEEL) at CU.

My PhD journey was also made much better by the friends that I along the way, namely Bojana Klepac Pogrmilovic, Nucharapon Liangruenrom and Douglas Pinto Sampaio Gomes. Together we explored Victoria, met for coffee and lunch and talked to help each other through the journey. The various colleagues I shared office and common spaces with; Dr. Rahul Wadhwani, Dr. Ayumi Ikeda, Dr. Malavika Arun, Dr. Ananya Thomas, Sesa Singha Roy, Thathsarani Kannangara, Charleston De Oliveira Bezerra, Maedeh Nadimi, Mahdi Shahrooz and Javier Piedrahita Solorzano also helped me to grow socially and professionally. I also thank Professor Paul Joseph for his friendly demeanour and chats we had in the corridors.

Overall, the level of helpfulness that I experienced at Victoria University (VU) and CU was extraordinary and something that I will cherish and aim to emulate for the rest of my life. I learnt great life lessons from all the people around me.

I would also like to thank my immediate family, Nyenge and LJ, for walking on this journey with me and making things so much easier for me at home. Even when things were difficult they soldiered on and supported me to get to this point.

VICTORIA UNIVERSITY
MELBOURNE AUSTRALIA

DETAILS OF INCLUDED PAPERS: THESIS BY PUBLICATION

Item/ Chapter No.	**Paper Title**	**Authors**	**Publication Status** (e.g. published, accepted for publication, to be revised and resubmitted, currently under review, unsubmitted but proposed to be submitted)	**Publication Title and Details** (e.g. date published, impact factor etc.)
2	Light transmitting substrates for convenient solar illumination of nanophotocatalyst coatings on membranes for low pressure water filtration	Lavern T. Nyamutswa, Stephen F. Collins, Dimuth Navaratna and Mikel C. Duke	Accepted	Book Chapter in "Advances in Water Desalination Technologies, published by World Scientific Publishing Company
3	Proof of Concept for Light Conducting Membrane Substrate for UV-Activated Photocatalysis as an Alternative to Chemical Cleaning	Lavern T. Nyamutswa, Bo Zhu, Dimuth Navaratna, Stephen F. Collins and Mikel C. Duke	Published	Membranes; SJR Q2 Impact Factor 3.180
4	Light conducting photocatalytic membrane for chemical-free fouling control in water treatment	Lavern T. Nyamutswa, Bo Zhu, Stephen F. Collins, Dimuth Navaratna and Mikel C. Duke	Published	Journal of Membrane Science; SJR Q1 Impact Factor 7.183
5	Sunlight-transmitting photocatalytic membrane for low energy and low maintenance water treatment	Lavern T. Nyamutswa, Blair D. Hanson, Dimuth Navaratna, Stephen F. Collins, Karl G. Linden and Mikel C. Duke	Submitted	Environmental Science and Technology; SJR Q1 Impact Factor 7.270

Declaration by: Lavern Tendayi Nyamutswa **Signature** [redacted] **Date:** 31-07-2020

CONFERENCE PROCEEDINGS

Oral Presentations

1. L. T. Nyamutswa, D. Navaratna, S.F. Collins and M. C. Duke, “Solar illuminated porous glass supported titanium dioxide photocatalytic MF membrane for remote low-maintenance/high-performance clean water recovery from impaired sources”, presented at Membrane Society of Australasia Annual Meeting, Monash University/CSIRO Clayton, Melbourne, 23-24 November 2020
2. L. T. Nyamutswa, D. Navaratna, S.F. Collins, K. G. Linden and M. C. Duke, “Water challenges in Zimbabwe and Australia and the potential application of a solar activated photocatalytic membrane to provide clean water”, presented at Environmental Engineering Seminars, University of Colorado, Boulder, 23 October 2019
3. L. T. Nyamutswa, D. Navaratna, S.F. Collins and M. C. Duke, “Solar activated photocatalysis as a solution to membrane fouling in water treatment”, presented at IEA SHC Task 62 - 3rd Expert Meeting, Freiburg, Germany, 8 – 9 October 2019
4. L. T. Nyamutswa, D. Navaratna, B. Zhu, S.F. Collins and M. C. Duke, “Light transmitting photocatalytic membrane for water treatment”, presented at the 12th conference of the Aseanian Membrane Society, Jeju, South Korea, 2 – 5 July, 2019
5. L. T. Nyamutswa, D. Navaratna, S.F. Collins and M. C. Duke, “In-situ photocatalysis on the surface of a light conducting membrane substrate as an effective strategy to mitigate organic fouling of membranes”, presented at the 6th Membrane Society of Australasia Early Career Researcher Symposium, Melbourne, Australia, 30 January – 1 February 2019
6. L. T. Nyamutswa, D. Navaratna, B. Zhu, S.F. Collins and M. C. Duke, “Photocatalytic sintered glass membrane for decentralized water treatment”, 8th International Symposium on Inorganic Membranes, Brisbane, Australia, 6 – 7 July 2018
7. L. T. Nyamutswa and M. C. Duke, “Photocatalytic membrane for decentralised water treatment”, presented at the Victoria University PhD Coursework Mini-Conference, Melbourne, Australia, 6 December, 2016

Poster Presentations

1. L. T. Nyamutswa, D. Navaratna, B. Zhu, S.F. Collins and M. C. Duke, “Light conducting membrane for UV-activated photocatalysis as an alternative to chemical-based membrane fouling control”, presented at the Taiwan Membrane Society & Membrane Society of Australasia (TA) Networking Event, Chung Yuan Christian University, Taiwan, 30 June – 1 July 2019
2. L. T. Nyamutswa, D. Navaratna, S.F. Collins and M. C. Duke, “Proof of concept for light conducting membrane *substrate for UV-activated photocatalysis as an alternative to chemical cleaning”, presented at the 11th conference of the Aseanian Membrane Society, Brisbane, Australia, 3 – 6 July, 2018*
3. L. T. Nyamutswa and M. C. Duke, “Risk *identification and management in lab-based water treatment experiments”, presented at the Victoria University PhD Coursework Mini-Conference, Melbourne, Australia, 6 December*, 2016

AWARDS AND GRANTS

1. Vice Chancellor’s Doctoral Industry Experience Placement (DIEP) stipend, awarded on 23 July 2020
2. Membrane Society of Australasia (MSA) Travel Award, awarded on 31 March 2019
3. Secomb Conference and Travel Fund, Victoria University, awarded on 29 May 2019
4. Best oral presentation award at the 6th Membrane Society of Australasia (MSA)-Early Career Researcher (ECR) Symposium, Melbourne, awarded on 1 February, 2019
5. Victoria University International Postgraduate Scholarship (VUIPRS), awarded on 5 July 2016

COURSEWORK UNITS

1. (ROP8003) Doctoral Industry Project Placement, Semester 2, 2019
2. (ROP8002) Research Integrity and Ethics, Semester 2, 2016

3. (ROP8001) Conceptualising/contextualising Research, Semester 2, 2016

RESEARCHER DEVELOPMENT TRAINING

1. Data Analytics Tools For Engineering Research, 24 April 2020
2. Systematically review the literature, 26 August 2019
3. Boost Your Research Track Record, 20 June 2019
4. EndNote: Advanced, 14 April 2019
5. Thinking Resiliently as a Researcher, 19 February 2019
6. Scholarly Publishing: The Changing Landscape, 13 September 2018

TABLE OF CONTENTS

LIST OF ABBREVIATIONS AND UNITS

AC	allyl cellulose
AMW	apparent molecular weight
ANFs	aramid nanofibers
ARB	antibiotic resistant bacteria
ARG	antibiotic resistant genes
BC	bacterial cellulose
BSA	bovine serum albumin
CBZ	carbamazepine
CEB	chemically enhanced backwash
CIP	clean-in-place
CMT	cimetidine
CVD	chemical vapour deposition
CS	chitosan
DAD	diode array detector
DC	direct current
DE	dairy effluent
DI water	deionised water
DMF	dimethyl formamide
DMSO	dimethyl sulfoxide
DOC	dissolved organic carbon
DOM	Dissolved organic matter
EDX	energy-dispersive X-ray spectroscopy
eV	electron volts
FLD	fluorescence detector
FQ	fluoroquinolone
FRR	flux recovery ratio
FSGOMs	Free standing graphene oxide membranes
FT-IR	Fourier transform infrared spectroscopy
g	gram
GO	graphene oxide
h	hour
HA	humic acid

HCE	hydraulic cleaning efficiency
HIFI	hydraulically irreversible fouling index
HPLC	high performance liquid chromatography
HPSEC	high performance size exclusion chromatography
HRT	hydraulic residence time
K	Kelvin
kDa	kilo Dalton
kPa	kilo Pascal
L	litre
LED	light emitting diode
MB	methylene blue
MF	microfiltration
MFCs	microbial fuel cells
mg	milligram
min	minute
mL	millilitre
MO	methyl orange
MW	molecular weight
NIPS	non-solvent induced phase separation
NF	nanofiltration
ng	nanogram
NOM	natural organic matter
NP	nanoparticles
NTU	nephelometric turbidity unit
OMW	olive mill wastewater
PAA	polyacrylic acid
PAN	Polyacrylonitrile
PDA	Polydopamine
PDMS	Polydimethylsiloxane
PE	primary effluent
PES	Polysulfone
pH	hydrogen ion concentration
PHEAAm	Poly(hydroxyethyl acrylamide)
pI	isoelectric point

PLA	polylactic acid
PMMA	poly(methyl methacrylate)
PMR	photocatalytic membrane reactor
PTFE	Polytetrafluoroethylene
PU	Polyurethane
PVA	polyvinyl alcohol
PVDF	polyvinylidene fluoride
RC	regenerated cellulose
rGO	reduced graphene oxide
RhB	Rhodamine
RO	reverse osmosis
S	Second
SA	sodium alginate
SEC	size exclusion chromatography
SEM	scanning electron microscopy
SFM	silk fibroin membrane
SOFs	side-glowing optical fibres
SPG	Shirasu porous glass
SWCNT	single-walled carbon nanotube
SWE	secondary wastewater effluent
TCFs	transparent conductive films
TOC	total organic carbon
TTIP	titanium tetraisopropoxide
UF	Ultrafiltration
UV	Ultraviolet
V	Volts
W	Watts
w/w	weight per weight
WWTP	wastewater treatment plant
XRD	X-ray diffraction

CHAPTER 1: INTRODUCTION

1.1 Background

Provision of safe water to the growing world population is an ongoing challenge that is subject of many research studies. Water recycling, as well as use of unconventional water sources, is increasingly becoming a necessity in order to sustain livelihoods, economies and ecosystems around the world. The quality of this recycled water varies widely, where harnessing poor quality water is necessitated by water scarcity around the world [1], increasing human population, industrialization and increasing negative environmental impacts [2]. Subsequently, more pressure is exerted on infrastructure and technology to make these waters fit for human, industrial and agricultural use, as well as disposal into natural water bodies. Improvements in the accessibility and operational simplicity of water treatment technologies would support initiatives aimed at improving wider access to clean water and lessening the impact of human activities on the environment.

Among the technologies available for treatment of water to meet stringent water quality guidelines is membrane micro and ultra-filtration. Membranes used for water treatment are porous, semi-permeable materials that allow water molecules to pass through while acting as a barrier to undesirable components such as pathogens and organic water pollutants [3, 4]. Membrane operations, however, are often regarded as complicated processes because they often need specifically trained operators to ensure they work effectively. This limits their uptake in many situations, including both industrialised and disadvantaged communities.

Due to their mode of operation of retaining undesirable components on their surfaces, membranes inevitably suffer from clogging, a phenomenon referred to as fouling. Membrane fouling is one of the largest barriers to wider adoption of membrane technology in water treatment, because it leads to operational inefficiencies such as reduced flux or increased energy use from higher pumping pressure in commonly used constant flux systems. Fouling also causes reduction of membrane lifespan, which in turn raises capital costs [5]. In considering any membrane process approaches to

manage membrane fouling have to be considered.

Approaches to reduce membrane fouling include, among others, adjustment of membrane properties, pre-treatment of feed water, optimization of module configuration and optimisation of operating conditions [6-8]. Although these reduce fouling to some extent, membrane cleaning is always employed in practice. Cleaning can be hydraulic, mechanical, electrical and chemical, with the former being the most common, followed by the latter. Chemical cleaning utilises reactions that occur with cleaning agents and foulants, which may lead to changes in the structure or properties of foulants, or alter the surface chemistry of fouling layers. These changes weaken adhesion between the foulant and membrane, or the foulant-foulant interactions, leading to easy flushing off the membrane [9]. However, cleaning results in loss of productivity and costs associated with labour, energy consumption as well as procurement, transportation, storage and disposal of chemicals [10].

Chemicals contribute a significant part of the operating costs (OPEX) of membrane systems [11]. Chemicals costs are widely variable and heavily dependent on proximity to manufacturing facilities and world markets, which can be a challenge in remote a community [12]. Disposal of the chemical containing concentrate from membrane operations is also known to be an environmental concern [11]. In the context of low pressure microfiltration (MF) and ultrafiltration (UF), the frequency of chemical use in the industry standard cleaning methods; chemical enhanced backwash (CEB), enhanced flux maintenance (EFM) and clean-in-place (CIP) can also significantly increase both the economic and environmental cost of chemical use. In laboratory and pilot plant operations, CEB can be as frequent as a couple of hours, while CIP and EFM can range from a couple of days to a few months [13, 14]. In a survey of 87 plants using UF and MF membranes for municipal water treatment backwash frequencies varied from 5 to 96 per day with a median of 32 days and lasted from 10 seconds to 10 minutes with a median of 77 seconds. Less than half the plants surveyed carried out EFM on average more than once a week while CIP cleaning frequency ranged from 0.2 to 50 times per year with a median of 4 per year [15]. With chemicals such as NaOCl used and concentrations as high as 5 g/L and size dependent volumes [9], the amount of chemicals required can be high if the frequency of use is also high.

A previous pilot study that applied commercial ceramic membranes for water recycling

required 22 L of 23% ‘as delivered’ polyaluminium chloride coagulant and 8 L of 13% ‘as delivered’ sodium hypochlorite CEB solution for the production of a million litres (ML) of treated water [13]. Assuming an individual has a water consumption of 150 L/day, a population of 100 people living in a remote community would need 0.45 ML for a 30-day supply of water. This water supply volume would require continuous supply of at least 10 L of coagulant and 4 L of hypochlorite (in concentrated supplied form) to cater for the community every month. Even though the volume of chemicals needed appears small, sourcing, paying for, and transporting it to a remote community may be a challenge, before the storage (including chemical shelf life), additional dosing equipment and training for correct and consistent usage required is even considered. After their use, the by-products of these chemicals also need to be disposed. It is therefore highly desirable to find non-chemical means to maintain membranes with available resources, and minimise any third party chemical use, additional equipment, expert training and associated spent chemical disposal.

To avoid (or minimise) chemical use, the modification of the membrane’s properties is an attractive method for fouling control because it can reduce the frequency of cleaning that is needed to keep the membrane functional [16, 17]. For example, hydrophilic modification of a membrane resulted in an increase of reversible fouling from 48% to 60%. An increase in reversible fouling can reduce chemical consumption because reversible fouling can be removed hydraulically without chemicals [16]. One of these modification methods is the immobilisation of heterogeneous photocatalysts, such as titanium dioxide (TiO_2), on the membrane surface [18]. Photocatalytic modification of membranes has a two-fold effect. Firstly, the photo-induced photocatalytic properties of TiO_2 induce partial or total decomposition of pollutants that approach the membrane. Secondly, the photo-induced super-hydrophilicity properties of TiO_2 leads to elimination of the remaining hydrophobic contaminants through simple water rinsing due to improved compatibility of water with the membrane allowing displacement of attached organic fouling modules [18]. This makes photocatalytic modification of membranes useful for both fouling control and the removal of water pollutants.

Photocatalytic membranes are well-studied materials that could offer an attractive method for tertiary water treatment. However, despite years of research and lab trials,

photocatalytic membranes are still to be widely adopted or commercialised. The system closest to commercialisation was developed by the Canadian company Purifics, although ceramic membranes are used to separate suspended photocatalyst particles, rather than having the photocatalyst coated on the membrane [19]. One of the reasons for this low uptake is that to date, researchers have mainly developed photocatalytic membranes for water treatment by coating high performance nano-sized photocatalysts on opaque materials such as ceramics and organic polymers [18]. In this arrangement, to activate the catalyst, light must be directed to the photocatalyst through the turbid, polluted water to be treated as well as the accumulated opaque fouling layer [20], bringing about inefficiencies because of significant light attenuation before it reaches the catalyst. Practical limitations on how to integrate light sources such as UV lamps and light emitting diodes (LEDs) into membrane elements also exist.

In understanding this major practical limitation of photocatalytic membrane technology, this PhD project sought to address this by providing the technical and scientific basis for replacing these opaque materials with transparent (light conducting) materials, starting with readily available, low cost, porous sintered borosilicate glass. Light, including solar radiation, can then be conveniently directed through the light-conducting sintered glass substrate and distributed by scattering the light from underneath to the photocatalyst coated on its surface [18, 21]. Even though light propagation in photocatalytic membranes is a recognised challenge in the literature [22, 23], the use of light conducting sintered glass, or indeed any transparent material, as a membrane substrate and subsequent alternative configurations has never been studied. A reduction in loss of light through can translate to more efficient use of energy. Moreover, as shown in Figure 1.1, using a light conducting substrate can also allow the integration of light sources into membrane modules or the end of enclosed membrane elements, with the light travelling down the length of the element and being scattered to the photocatalyst coating.

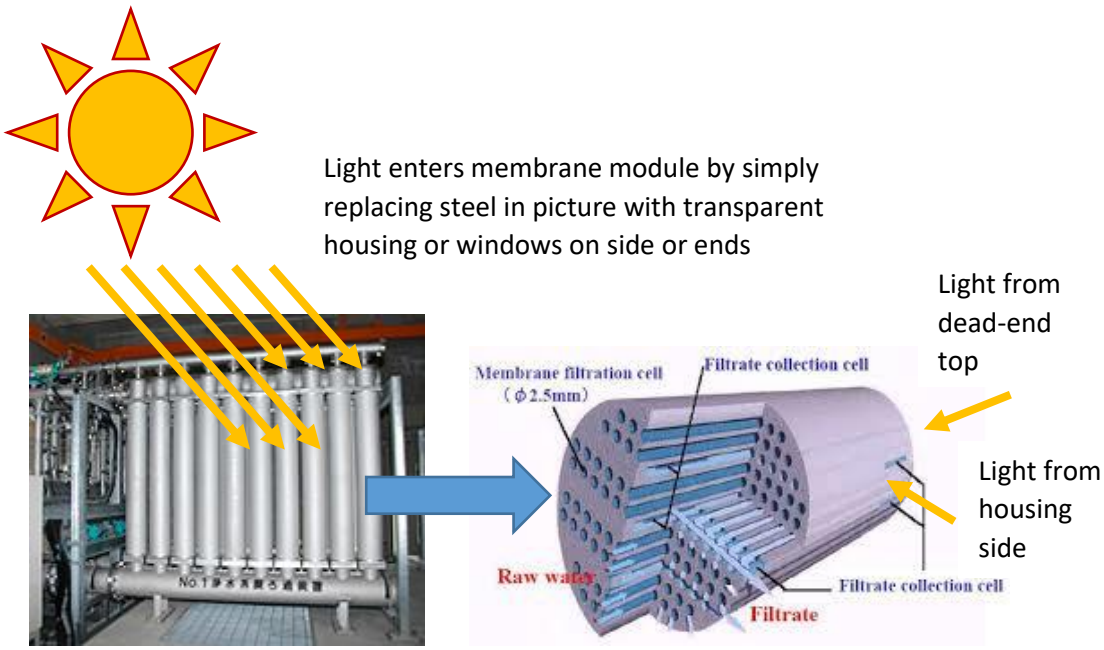

Figure 1.1. A typical ceramic membrane plant (left) and monolith (right) [24] used to propose how a light source can be directed to an equivalent monolith made of porous glass (or polymer). Overlaid orange arrows show how light can be introduced into the membrane plant housings, and how it reaches the photocatalytic TiO_2 coated channels inside the monolith which receive the raw water.

Light propagation through the foulant-free substrate also ensures that any cake layer which builds up on the membrane's active surface becomes a non-factor in the transmission of light to the photocatalyst beneath it. Subsequently, efficient light transmission to the membrane active layer also translates to efficient photocatalysis and minimised fouling of the membrane. Such membranes could be incorporated into a point-of-use (decentralised) water purification device which can be used in remote or disaster-hit areas, where it physically reject pollutants such as organics, bacteria and viruses and then deactivates them by photocatalytic oxidation when it is exposed to the sun. The chemical requirement (and associated equipment, training and spent

chemical disposal) for the 100-people remote community given as an example earlier can be completely avoided, or at least greatly reduced. Cleaning the membrane with the sun's power can give options to keep the treatment plant functional until the chemicals eventually arrive from difficult to reach source markets into the remote community. Further, any spent chemical products produced would be greatly reduced and could be managed safely and with minimal environmental impact.

1.2 Research Objectives

The main aim of this project was to validate a new, innovative idea featuring a photocatalytic MF membrane made from light conducting (i.e. with transparency and scattering properties) sintered glass discs and titanium dioxide nanoparticles and validate its performance in decentralised water treatment application. The objectives were to:

i. Evaluate the light transmitting properties of porous sintered glass discs and prepare light transmitting photocatalytic membrane by dip-coating with TiO_2;
ii. Validate membrane's photocatalytic degradation of typical organic water pollutants in *ex-situ* testing under model UV light;
iii. Assess the anti-fouling and rejection capabilities of the membrane under model UV and solar light activated photocatalysis in *in-situ* testing;
iv. Investigate the mechanism of fouling reduction and formation of hydroxyl radicals through photocatalytic activation; and
v. Demonstrate with quantitative evidence the novel idea that proposes to solve the challenge of distributing light to a photocatalyst coated on a membrane surface, through chemical and energy reduction, as well as practical performance improvements in membrane water treatment.

1.3 Thesis Outline

The thesis is presented in six chapters.

In **Chapter 1,** the background to the research question and the research objectives are provided. The thesis' significance in addressing a gap in current knowledge is also provided.

Chapter 2 is a review of the existing literature on photocatalytic membranes used in water treatment. Chapter 2 is divided into Section A and B. Section A is from a

peer reviewed book chapter, which covers light conducting materials with the potential of being used as membrane substrates. It reviews TiO_2 use as a heterogeneous photocatalyst in water treatment, and how it is immobilised to develop photocatalytic membranes. Section B is a supplementary literature review which covers the light energy needs of photocatalytic membranes and the adoption of alternative energy sources.

Chapter 3 presents results and discussion of the proof of the proposed novel concept of light conducting photocatalytic membranes by *ex-situ* testing. Preparation of the membrane, validation of its photocatalytic properties and its light conducting properties are also given in this chapter.

Chapter 4 presents evaluation of the membrane's performance in the treatment of synthetic solutions that mimic water pollutants in water via *in-situ* testing. In this chapter an improved preparation method, morphology of the membrane, and fouling indices towards representative water pollutants are also provided.

Chapter 5 presents the practical validation of membrane performance in the treatment of real surface water samples. The membrane's performance under simulated solar radiation is also evaluated. The chapter demonstrates the potential for reduced chemical and energy use during water treatment using the developed membrane system.

Chapter 6 includes the conclusions that were drawn from this PhD project, as well as their implications for future studies.

References

[1] C. Tortajada and A. K. Biswas, "Achieving universal access to clean water and sanitation in an era of water scarcity: strengthening contributions from academia," *Current Opinion in Environmental Sustainability,* vol. 34, pp. 21-25, 2018/10/01/ 2018.

[2] T. Distefano and S. Kelly, "Are we in deep water? Water scarcity and its limits to economic growth," *Ecological Economics,* vol. 142, pp. 130-147, 2017/12/01/ 2017.

[3] Z. He, Z. Lyu, Q. Gu, L. Zhang, and J. Wang, "Ceramic-based membranes for water and wastewater treatment," *Colloids and Surfaces A: Physicochemical and Engineering Aspects,* vol. 578, p. 123513, 2019/10/05/ 2019.

[4] S. Riaz and S.-J. Park, "An overview of TiO2-based photocatalytic membrane reactors for water and wastewater treatments," *Journal of Industrial and Engineering Chemistry,* vol. 84, pp. 23-41, 2020/04/25/ 2020.

[5] Z. Geng *et al.*, "Self-cleaning anti-fouling hybrid ultrafiltration membranes via side chain grafting of poly(aryl ether sulfone) and titanium dioxide," *Journal of Membrane Science,* vol. 529, pp. 1-10, 5/1/ 2017.

[6] W. J. Lee *et al.*, "Fouling mitigation in forward osmosis and membrane distillation for desalination," *Desalination,* vol. 480, p. 114338, 2020/04/15/ 2020.

[7] C. Li, W. Sun, Z. Lu, X. Ao, and S. Li, "Ceramic nanocomposite membranes and membrane fouling: A review," *Water Research,* vol. 175, p. 115674, 2020/05/15/ 2020.

[8] J. Xu, C.-Y. Chang, J. Hou, and C. Gao, "Comparison of approaches to minimize fouling of a UF ceramic membrane in filtration of seawater," *Chemical Engineering Journal,* vol. 223, pp. 722-728, 2013/05/01/ 2013.

[9] C. Liu, "Membrane cleaning: From theory to practice," *Water e-Journal,* vol. 2, no. 2, 2017.

[10] S. S. Madaeni and N. Ghaemi, "Characterization of self-cleaning RO membranes coated with TiO2 particles under UV irradiation," *Journal of Membrane Science,* vol. 303, no. 1–2, pp. 221-233, 10/15/ 2007.

[11] S. Bhojwani, K. Topolski, R. Mukherjee, D. Sengupta, and M. M. El-Halwagi, "Technology review and data analysis for cost assessment of water treatment systems," *Science of The Total Environment,* vol. 651, pp. 2749-2761, 2019/02/15/ 2019.

[12] H. M. Ettouney, H. T. El-Dessouky, R. S. Faibish, and P. J. Gowin, "Evaluating the economics of desalination," *Chemical Engineering Progress,* Article vol. 98, no. 12, pp. 32-39, 2002.

[13] N. Dow *et al.*, "Fouling mechanisms and reduced chemical potential of ceramic membranes combined with ozone," *Water Practice and Technology,* vol. 10, no. 4, pp. 806-813, 2015.

[14] S. S. Yoo, K. H. Chu, I.-H. Choi, J. S. Mang, and K. B. Ko, "Operating cost reduction of UF membrane filtration process for drinking water treatment attributed to chemical cleaning optimization," *Journal of Environmental Management,* vol. 206, pp. 1126-1134, 2018/01/15/ 2018.

[15] N. Porcelli and S. Judd, "Chemical cleaning of potable water membranes: A review," *Separation and Purification Technology,* vol. 71, no. 2, pp. 137-143, 2010/02/18/ 2010.

[16] Q. Gu *et al.*, "Interfacial diffusion assisted chemical deposition (ID-CD) for confined surface modification of alumina microfiltration membranes toward high-flux and anti-fouling," *Separation and Purification Technology,* vol. 235, p. 116177, 2020/03/18/ 2020.

[17] J. Wang *et al.*, "Hydrophilic modification of PTFE microfiltration flat membrane by crosslinking OCMCS-PEI to enhance anti-fouling property," *Progress in Organic Coatings,* vol. 135, pp. 565-573, 2019/10/01/ 2019.

[18] L. T. Nyamutswa, B. Zhu, S. F. Collins, D. Navaratna, and M. C. Duke, "Light conducting photocatalytic membrane for chemical-free fouling control in water treatment," *Journal of Membrane Science,* vol. 604, p. 118018, 2020/06/01/ 2020.

[19] Purifics. (2020, 10 July 2020). *Complete Water Purification Using Ceramic Membrane Technologies*. Available: http://www.purifics.com/

[20] M. Ren, M. Drosos, and F. H. Frimmel, "Inhibitory effect of NOM in photocatalysis process: Explanation and resolution," *Chemical Engineering Journal,* vol. 334, pp. 968-975, 2018/02/15/ 2018.

[21] L. Nyamutswa, B. Zhu, D. Navaratna, S. Collins, and M. Duke, "Proof of Concept for Light Conducting Membrane Substrate for UV-Activated Photocatalysis as an Alternative to Chemical Cleaning," *Membranes,* vol. 8, no. 4, p. 122, 2018.

[22] I. Horovitz *et al.*, "Carbamazepine degradation using a N-doped TiO2 coated photocatalytic membrane reactor: Influence of physical parameters," *Journal of Hazardous Materials,* vol. 310, pp. 98-107, 2016/06/05/ 2016.

[23] B. J. Starr, V. V. Tarabara, M. Herrera-Robledo, M. Zhou, S. Roualdès, and A. Ayral, "Coating porous membranes with a photocatalyst: Comparison of LbL self-assembly and plasma-enhanced CVD techniques," *Journal of Membrane Science,* vol. 514, pp. 340-349, 2016/09/15/ 2016.

[24] K. Hattori, "Operation with ceramic membrane filtration system for DWTP in Japan," presented at the Sborník Konference Pitná voda České Budějovice, 2010. Available: http://www.wet-team.cz/files/konference/2010/PV2010%20sbornik/18-Hattori.pdf

CHAPTER 2: LITERATURE REVIEW

2.1. Chapter Overview

Chapter 2 is divided into two sections, A and B. Section A presents a review of the literature on materials that could be adopted as light conducting substrates for photocatalytic membranes. It is also a review of titanium dioxide's use as a heterogeneous photocatalyst in water treatment, and how it is immobilised to develop photocatalytic membranes. This section was accepted for publishing as a peer reviewed chapter in the book "Advances in Water Desalination Technologies'', edited by Matthew Tirrell, Benny Freeman and Yoram Cohen, published by World Scientific Publishing Company. The chapter is titled "Light transmitting substrates for convenient solar illumination of nanophotocatalyst coatings on membranes for low pressure water filtration" by Lavern T. Nyamutswa, Stephen F. Collins, Dimuth Navaratna and Mikel C. Duke. It is presented here in the final accepted format.

Section B is a supplementary literature review which covers the light energy needs of photocatalytic membranes and the use of light emitting diodes (LEDs) and solar as alternative energy sources. These were not covered in the book chapter that makes up Section A. Section B also gives the overall conclusion of the literature review and how it was used to shape the research project.

SECTION A

2.2. Declaration of Co-Authorship and Co-Contribution to the Chapter

VICTORIA UNIVERSITY

THE NEW WAY TO DO UNI

OFFICE FOR RESEARCH TRAINING, QUALITY AND INTEGRITY

DECLARATION OF CO-AUTHORSHIP AND CO-CONTRIBUTION: PAPERS INCORPORATED IN THESIS

This declaration is to be completed for each conjointly authored publication and placed at the beginning of the thesis chapter in which the publication appears.

1. PUBLICATION DETAILS (to be completed by the candidate)

Title of Paper/Journal/Book: **Light transmitting substrates for convenient solar illumination of nanophotocatalyst coatings on membranes for low pressure water filtration**

Surname: **Nyamutswa** First name: **Lavern**

Institute: **Institute for Sustainable Industries and Liveab** Candidate's Contribution (%): **80**

Status:

Accepted and in press: ☑ Date: **30/04/2020**

Published: ☐ Date:

2. CANDIDATE DECLARATION

I declare that the publication above meets the requirements to be included in the thesis as outlined in the HDR Policy and related Procedures – policy.vu.edu.au.

Lavern Nyamutswa Digitally signed by Lavern Nyamutswa Date: 2020.07.27 18:41:07 +10'00'	27/07/2020
Signature	**Date**

3. CO-AUTHOR(S) DECLARATION

In the case of the above publication, the following authors contributed to the work as follows:

The undersigned certify that:

1. They meet criteria for authorship in that they have participated in the conception, execution or interpretation of at least that part of the publication in their field of expertise;
2. They take public responsibility for their part of the publication, except for the responsible author who accepts overall responsibility for the publication;

PO Box 14428, Melbourne,
Vic 8001, Australia
+61 3 9919 6100

Victoria University ABN 83776954731
CRICOS Provider No. 00124K (Melbourne),
02475D (Sydney), RTO 3113

3. There are no other authors of the publication according to these criteria;

4. Potential conflicts of interest have been disclosed to a) granting bodies, b) the editor or publisher of journals or other publications, and c) the head of the responsible academic unit; and

5. The original data will be held for at least five years from the date indicated below and is stored at the following **location(s):**

Institute for Sustainable Industries and Liveable Cities, Victoria University, Werribee Campus, Melbourne, Australia

Name(s) of Co-Author(s)	Contribution (%)	Nature of Contribution	Signature	Date
Lavern T. Nyamutswa	80	Concept development and manuscript writing	[redacted]	27/07/2020
Stephen F. Collins	5	Manuscript review and editing		29 Jul '20
Dimuth Navaratna	5	Manuscript review and editing		29/07/2020
Mikel C. Duke	10	Concept development and manuscript review and editing		27/07/2020

Updated: September 2019

PO Box 14428, Melbourne,
Vic 8001, Australia
+61 3 9919 6100

Victoria University ABN 83776954731
CRICOS Provider No. 00124K (Melbourne),
02475D (Sydney), RTO 3113

Light Transmitting Substrates for Convenient Solar Illumination of Nanophotocatalyst Coatings on Membranes for Low Pressure Water Filtration

Lavern T. Nyamutswa, Stephen F. Collins, Dimuth Navaratna, and Mikel C. Duke.

Advances in Water Desalination Technologies. August 2021, 459-489

https://doi.org/10.1142/9789811226984_0013

The full-text of this article is subject to copyright restrictions, and cannot be included in the online version of the thesis.

SECTION B

2.4. Identification and minimisation of energy requirements in photocatalytic membrane systems

Energy is an important input in photocatalytic membrane processes for water treatment. Energy is required for pump operation, as well as for powering the artificial light sources needed to activate the photocatalyst. The energy consumed by the light source can be a significant contribution to energy requirements [1]. In a photocatalytic membrane setup with a treatment capacity of 4.2 L/h, for example, energy consumption by UV lamps used for photocatalytic activation was 9.3 kWh/m^3 [2]. In comparison, state of the art large scale sea water reverse osmosis (RO) plants (which are generally regarded as energy intensive) typically have total energy consumption of less than 4 kWh/m^3 [3-5] while microfiltration (MF) water treatment systems use less than 1 kWh/m^3 [6].

The importance of reducing or eliminating the photocatalyst's reliance on lamps which use electrical energy was well illustrated in a study by Athanasekou *et al*. in 2015 [7]. In considering the total electrical energy demand, they compared the energy consumed by a pump in both photocatalytic and non-photocatalytic membrane treatment processes. By using Equation 1, they calculated the energy consumed by a pump to drive 100 m^3 of water through a membrane in crossflow mode:

$$E\ (kWh) = 100 \frac{P}{S} \frac{\rho_w}{36} \qquad (1)$$

where E is the energy, P is the pressure on the retentate side of the membrane (bar), ρ_w (g/cm^3) is the density of the fluid and S is the pump efficiency [7]. However, for comparative purposes, the more conventional units of kWh/m^3 will be used. A GO-TiO_2/γ Al_2O_3 UF tubular membrane had pump energy consumption values of less than 0.05 kWh/m^3 for both methyl orange (MO) and methylene blue (MB) filtration during dark, UV and visible light treatment. This was far less than values of a commercial ceramic nanofiltration (NF) which needed 0.85 kWh/m^3 to treat MO solution by size exclusion, while a reverse osmosis (RO) system needed about 1.20 kWh/m^3 for the same task. When the energy consumed in powering the light sources was also taken into consideration, the total energy needed for the hybrid process was equivalent to

that required by the commercial polymeric NF membrane (i.e. 0.85 kWh/m^3) to treat the same amount of water, clearly showing that most of the energy in a photocatalytic membrane reactor (PMR) goes to the light source. However, the hybrid system operates at lower pressures, and has above 99% water recovery (low fouling solution, therefore no backwashing needed), hence it treats the same volume of water in less time. In another study using the same materials, the authors further concluded that the largest consumer of energy in PMR processes is the light source [1]. Reducing the light energy demand is therefore a critical driver for PMR research.

The fact that lighting requirements are the primary consumer of energy was also demonstrated in the removal of MO by γ-alumina UF membranes dip coated with TiO_2 or modified by chemical vapour deposition (CVD) techniques [8]. The energy consumed by the pump to collect a certain volume of permeate was measured. The dip-coated membranes were operated in the dead-end mode, while the rest were operated in the cross-flow mode. The energy consumed by 36 W UV sources for the dip-coated membranes while maintaining permeation demonstrated that the light source is one of the biggest consumers of energy in the system. To treat 200 mL of water in a period of about 2 h, energy consumption of the dip-coated membrane system with a membrane surface area of 50 cm^2 was about 500 kWh/m^3 with the UV sources switched on and 0.05 kWh/m^3 when they were switched off, a difference of four orders of magnitude with the larger value being essentially completely impractical.

2.4.1. Light emitting diodes

To reduce this energy footprint, alternative sources of light energy have been explored, among them energy efficient light emitting diodes (LEDs) [9-11]. Low pressure mercury and xenon arc lamps are the traditional radiation energy sources that they have been used for photocatalytic membrane systems, but the advent of more energy efficient sources and concerns over mercury have seen their use being phased out [12-14]. LEDs have increasingly attracted attention due their numerous advantages over traditional lamps used in photocatalytic applications, which include longer lifetime, higher energy efficiency, high spectral purity for targeted performance, flexible configuration, small size and potential to be used in compact PMRs [15, 16]. The low voltage requirements of LEDs of between 6-30 V DC mean they can be driven by

battery or solar cells with simpler low voltage power converters, which is important for building point of use devices, especially for remote or off-grid areas.

A review of electrical energy per order (E_{EO}) of several UV/TiO_2 systems which used traditional lamps and LED light sources conducted by Matafonova and Batoev [17] found that the E_{EO} of LED systems was comparable, and sometimes significantly lower than that of traditional lamps. The E_{EO} is defined as the electrical energy required to reduce the concentration of a pollutant by one order of magnitude per cubic metre of contaminated water [18]. For example, treatment of Basic Red 46 with UV LEDs led to up to 4.8-fold reduction in the E_{EO} compared to traditional UV lamps [19]. Building on the studies in which the E_{EO} of LED systems were significantly lower than that of traditional lamps will contribute to the lamps being phased out and the energy efficiency of photocatalytic membrane treatment systems being improved. LEDs, unlike mercury and xenon arc lamps, can give pulsed illumination, which is known to reduce electric consumption while maintaining the same efficiency [20].

It is now generally regarded that LEDs can be successfully used in membrane photocatalytic experiments instead of traditional lamps. UVA from 3 W, 365 nm LED sources have been used for TiO_2 photocatalysed degradation of Ciprofloxacin (CIP), a fluoroquinolone (FQ) antibiotic used for treatment of bacterial infections [21]. 12 LED lamps in total were connected to a DC power supply to give an incident light intensity of 10 mW/cm^2. The light caused minimal photolysis but was very effective in initiating photocatalysis, as seen from the pseudo first order constants of 0.0091 ± 0.0011 min^{-1} for CIP and 0.2217 ± 0.0179 min^{-1} for FQ.

2.4.2. Solar energy

The ultimate alternative to electrical energy demanding artificial light sources is the naturally occurring abundant source of solar light. The biggest disadvantage of relying on solar energy, however, is that intensity is widely variable, depending on the geographical location, weather, season and time of day. As a reference, the average annual solar intensity in Melbourne from 1 July 2019 to 30 June 2020 was 18 mW/cm^2. The average intensity peaks in the summer months (28-31 mW/cm^2) and is lowest in winter (7-10 mW/cm^2) [22]. Further, the most widely available commercial types of

TiO_2, Degussa P25, is activated by light of wavelengths of 385 nm or lower, which lie in the UV region and is just 4 % of total sunlight radiation [23].

Even though the fraction of UV in solar radiation is only about 4%, it can still be used to excite unmodified TiO_2, provided adequate intensity is available. To demonstrate this, a P25 TiO_2-poly[(vinylidenefluoride-trifluoroethylene] [(P(VDF–TrFE)] UF membrane was applied in the degradation of 10 mg/L tartrazine under solar light of intensity 60-100 mW/cm^2 and a UV lamp with maximum emission at 365 nm and intensity of appproximately 6 mW/cm^2 [24]. After 5 hours, the degradation under solar and UV lamp was 78% and 37% respectively.

In another study of the degradation of tartrazine facilitated by P25 TiO_2 immobilised on glass plates, solar radiation gave a 99% degradation, and a 24 W, 65 nm UV lamp a 30% degradation after 3.3 hours [25]. In another study, the degradation of 1,4-dioxane in a PMR consisting of suspended TiO_2 and a PVDF membrane under solar radiation was compared to that under artificial UV irradiation [2]. The UV flux from sunlight was measured at 1.31 ± 0.24 mW/cm^2, corresponding to a UV dose of 0.25 ± 0.05 W/L. Degradation of 1,4 dioxane occurred under both solar and UV lamp radiation at a first order rate a constant of 0.028 min^{-1} and 0.037 min^{-1} respectively. 100% degradation occurred in about 1.8 h under UV irradiation, and 3.2 h under solar, clearly showing that the use of sunlight in PMRs is feasible. It was estimated that for a treatment capacity of 4.2 L/h in this PMR, 9.3 kWh/m^3 of energy from UV lamps is needed. Use of sunlight instead of UV lamps therefore results in significant savings on energy costs.

TiO_2 has also been modified to use solar energy more efficiently through methods such as impurity doping, dye sensitisation [23, 26] and compositing with other materials such as graphene oxide [27, 28]. Absorption peak shifts for TiO_2 from 365 nm in the UV region to 700 nm in the visible light region, and even into the infrared region, have been achieved through such modifications [29].

Visible light LEDs, as energy efficient artificial light sources and solar simulating devices, have also been shown to be a suitable radiation source for photocatalytic membrane applications. This was demonstrated in a submerged membrane reactor consisting of carbon, nitrogen and sulphur tri-doped TiO_2 and a hollow fibre polyvinylidene fluoride (PVDF) MF membrane operated in a continuous flow-through

mode for the degradation of carbamazepine (CBZ). The LEDs with an average power of 15 W emitted blue light at 450 nm, and a broadband emission between 500-600 nm at an average intensity of 0.4 mW/cm^2. CBZ removals of up to 68% were achieved with hydraulic residence times (HRTs) ranging from 30 to 300 min [15].

The efficacy of visible light LEDs as solar energy simulators in facilitating photocatalytic degradation of MO and MB in in a PMR consisting of ceramic γ-alumina membranes dip-coated with nitrogen doped TiO_2 was also investigated [8]. >99% water recovery (dead-end filtration and no backwashing applied) and 45% dye reduction was realised, compared to commercial polymeric NF membranes which had 80% water recovery and 95% dye rejection. The authors proposed that recycling the feed in the PMR system would give the same efficiency as the commercial NF systems since the PMR system uses only 10% of the energy used by the NF system.

2.4.3. Summary of photocatalytic performance of systems with lamps and LED light sources

Performance characteristics of PMR systems which applied both LEDs and traditional lamps over a range of light wavelengths (UV and visible) are summarised in Table 2.1. To give sufficient residence time for complete degradation of the targeted organic compounds to occur, these studies employed a variety of techniques, which included recirculation of the feed or permeate [30], and submerged membrane systems with suspended photocatalysts for higher contact area [2]. It is noted that in all cases, removal of the target organic occurs in the order of hours, since this has been the focus of their studies. One-pass filtration is standard practice in MF and UF operations, where contact time with the membrane is much less than this. Reduction of organics due to oxidation would therefore be unlikely. Since this thesis is focussed on the industry standard dead-end, one-pass system, the first effect of reduced fouling from photocatalysis will be the main interest, and the secondary interest will be on potential for organics removal due to oxidation (although unlikely to occur due to the short contact times).

Table 2.1. Summary of contaminant removal performance of various photocatalytic studies using UV lamps and LEDs for the removal of compounds from water, which include methylene blue (MB), carbamazepine (CBZ), methyl orange (MO) and bovine serum albumin (BSA)

Membrane	**Light source**	**Intensity, peak wavelength**	**Contaminant**	**k (x 10^{-3} min^{-1})**	**% Removal**	**Time for removal (hours)**	**Reference**
TiO_2/PMMA	8 W UV Lamp,	1.1 mW/cm^2, 368 nm	~10^{-5} M MB	3.0	100	4	[31]
TiO_2/PMMA	8 W UV Lamp,	2 mW/cm^2, 368 nm	~10^{-5} M MB	2.4	100	1	[32]
N-TiO_2/Al_2O_3	300 W ozone-free Xe arc lamp solar simulator		4.24 × 10^{-6} M CBZ	8.5	~80	2	[10]
TiO_2/PAA/PVDF	15 W UV Lamp		40 ppm Reactive Black 5	2.8	99	5	[33]
TiO_2/PTFE	300 W UV Lamp		10 ppm MB	18.7	90	1.7	[34]
TiO_2/PES	16 W UVA Lamp		5 ppm MO	4.1	90	9	[35]
TiO_2/GO-Psf	150 W UV Lamp		50 ppm MB	3.7	70	5	[36]
	70 W Full spectrum light bulb			3.3	65	5	
TiO_2/GO/PVDF	11 W UV Lamp,	0.6 mW/cm^2	1000 ppm BSA	14.2	80	2	[37]
TiO_2/PVDF/TrFE	Sunlight		10 ppm Tartrazine	300	78	5	[24]
TiO_2/PVDF	6 x 4 W UV lamps	350-400 nm	10 μM Bisphenol A	36.1	100	2	[38]
				102.5	100	2	
			10 × 10^{-6} M Cimetidine	31.4	100	2	
			10 × 10^{-6} M 4-				

Membrane	Light source	Intensity, peak wavelength	Contaminant	k (x 10^{-3} min^{-1})	% Removal	Time for removal (hours)	Reference
			Chlorophenol				
TiO_2/PTi	6 x UV-LEDs,	0.390 mW/cm^2, 365 nm	0.004 ppm 17α-ethinylestradiol	24.5	48	3	[20]
				3.4	10	3	
				14.4	30	3	
			0.004 ppm 17β-estradiol	18.9	25	3	
				7.3	20	3	
			0.004 ppm Estrone				
			0.004 ppm Estriol				
			0.004 ppm Bisphenol A				
TiO_2/PVDF	36 W UVA Lamp		10 ppm nonylphenol	17.3	100	2.5	[39]
N-Pd/TiO_2/Psf	Solar simulator with 500 W Xe lamp,	100 mW/cm^2	100 ppm Eosin Yellow	16.9	97	4	[40]
TiO_2/Fibreglass	Solar simulator with 150 W Xe-Hg Light		5 ppm MB	3.9	80	8	[41]
TiO_2/SiO_2/SiC	UV lamp		30 × 10^{-6} M MB	9.8	69	1	[42]
Au-TiO_2/pDA/PVDF	300 W Xe visible light lamp		10 ppm Tetracycline	21.9	92	2	[43]
TiO_2/PVDF-TrFE	6 x 8 W UV lamps	3.8 mW/cm^2, 365 nm	10^{-5} M MB	40	100	1.5	[44]
Ag_2O/TiO_2/Chitosan	150 W visible tungsten–halogen lamp		10 ppm MB	16.4	96	0.25	[45]

Membrane	Light source	Intensity, peak wavelength	Contaminant	k (x 10^{-3} min^{-1})	% Removal	Time for removal (hours)	Reference
TiO_2/Al_2O_3	4 x 8.7 W UV lamps	53 W/m^2, 350 nm	1 ppm diuron	323	95	3	[46]
			1 ppm chlorfenvinphos	289	78	3	
TiO_2/Ti	300 W Xe UV-visible lamp		5 ppm Rhodamine B	32.3	85	1	[47]
TiO_2/PEG/PVDF	8 W UV lamps, 365 nm		100 ppm Nonylphenol	8.1	99	5	[48]
TiO_2/ZnO/PVDF	200 W Xe light, with filters	400–780 nm	10^{-5} M MB	83.8	80	0.5	[49]
TiO_2/(P(VDF-TrFE)	6 x 8 W UV lamps,	1.7 mW/cm^2, 365 nm	17.6 × 10^{-6} M MB	5	85	5	[50]

2.5. Conclusions

Studies often report energy as a significant cost source in the operation of membranes in water treatment, and is regarded as a critical parameter in selecting a water treatment process. In traditional membranes, pumps in the case of pressure driven operations such as NF and RO, consume most of the energy. In photocatalytic MF and UF membranes, the possibility of carrying out filtration at lower pressures means that the light source, rather the pump, is the most significant consumer of energy. Nevertheless, a process that can remove/breakdown organic contaminants without significant reject/concentrate disposal requirements (as compared to the higher energy/lower volume recovery NF and RO) is highly desirable. Further reductions in the energy consumed by photocatalytic membranes has been made possible by replacing traditional UV lamps with light emitting diodes (LEDs). Complete replacement of artificial light sources with solar energy has also been shown to be possible. This results in more energy savings in photocatalytic membranes.

The use of photocatalytic membranes in real water treatment is promising and has been shown to give superior performance. Among these are increased pollutant degradation, increased flux, reduced fouling, shortened treatment times and higher longevity of membranes due to less frequent cleaning procedures, which can lead to

membrane damage. However, photocatalytic membranes are still not adopted by industry despite research interest which began in 1991 [51] and the first functional photocatalytic membrane being reported in 2006 [52]. As discussed in Section A and B, barriers to wider adoption that are frequently cited are the low efficiency of the photocatalysts, dependency on high energy artificial UV instead of visible (solar) light, short membrane life due to loss of photocatalyst and practical integration of light sources with water treatment systems.

Progress has been made in most of these issues, except on the question of the best way to integrate light sources into treatment systems and membrane modules to better harness the abundant sunlight instead of using electricity to provide the light source. By solving the light transmission challenges identified in Section A (which include light scattering by the feed) through using light transmitting substrates and reducing the energy footprint of photocatalytic membranes identified in Section B, the attractiveness of photocatalytic membranes as a practical low cost, reduced fouling, and superior performance alternative can be enhanced. The thesis is mainly motivated to harness photocatalysis as a means to reduce cleaning chemical consumption for sustainable membrane water treatment, as well as the degradation of pollutants. Photocatalysis was identified as an alternative to chemical cleaning, whereby induced super-hydrophilicity discussed in Section A helps in minimising fouling, while oxidation degrades water pollutants. Using a light transmitting porous sintered glass substrate allowed light to be directed through the substrate itself and distributing to the photocatalyst coating by light scattering from underneath, where the quality of the water being treated and accumulated fouling layers no longer affect the efficiency of light transmission to the photocatalysts. This also allows light sources to be installed at the ends of monolithic membrane designs as proposed in the introduction chapter, where it travels down the substrates length and the scattered light activates the photocatalyst beneath the membrane surface. Light transmission give the possibility of simple exposure of the membrane to the sun to control fouling *in-situ*, eliminating or reducing the need for chemically cleaning the membrane, while decontaminating water for potable or other fit-for-purpose use. In the thesis, a one-pass filtration system was employed, meaning the contact time between the photocatalyst and organic pollutants would not be sufficient to allow complete degradation.

References

[1] C. P. Athanasekou *et al.*, "Prototype composite membranes of partially reduced graphene oxide/TiO2 for photocatalytic ultrafiltration water treatment under visible light," *Applied Catalysis B: Environmental,* vol. 158-159, pp. 361-372, 2014/10/01/ 2014.

[2] K.-C. Lee, H.-J. Beak, and K.-H. Choo, "Membrane photoreactor treatment of 1,4-dioxane-containing textile wastewater effluent: Performance, modeling, and fouling control," *Water Research,* vol. 86, pp. 58-65, 2015/12/01/ 2015.

[3] C. R. Bartels and K. Andes, "Consideration of energy savings in SWRO," *Desalination and Water Treatment,* vol. 51, no. 4-6, pp. 717-725, 2013/01/01 2013.

[4] R. Dashtpour and S. N. Al-Zubaidy, "Energy efficient reverse osmosis desalination process," *International Journal of Environmental Science and Development,* vol. 3, no. 4, p. 339, 2012.

[5] R. Semiat, "Energy Issues in Desalination Processes," *Environmental Science & Technology,* vol. 42, no. 22, pp. 8193-8201, 2008/11/15 2008.

[6] K. Zuo *et al.*, "Coupling microfiltration membrane with biocathode microbial desalination cell enhances advanced purification and long-term stability for treatment of domestic wastewater," *Journal of Membrane Science,* vol. 547, pp. 34-42, 2018/02/01/ 2018.

[7] C. P. Athanasekou *et al.*, "Ceramic photocatalytic membranes for water filtration under UV and visible light," *Applied Catalysis B: Environmental,* vol. 178, pp. 12-19, 2015/11/01/ 2015.

[8] N. G. Moustakas, F. K. Katsaros, A. G. Kontos, G. E. Romanos, D. D. Dionysiou, and P. Falaras, "Visible light active TiO2 photocatalytic filtration membranes with improved permeability and low energy consumption," *Catalysis Today,* vol. 224, pp. 56-69, 2014/04/01/ 2014.

[9] D. M. A. Alrousan, M. I. Polo-López, P. S. M. Dunlop, P. Fernández-Ibáñez, and J. A. Byrne, "Solar photocatalytic disinfection of water with immobilised titanium dioxide in re-circulating flow CPC reactors," *Applied Catalysis B: Environmental,* vol. 128, pp. 126-134, 2012/11/30/ 2012.

[10] I. Horovitz *et al.*, "Carbamazepine degradation using a N-doped TiO2 coated photocatalytic membrane reactor: Influence of physical parameters," *Journal of Hazardous Materials,* vol. 310, pp. 98-107, 2016/06/05/ 2016.

[11] B. J. Starr, V. V. Tarabara, M. Herrera-Robledo, M. Zhou, S. Roualdès, and A. Ayral, "Coating porous membranes with a photocatalyst: Comparison of LbL self-assembly and plasma-enhanced CVD techniques," *Journal of Membrane Science,* vol. 514, pp. 340-349, 2016/09/15/ 2016.

[12] S.-K. Back *et al.*, "Correlation between mercury content and leaching characteristics in waste phosphor powder from spent UV curing lamp after thermal treatment," *Journal of Hazardous Materials,* vol. 382, p. 121094, 2020/01/15/ 2020.

[13] Y. Hu and H. Cheng, "Mercury risk from fluorescent lamps in China: Current status and future perspective," *Environment International,* vol. 44, pp. 141-150, 2012/09/01/ 2012.

[14] P. Nance, J. Patterson, A. Willis, N. Foronda, and M. Dourson, "Human health risks from mercury exposure from broken compact fluorescent lamps (CFLs)," *Regulatory Toxicology and Pharmacology,* vol. 62, no. 3, pp. 542-552, 2012/04/01/ 2012.

[15] P. Wang, A. G. Fane, and T.-T. Lim, "Evaluation of a submerged membrane vis-LED photoreactor (sMPR) for carbamazepine degradation and TiO2 separation," *Chemical Engineering Journal,* vol. 215-216, pp. 240-251, 2013/01/15/ 2013.

[16] M. Martín-Sómer, C. Pablos, R. van Grieken, and J. Marugán, "Influence of light distribution on the performance of photocatalytic reactors: LED vs mercury lamps," *Applied Catalysis B: Environmental,* vol. 215, pp. 1-7, 2017/10/15/ 2017.

[17] G. Matafonova and V. Batoev, "Recent advances in application of UV light-emitting diodes for degrading organic pollutants in water through advanced oxidation processes: A review," *Water Research,* vol. 132, pp. 177-189, 2018/04/01/ 2018.

[18] P. Puspita, F. A. Roddick, and N. A. Porter, "Decolourisation of secondary effluent by UV-mediated processes," *Chemical Engineering Journal,* vol. 171, no. 2, pp. 464-473, 2011/07/01/ 2011.

[19] M. Rasoulifard, R. Marandi, H. Majidzadeh, and I. Bagheri, "Ultraviolet Light-Emitting Diodes and Peroxydisulfate for Degradation of Basic Red 46 from Contaminated Water," *Environmental Engineering Science,* vol. 28, no. 3, pp. 229-235, 2011.

[20] M. J. Arlos *et al.*, "Photocatalytic decomposition of selected estrogens and their estrogenic activity by UV-LED irradiated TiO2 immobilized on porous titanium sheets via thermal-chemical oxidation," *Journal of Hazardous Materials,* vol. 318, pp. 541-550, 2016/11/15/ 2016.

[21] S. Li and J. Hu, "Transformation products formation of ciprofloxacin in UVA/LED and UVA/LED/TiO2 systems: Impact of natural organic matter characteristics," *Water Research,* vol. 132, pp. 320-330, 2018/04/01/ 2018.

[22] A. B. o. Meteorology. (2020, 10 July 2020). *Solar exposure : Monthly, seasonal and annual solar exposure*. Available: http://www.bom.gov.au/jsp/ncc/climate_averages/solar-exposure/index.jsp?period=mar#maps

[23] H. Xu, M. Ding, W. Chen, Y. Li, and K. Wang, "Nitrogen–doped GO/TiO2 nanocomposite ultrafiltration membranes for improved photocatalytic performance," *Separation and Purification Technology,* vol. 195, pp. 70-82, 2018/04/29/ 2018.

[24] L. Aoudjit, P. M. Martins, F. Madjene, D. Y. Petrovykh, and S. Lanceros-Mendez, "Photocatalytic reusable membranes for the effective degradation of tartrazine with a solar photoreactor," *Journal of Hazardous Materials,* vol. 344, pp. 408-416, 2018/02/15/ 2018.

[25] N. Chekir *et al.*, "A comparative study of tartrazine degradation using UV and solar fixed bed reactors," *International Journal of Hydrogen Energy,* vol. 42, no. 13, pp. 8948-8954, 2017/03/30/ 2017.

[26] S. Livraghi, M. Pelaez, J. Biedrzycki, I. Corazzari, E. Giamello, and D. D. Dionysiou, "Influence of the chemical synthesis on the physicochemical properties of N-TiO2 nanoparticles," *Catalysis Today,* vol. 209, pp. 54-59, 6/15/ 2013.

[27] M. A. Mohamed *et al.*, "Regenerated cellulose membrane as bio-template for in-situ growth of visible-light driven C-modified mesoporous titania," *Carbohydrate Polymers,* vol. 146, pp. 166-173, 2016/08/01/ 2016.

[28] L. Lin, H. Wang, W. Jiang, A. R. Mkaouar, and P. Xu, "Comparison study on photocatalytic oxidation of pharmaceuticals by TiO2-Fe and TiO2-reduced graphene oxide nanocomposites immobilized on optical fibers," *Journal of Hazardous Materials,* vol. 333, pp. 162-168, 2017/07/05/ 2017.

[29] Y. Shi, J. Huang, G. Zeng, W. Cheng, and J. Hu, "Photocatalytic membrane in water purification: is it stepping closer to be driven by visible light?," *Journal of Membrane Science,* vol. 584, pp. 364-392, 2019/08/15/ 2019.

[30] A. K. Nair and P. E. JagadeeshBabu, "Ag-TiO2 nanosheet embedded photocatalytic membrane for solar water treatment," *Journal of Environmental Chemical Engineering,* vol. 5, no. 4, pp. 4128-4133, 2017/08/01/ 2017.

[31] M. Cantarella, R. Sanz, M. A. Buccheri, L. Romano, and V. Privitera, "PMMA/TiO2 nanotubes composites for photocatalytic removal of organic compounds and bacteria from water," *Materials Science in Semiconductor Processing,* vol. 42, pp. 58-61, 2016/02/01/ 2016.

[32] M. Cantarella *et al.*, "Immobilization of nanomaterials in PMMA composites for photocatalytic removal of dyes, phenols and bacteria from water," *Journal of Photochemistry and Photobiology A: Chemistry,* vol. 321, pp. 1-11, 2016/05/01/ 2016.

[33] N. K. O. Cruz, G. U. Semblante, D. B. Senoro, S.-J. You, and S.-C. Lu, "Dye degradation and antifouling properties of polyvinylidene fluoride/titanium oxide membrane prepared by sol–gel method," *Journal of the Taiwan Institute of Chemical Engineers,* vol. 45, no. 1, pp. 192-201, 2014/01/01/ 2014.

[34] Y. Qian *et al.*, "Fabrication of TiO2-modified polytetrafluoroethylene ultrafiltration membranes via plasma-enhanced surface graft pretreatment," *Applied Surface Science,* vol. 360, pp. 749-757, 2016/01/01/ 2016.

[35] Z. A. M. Hir, P. Moradihamedani, A. H. Abdullah, and M. A. Mohamed, "Immobilization of TiO2 into polyethersulfone matrix as hybrid film photocatalyst for effective degradation of methyl orange dye," *Materials Science in Semiconductor Processing,* vol. 57, pp. 157-165, 2017/01/01/ 2017.

[36] Y. Gao, M. Hu, and B. Mi, "Membrane surface modification with TiO2–graphene oxide for enhanced photocatalytic performance," *Journal of Membrane Science,* vol. 455, pp. 349-356, 2014/04/01/ 2014.

[37] Z. Xu *et al.*, "Photocatalytic antifouling PVDF ultrafiltration membranes based on synergy of graphene oxide and TiO2 for water treatment," *Journal of Membrane Science,* vol. 520, pp. 281-293, 2016/12/15/ 2016.

[38] S. Ramasundaram *et al.*, "Photocatalytic applications of paper-like poly(vinylidene fluoride)–titanium dioxide hybrids fabricated using a combination of electrospinning and electrospraying," *Journal of Hazardous Materials,* vol. 285, pp. 267-276, 2015/03/21/ 2015.

[39] H. Dzinun, M. H. D. Othman, A. F. Ismail, M. H. Puteh, M. A. Rahman, and J. Jaafar, "Photocatalytic degradation of nonylphenol using co-extruded dual-layer hollow fibre membranes incorporated with a different ratio of TiO2/PVDF," *Reactive and Functional Polymers,* vol. 99, pp. 80-87, 2016/02/01/ 2016.

[40] A. T. Kuvarega, N. Khumalo, D. Dlamini, and B. B. Mamba, "Polysulfone/N,Pd co-doped TiO2 composite membranes for photocatalytic dye degradation," *Separation and Purification Technology,* vol. 191, pp. 122-133, 2018/01/31/ 2018.

[41] M. Coto, S. C. Troughton, J. Duan, R. V. Kumar, and T. W. Clyne, "Development and assessment of photo-catalytic membranes for water purification using solar radiation," *Applied Surface Science,* vol. 433, pp. 101-107, 2018/03/01/ 2018.

[42] R. M. Huertas, M. C. Fraga, J. G. Crespo, and V. J. Pereira, "Sol-gel membrane modification for enhanced photocatalytic activity," *Separation and Purification Technology,* vol. 180, pp. 69-81, 2017/06/08/ 2017.

[43] C. Wang *et al.*, "Bioinspired Synthesis of Photocatalytic Nanocomposite Membranes Based on Synergy of Au-TiO2 and Polydopamine for Degradation of Tetracycline under Visible Light," *ACS Applied Materials & Interfaces,* vol. 9, no. 28, pp. 23687-23697, 2017/07/19 2017.

[44] P. M. Martins, R. Miranda, J. Marques, C. J. Tavares, G. Botelho, and S. Lanceros-Mendez, "Comparative efficiency of TiO2 nanoparticles in suspension vs. immobilization into P(VDF–TrFE) porous membranes," *RSC Advances,* 10.1039/C5RA25385C vol. 6, no. 15, pp. 12708-12716, 2016.

[45] Y. Zhao, C. Tao, G. Xiao, and H. Su, "Controlled synthesis and wastewater treatment of Ag2O/TiO2 modified chitosan-based photocatalytic film," *RSC Advances,* 10.1039/C6RA27295A vol. 7, no. 18, pp. 11211-11221, 2017.

[46] S. Sanches, C. Nunes, P. C. Passarinho, F. C. Ferreira, V. J. Pereira, and J. G. Crespo, "Development of photocatalytic titanium dioxide membranes for degradation of recalcitrant compounds," *Journal of Chemical Technology & Biotechnology,* vol. 92, no. 7, pp. 1727-1737, 2017.

[47] Y. Chang *et al.*, "Effect of post-heat treatment on the photocatalytic activity of titanium dioxide nanowire membranes deposited on a Ti substrate," *RSC Advances,* 10.1039/C7RA02092A vol. 7, no. 35, pp. 21422-21429, 2017.

[48] H. Dzinun, M. H. D. Othman, A. F. Ismail, M. H. Puteh, M. A. Rahman, and J. Jaafar, "Performance evaluation of co-extruded microporous dual-layer hollow fiber membranes using a hybrid membrane photoreactor," *Desalination,* vol. 403, pp. 46-52, 2017/02/01/ 2017.

[49] N. Li *et al.*, "Precisely-controlled modification of PVDF membranes with 3D TiO2/ZnO nanolayer: enhanced anti-fouling performance by changing hydrophilicity and photocatalysis

under visible light irradiation," *Journal of Membrane Science,* vol. 528, pp. 359-368, 2017/04/15/ 2017.

[50] S. Teixeira, P. M. Martins, S. Lanceros-Méndez, K. Kühn, and G. Cuniberti, "Reusability of photocatalytic TiO2 and ZnO nanoparticles immobilized in poly(vinylidene difluoride)-co-trifluoroethylene," *Applied Surface Science,* vol. 384, pp. 497-504, 2016/10/30/ 2016.

[51] J. Sabate, M. A. Anderson, H. Kikkawa, M. Edwards, and C. G. Hill, "A kinetic study of the photocatalytic degradation of 3-chlorosalicylic acid over TiO2 membranes supported on glass," *Journal of Catalysis,* vol. 127, no. 1, pp. 167-177, 1991/01/01 1991.

[52] H. Choi, A. C. Sofranko, and D. D. Dionysiou, "Nanocrystalline TiO2 Photocatalytic Membranes with a Hierarchical Mesoporous Multilayer Structure: Synthesis, Characterization, and Multifunction," *Advanced Functional Materials,* vol. 16, no. 8, pp. 1067-1074, 2006.

CHAPTER 3: PROOF OF CONCEPT FOR LIGHT CONDUCTING MEMBRANE SUBSTRATE FOR UV-ACTIVATED PHOTOCATALYSIS AS AN ALTERNATIVE TO CHEMICAL CLEANING

3.1. Chapter Overview

Chapter 3 presents the proof of the proposed novel concept of light conducting photocatalytic membranes. Preparation of the membrane, validation of its photocatalytic properties, its light conducting properties and chemical composition are given in this chapter. The chapter also looks at the anti-fouling properties of the membrane when it is exposed to UV radiation outside the module. This chapter was published as a research article titled “Proof of Concept for Light Conducting Membrane Substrate for UV-Activated Photocatalysis as an Alternative to Chemical Cleaning’’, by Lavern T. Nyamutswa, Bo Zhu, Dimuth Navaratna, Stephen F. Collins and Mikel C. Duke in the peer reviewed journal “Membranes” (2018), 8 (4) 122. https://doi.org/10.3390/membranes8040122. It is presented here in the final published format.

3.2. Declaration of Co-Authorship and Co-Contribution of the Chapter

VICTORIA UNIVERSITY

THE NEW WAY TO DO UNI

OFFICE FOR RESEARCH TRAINING, QUALITY AND INTEGRITY

DECLARATION OF CO-AUTHORSHIP AND CO-CONTRIBUTION: PAPERS INCORPORATED IN THESIS

This declaration is to be completed for each conjointly authored publication and placed at the beginning of the thesis chapter in which the publication appears.

1. PUBLICATION DETAILS (to be completed by the candidate)

Title of Paper/Journal/Book: **Proof of Concept for Light Conducting Membrane Substrate for UV-Activated Photocatalysis as an Alternative to Chemical Cleaning**

Surname: **Nyamutswa** First name: **Lavern**

Institute: **Institute for Sustainable Industries and Liveab** Candidate's Contribution (%): **75**

Status:

Accepted and in press: ☑ Date: **26/11/2018**

Published: ☑ Date: **2/12/2018**

2. CANDIDATE DECLARATION

I declare that the publication above meets the requirements to be included in the thesis as outlined in the HDR Policy and related Procedures – policy.vu.edu.au.

[redacted]	30/07/2020
Signature	**Date**

3. CO-AUTHOR(S) DECLARATION

In the case of the above publication, the following authors contributed to the work as follows:

The undersigned certify that:

1. They meet criteria for authorship in that they have participated in the conception, execution or interpretation of at least that part of the publication in their field of expertise;
2. They take public responsibility for their part of the publication, except for the responsible author who accepts overall responsibility for the publication;

PO Box 14428, Melbourne,
Vic 8001, Australia
+61 3 9919 6100

Victoria University ABN 83776954731
CRICOS Provider No. 00124K (Melbourne),
02475D (Sydney), RTO 3113

3. There are no other authors of the publication according to these criteria;

4. Potential conflicts of interest have been disclosed to a) granting bodies, b) the editor or publisher of journals or other publications, and c) the head of the responsible academic unit; and

5. The original data will be held for at least five years from the date indicated below and is stored at the following **location(s)**:

Institute for Sustainable Industries and Liveable Cities, Victoria University, Werribee Campus, Melbourne, Australia

Name(s) of Co-Author(s)	Contribution (%)	Nature of Contribution	Signature	Date
Lavern T. Nyamutswa	75	Concept development and manuscript writing	[redacted]	30/07/2020
Bo Zhu	5	Manuscript review and editing	[redacted]	28/7/2020
Dimuth Navaratna	5	Concept development, manuscript review and editing	[redacted]	29/07/2020
Stephen F. Collins	5	Concept development, manuscript review and editing	[redacted]	29 Jul '20
Mikel C. Duke	10	Concept development, manuscript review and editing	[redacted]	27/7/2020

Updated: September 2019

PO Box 14428, Melbourne,
Vic 8001, Australia
+61 3 9919 6100

Victoria University ABN 83776954731
CRICOS Provider No. 00124K (Melbourne),
02475D (Sydney), RTO 3113

3.3. Research Article

Article

Proof of Concept for Light Conducting Membrane Substrate for UV-Activated Photocatalysis as an Alternative to Chemical Cleaning

Lavern T. Nyamutswa [1,*], Bo Zhu [1], Dimuth Navaratna [1,2], Stephen Collins [2] and Mikel C. Duke [1]

[1]Institute for Sustainable Industries and Liveable Cities, Victoria University, P.O. Box 14428, Melbourne, 8001 Australia; bo.zhu@vu.edu.au (B.Z.); dimuth.navaratna@vu.edu.au (D.N.); mikel.duke@vu.edu.au (M.C.D.)

[2]College of Engineering and Science, Victoria University, P.O. Box 14428, Melbourne, 8001, Australia; stephen.collins@vu.edu.au

*****Correspondence: lavern.nyamutswa@live.vu.edu.au; Tel.: +61-3-9919-8111

Received: 31 October 2018; Accepted: 26 November 2018; Published: date

Abstract: Adopting an effective strategy to control fouling is a necessary requirement for all membrane processes used in the water/wastewater treatment industry to operate sustainably. The use of ultraviolet (UV) activated photocatalysis has been shown to be effective in mitigating ceramic membrane fouling by natural organic matter. The widely used configuration in which light is directed through the polluted water to the membrane's active layer suffers from inefficiencies brought about by light absorption by the pollutants and light shielding by the cake layer. To address these limitations, directing light through the substrate, instead of through polluted water, was studied. A UV conducting membrane was prepared by dip coating TiO_2 onto a sintered glass substrate. The substrate could successfully conduct UV from a lamp source, unlike a typical alumina substrate. The prepared membrane was applied in the filtration of a humic acid solution as a model compound to study natural organic matter membrane fouling. Directing UV through the substrate showed only a 1 percentage point decline in the effectiveness of the cleaning method over two cleaning events from 72% to 71%, while directing UV over the photocatalytic layer had a 9 percentage point decline from 84% to 75%. Adapting the UV-through-substrate configuration could

be more useful in maintaining membrane functionality during humic acid filtration than the current method being used.

Keywords: Titanium dioxide; photocatalytic membrane; water treatment; membrane fouling

1. Introduction

Water scarcity affects about two-thirds of the world's population for at least a month of every year [1]. Existing water resources of suitable quality are already over-subscribed or rapidly approaching their limits in most parts of the world. To address this gap, conveniently available poorer quality waters may be used, but they first have to be treated to meet quality standards. However, current treatments are beset with several issues, among them high costs, non-effectiveness in removing recalcitrant pollutants such as azo dyes and nitroaromatic compounds [2], and the generation of toxic secondary by-products. Improving accessibility and operational simplicity of treatment technologies would support initiatives to improve wider access to clean water.

Treatment of municipal and industrial wastewater is also becoming an important source of water for industrial and agricultural use [3]. To meet increasingly stringent water quality regulations, natural organic matter, soluble microbial products and micro-pollutants should also be removed from wastewater. Processes that have been used in tertiary water treatment processes include advanced oxidation, activated carbon adsorption, ion exchange and membrane filtration. Membrane filtration, in particular, is gaining increased use because of its lower energy footprint, compact design, lower chemical consumption and the ease with which it can be maintained and automated [3].

Membrane processes, however, have several issues which limit their use on a wider scale. One such issue is fouling, which reduces membrane separation efficiency, membrane lifespan and can raise energy costs. Maintaining performance and improving the simplicity of operation of membrane systems is necessary to make the technology more widely available to communities worldwide.

The approaches that have been used to reduce membrane fouling include pre-treating the feed, modification of membrane properties, optimisation of operating conditions,

as well as optimization of module arrangement and configuration [4]. Although these reduce fouling to some extent, membrane cleaning is always employed in practice. Cleaning can be achieved hydraulically, mechanically, electrically or chemically, with the former being the most common, followed by the latter. More than one of these cleaning methods can also be applied in combination. However, these result in significant downtime and costs associated with loss of productivity, labour, energy as well as procurement, transportation, storage, and disposal of chemicals [4].

In-situ self-cleaning methods are therefore necessary to solve the fouling problem without stopping the water filtration process. One such method is coupling membrane filtration with photocatalysis. The photocatalytic properties of semiconductor photocatalysts such as TiO_2 lead to the photo-induced partial or total decomposition of pollutants present on the surface of the membrane while photo-induced ultra-hydrophilicity leads to elimination of the remaining hydrophobic contaminants through a simple water rinsing operation. Photocatalysis and induced hydrophilicity can occur on the same surface simultaneously to give a “self-cleaning” membrane which leads to savings on cleaning procedures [5,6].

Several configurations have been used to combine filtration with photocatalysis to give an integrated hybrid water treatment process, known as a photocatalytic membrane reactor (PMR). The configurations include a slurry photocatalytic reactor with a membrane submerged in it, a slurry reactor that precedes a membrane filtration unit and a porous photocatalytic membrane in which the photocatalyst is coated onto the membrane substrate [7]. Of these three configurations, the latter is the most interesting for future water treatment because it combines both filtration and photocatalysis in one unit.

A novel configuration in which the feed solution was fed from the uncoated side of the membrane was studied, mainly to independently control the separation and photocatalytic functions of the membrane [6]. Separating the separation and photocatalysis functionalities increases process robustness because failure of one does not necessarily result in the failure of the other [8]. Another advantage cited for this configuration is retention of particulates capable of shielding UV light on the feed side of the membrane, thus making photocatalysis more efficient because the permeated side has more optical transparency than the feed side. This was envisaged

to make UV disinfection of highly turbid waters more efficient in terms of UV dosage, though it could come at the expense of increased membrane fouling.

To date, researchers have focused on making photocatalytic membranes for water treatment by coating nano-sized photocatalysts on opaque materials such as ceramics, organic membranes and metals. These membranes lack light transparency, requiring light to be directed through the water being treated to reach the photocatalyst coating on the substrate surface. Directing light this way in complex membrane element designs, such as ceramic monoliths, results in light attenuation before it reaches the photocatalyst coated inside the channels. Organic pollutants present in water can also strongly absorb light which was meant to reach the photocatalyst coating, reducing photocatalytic efficiency [9]. In this study, the potential of replacing these materials with optically transparent sintered glass was investigated. UV light (including solar) can then be conveniently directed through the light-transmitting sintered glass substrate to reach the photocatalyst coated on its surface. The use of sintered glass in this way was not found in the literature. If loss of light through absorption or reflection by the membrane substrate or organic pollutants present in the water being treated are minimised, it can translate to more efficient use of energy and reduced costs, and long term mitigation of fouling with minimal chemical and physical membrane cleaning. The concept is depicted in Figure 1.

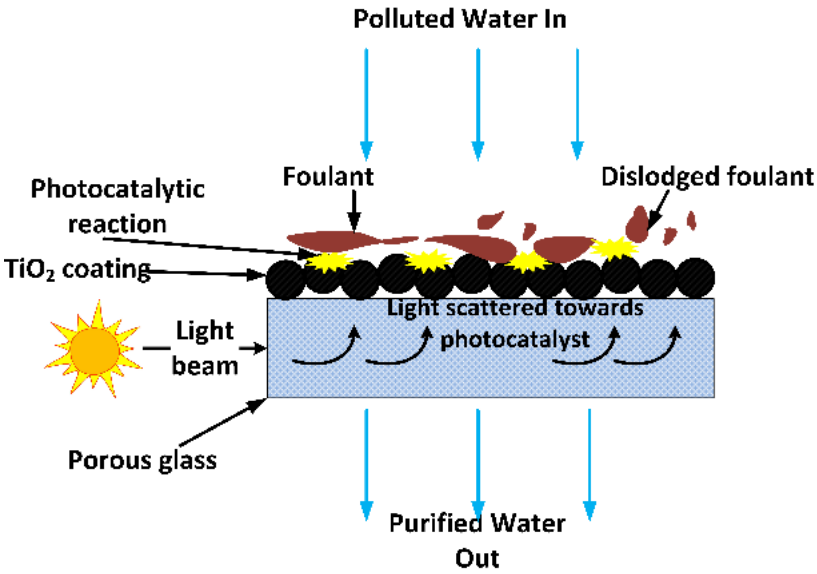

Figure 1. The concept of a light-conducting membrane substrate for practical implementation of a photocatalytic reaction for improved membrane performance.

The key aim of this research study was to verify the concept by coating porous glass membranes with a photocatalyst and observing ex-situ if the photocatalytic reaction can be engaged by directing light through the substrate in comparison to applying the light directly to the photocatalytic layer. The model synthetic dye, screened methyl orange (sMO), was used to observe a practical photocatalytic reaction utilising the well-known commercial catalyst, Aeroxide P25 TiO_2. The model membrane foulant and pollutant, humic acid (HA) was used as a filtration feed solution to study the effect of applying this concept in mitigating membrane fouling.

2. Materials and Methods

2.1. Materials

Humic acid was purchased from Fluka AG Cheische Fabrik., Buchs, Switzerland and used as a representative natural organic matter compound. Titanium dioxide P25 with 99.8% purity and composed of 80% anatase and 20% rutile phases was acquired from Evonik. The TiO_2 had an average particle size of 30 nm and a specific surface area of 50 m^2/g). Bovine Serum Albumin (BSA) of molecular weight 66 kDA was purchased from Sigma Aldrich (St. Louis, MO, USA). Screened methyl orange used as a model dye was purchased from Ajax Chemicals, Australia. Methanol was acquired from Chem-Supply, Australia. Nitric acid was purchased from Merck Pty Limited, Kilsyth, Australia. Acetone (99.9%) was purchased from Sigma-Aldrich, Australia. Sintered glass used as the membrane substrate was acquired from Ningbo Ja-Hely Technology Co., Ltd., Ningbo, China. This was in the form of flat circular discs of 25 mm diameter, 2 mm thickness and G5 porosity grade.

2.2. Apparatus

A panel consisting of 6 × 18 W UVA lamps (A.U.V.S (Ops), Pty. Ltd., Australia) with an emission peak at 365 nm was used to illuminate the membrane outside the module. The UV intensity at 365 nm was measured by a UV irradiance meter from Photoelectric Instrument Factory of Beijing Normal University, Beijing, China. A TPI 665L digital manometer from Accutherm, Melbourne, Australia was used to measure transmembrane pressure (TMP) changes. The membrane was placed in a custom made filtration module made from stainless steel, giving an effective membrane area of 2.5 cm^2. A programmable Vulcan 3-550PD NEY furnace, (Extech Equipment, Victoria, Australia) was used for heat treating the membrane after coating with TiO_2.

A peristaltic pump (Masterflex 7592-45, Cole-Parmer, Vernon Hills, IL, USA) was used to drive the feed through the membrane in dead-end mode. The amount of permeate collected was measured by an electronic balance (FX-3000i WP, A&D Company Ltd., South Korea) with real time monitoring software. A sonic bath (Soniclean 500HT, Transtek Systems, Melbourne, Australia) was used to ultrasonically clean the membranes before coating, as well as to remove air bubbles in the coating suspension.

2.3. Preparation of Membranes

The sintered glass discs were first cleaned by washing in acetone, ethanol then water in a sonic bath to remove loose particles and possible contaminants. Each sonic wash was 20 min long. The last wash was followed by deionised water (DI water) rinsing and drying in a fan-forced oven at 80 °C for 3 h. The washed discs were weighed, labelled and stored in an air tight container until use.

To ensure coating on only one side of the membrane, one side was covered with masking tape. The coating suspension was prepared by adding 2 g of Evonik P25 TiO_2 to 60 mL of 70/30% (*v*/*v*) water/methanol water acidified to pH 3 with nitric acid. The suspension was sonicated for 20 min followed by magnetic stirring for 2 h before the commencement of coating.

The disc was then dipped into the suspension using a custom made mechanical device and withdrawn at a dipping/withdrawal speed of 2 cm/min. The process was repeated three times. The coated membranes were then air dried over 12 h and the tape carefully removed, followed by heat treatment to 450 °C at a heating rate of 1 °C/min in a programmable muffle furnace. The temperature was held at 450 °C for 2 h, and then cooled to room temperature at 1 °C/min. The membranes were then washed with DI water and oven dried at 80 °C for 5 h. The membranes were weighed before and after coating to determine the amount of TiO_2 that was immobilised on the surface.

2.4. Membrane Characterisation and Chemical Analysis

Fourier transform infrared spectroscopy (FTIR) analysis was used to explore surface functional groups and was performed with a Perkin Elmer Frontier FTIR Spectrometer equipped with an attenuated total reflectance (ATR) accessory. The crystal structure

of the photocatalyst after coating was confirmed by powder X-ray diffraction (XRD) using a Rigaku Mini Flex 600 diffractometer operating with CuKα (λ = 1.54060 Å) radiation at 15 mA and 40 kV with a Ni filter. The analysis range was 20°–80° 2θ with 0.02° step and 1.2 s acquisition for steps. The step time was chosen to adequately obtain a good signal to noise ratio in the mean reflections of (1 0 1) and (1 1 0) planes, which are the two main anatase and rutile planes of TiO_2 [10]. The substrate was ground by mortar and pestle before XRD analysis. The pore size of the substrate was determined by capillary flow porometry using a Quantachrome Porometer 3 GZ series. The method involves measuring nitrogen gas flow as a function of TMP through the dry and wetted membrane. The pore size is then calculated using the Washburn equation. The wetting liquid was Porofil from Quantachrome Corp, Florida, USA. The absorbance of the sMO solution at 642 nm was measured by a UV-Visible-Biochrom Libra 522 UV-visible spectrophotometer. Total organic carbon (TOC) of BSA was determined by a Shimadzu TOC-V CSH analyzer.

2.5. Degradation of Screened Methyl Orange

The developed membranes were tested for photocatalytic activity under several configurations in UV light. The naked UV lamp had an intensity of 2.5 mW/cm^2 at 365 nm and a distance of 10 cm as measured by the UV irradiance meter. The membranes were placed in a beaker with 100 mL 0.01 mM solutions of sMO and the discoloration of the dye monitored by UV-Visible light absorption measurements at 642 nm of 1 mL samples withdrawn by a micropipette at 30 min intervals. The membrane was placed such that only a thin layer of liquid was above the membrane. The first hour of each experiment was carried out in the dark to allow adsorption of the dye onto the membrane. The degradation experiments carried out are summarised in Table 1.

Table 1. Description of the screened methyl orange (sMO) degradation experiments.

Designation	Description	Purpose
A1	Coated membrane. Coated side facing UV source.	To determine effect of shining UV directly onto active layer.
A2	Coated membrane. Coated side facing away from UV source.	To determine the effect of transmitting light through the substrate.
A3	Coated membrane. Coated side facing away from UV source. Top part of membrane covered with aluminium foil.	To determine whether the apparent photocatalytic activated is due to light reflected from the base of the beaker, rather than light passing through the filter.
A4	Coated membrane. Coated side facing away from UV source. Every area of the beaker blocked except the top part of the membrane.	To focus the light source onto the filter, to determine whether it can transmit light that is sufficient enough to trigger photocatalytic reactions.
A5	Uncoated filter, in the presence of UV light.	To eliminate photocatalytic effect.
A6	Filter coated with P25, without UV light.	To determine adsorption property of coated membrane.
A7	Uncoated filter, without UV light.	To determine adsorption property of uncoated membrane.
A8	UV light only.	To determine the extent of photolysis.

The pseudo first order rate constant of the dye degradation was calculated using the Langmuir-Hinshelwood equation:

$$\ln\left(\frac{C}{C_0}\right) = -kt \quad (1)$$

where C_0 is the initial concentration of dye, C is the concentration in mmol/L at time t (min), and k (min^{-1})is the rate constant [11].

2.6. Filtration of Humic Acid and BSA Rejection Tests

A 20 mg/L HA solution prepared by the appropriate dilution of a previously prepared stock solution was used as the feed. Generally, the concentration range of humic substances in surface and ground water is 20 µg/L–30 mg/L [12]; therefore, 20 mg/L was specifically chosen to fall within the upper region of this range to represent a more challenging wastewater where there is a stronger need for membrane cleaning. To prepare the stock solution, 6 g of HA was mixed in 2 L of deionized water over 2 days by aid of a magnetic stirrer. Suspended solids were removed by vacuum filtration through a 0.45 µm membrane filter (ADVANTEC, Tokyo, Japan). The filtration setup is depicted in Figure 2, and it consisted of a feed tank, a peristaltic pump, membrane module, needle to close the retentate line such that the filtration mode was dead-end, pressure transducer to measure the change in transmembrane pressure (TMP), and a permeate collection tank placed on a balance connected to a data logger. The experiments were carried out at a constant flux of 450 L m^{-2} h^{-1}. The membrane was first compacted with simulated tap water (100 mg/L NaCl solution) for 30 min, followed by filtration of the 20 mg/L HA solution for 30 min. Simulated tap water was used instead of real tap water so that the actual composition of the water was known, controllable and replicable. The membrane was then removed from the module and cleaned by either UV exposure under the lamp for 30 min, chemical cleaning using a 1% NaOH solution and 0.5% NaOCl, or simple rinsing in distilled water. After the cleaning process, the membranes were reloaded onto the module and the membrane recovery determined by measuring the new TMPs while continuing HA filtration for 30 min, cleaning and another HA filtration cycle. The cleaning methods used are summarised in Table 2.

Table 2. Description of the cleaning methods used to regenerate the membrane after fouling.

Designation	Description of Cleaning Method
B1	No cleaning employed
B2	UV exposure over the active layer
B3	UV exposure through the substrate
B4	Rinsing in DI water
B5	Rinsing in NaOH and NaOCl solutions

The apparent fouling rate, *r*, in kPa/min between two adjacent cleaning events was calculated as:

$$r = \frac{P_{max} - P_{min}}{\Delta t} \tag{2}$$

where P_{max} is the TMP value immediately after the second cleaning event, P_{min} is the TMP value immediately after the first cleaning event, and Δt is the time between these two recorded TMP values.

The efficiency of each cleaning event was calculated as:

$$E = \frac{P_{before} - P_{after}}{P_{before} - P_0} \times 100\% \tag{3}$$

where P_{before} and P_{after} are the TMP values immediately before and after the cleaning event, and P_0 is the pressure required to overcome the intrinsic membrane resistance [13].

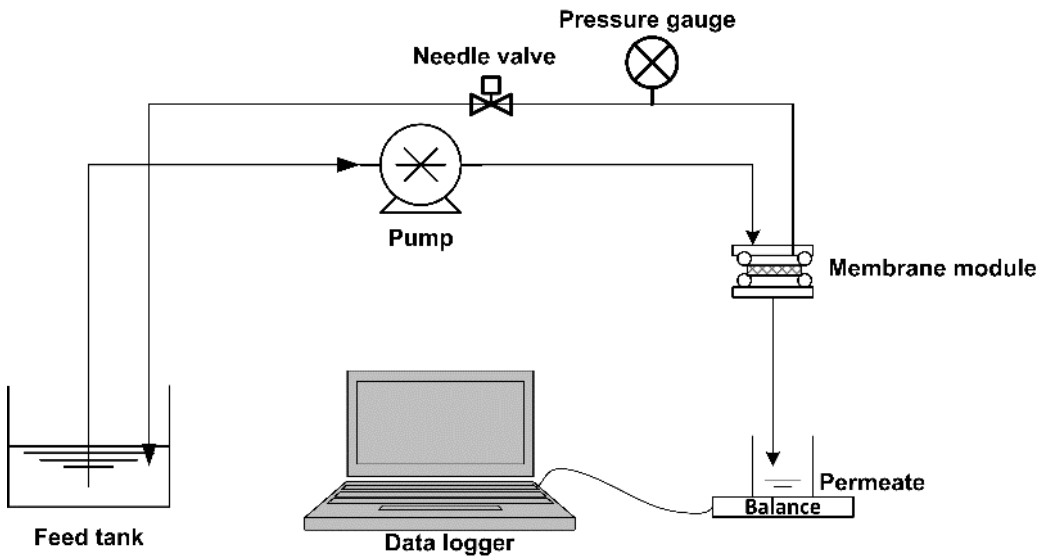

Figure 2. Schematic representation of the filtration setup.

To determine the selectivity of the substrate and prepared membrane, a 50 mg/L BSA solution was prepared by appropriate dilution of a 1 mg/mL BSA stock solution containing 1 mM $CaCl_2$ and 7 mM NaCl in DI water. The BSA solution was then filtered through the uncoated substrate as well as the prepared membrane. The change in TOC was measured and the rejection, *R*, is calculated by

$$R = (1 - \frac{C_p}{C_f}) \text{ x } 100\% \quad (4)$$

where C_p and C_f are the TOC concentrations in the permeate and feed, respectively.

3. Results and Discussion

3.1. Membrane Characterisation

The average pore size of the substrate as measured by porometry was 1.4 µm. After coating with TiO_2, the normalized weight of the coating was measured on the membranes to be 4 ± 0.2 mg/cm^2. The results of the XRD analysis of the photocatalyst and substrate are shown in Figure 3.

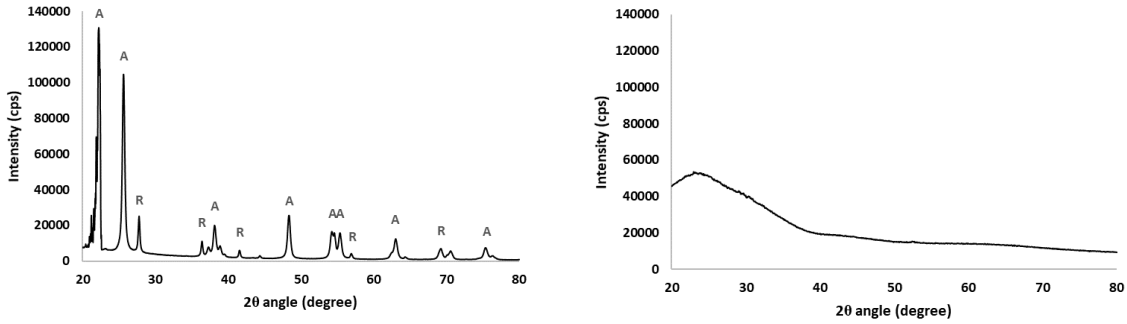

(**a**) (**b**)

Figure 3. The X-ray diffraction (XRD) patterns of the (**a**) TiO_2 photocatalyst; (**b**) the substrate with markers to indicate the Bragg peaks associated with the anatase (A) and rutile (R) phases.

The diffraction pattern of the TiO_2 immobilized on the membranes shows that the anatase phase is predominant, while the rutile phase is also present [14]. Typical anatase peaks include 25.7° (1 0 1), 38.1° (0 0 4), 48.5° (2 0 0), 54.3° (1 0 5), 55.3° (2 1 1) and 63.0° (1 1 8) [15,16], while rutile peaks appeared at 27.8° (1 1 0) [17], 36.4° (1 0 1), 41.6° (1 1 1), 57.1° (2 2 0) and 69.3 (3 0 1) [14]. The substrate is amorphous, therefore no distinct crystalline phases were detected.

Figure 4 shows the Fourier Transform Infrared (FT-IR) spectrum of the sintered glass substrate and the P25 photocatalyst

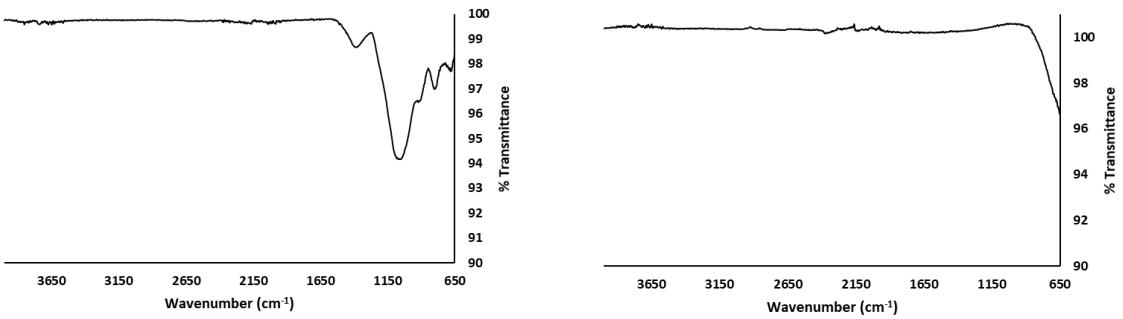

(**a**) (**b**)

Figure 4. FT-IR spectrum of the: (**a**) sintered glass substrate and; (**b**) P25 powder.

Borosilicate glass is a composite of the three network forming units whose proportions depend on each particular type of glass. The units are trigonally coordinated boron (BO_3), tetrahedrally coordinated boron (BO_4), and tetrahedral SiO_4 structural units. It can also consist of network modifiers such as alkali and or alkaline earth metal oxides. The peak appearing at 680 cm^{-1} is assigned to the bending vibrations of Si–O–B bridges. The peak at 920 cm^{-1} is due to the stretching vibrations of B–O bonds in tetrahedral BO_4 units. The band between 1000–1120 cm^{-1} is thought to arise from overlapping contributions of silicate and borate groups containing BO_3 and BO_4 units. The absorption band which peaks at 1379 cm^{-1} is attributed to the B–O stretching vibrations of polymerized BO_3 units. Broad bands which normally appear from 2200 cm^{-1} and extend beyond due to OH, water and hydroxyl groups, were not observed, mainly due to the heating process which drives out water. The barely noticeable peaks in this region are attributed to the stretching vibrations of O–H bonds which are formed at non-bridging oxygen sites [18,19]. FT-IR thus confirmed that the substrate consists of the borosilicate glass functional units. For the P25 samples, no significant peaks were observed.

3.2. UV Intensity

The intensity of the UV radiation at 365 nm passing through the membrane substrate was measured at 0.45 mW/cm^2 at a distance of 10 cm from the light source. In contrast, 0.00 mW/cm^2 was detected from a similar substrate with the same dimensions made from α-Al_2O_3. The sintered glass substrate is therefore better at conducting light than typical alumina substrates commonly used to make ceramic membranes.

3.3. Degradation of Screened Methyl orange

Figure 5 shows relative changes of dye concentration with time for the various batch experiment setups. When light was directed onto the coated surface, about 58% of the dye had been degraded after 5 h (A1). This configuration can work well in cases of low turbidity waters, or low concentration dyes where there is minimal absorption of radiation by organic molecules or scattering and attenuation of radiation by minute particles present in the water. It is also of interest to note that the depth of the liquid above the coated layer was just 2 mm, therefore, no significant absorption of radiation by organic molecules would be expected. To address these limitations, UV directed through the substrate was investigated. After 5 h, the dye degradation percentage was 52% (A2). Although lower than when the UV was directed to the active layer, this configuration can be useful in turbid waters or high concentration organic solutions as mentioned before. The kinetics of screened methyl orange degradation thus showed that UV light could be successfully directed through the substrate to initiate photocatalytic reactions on the coated surface.

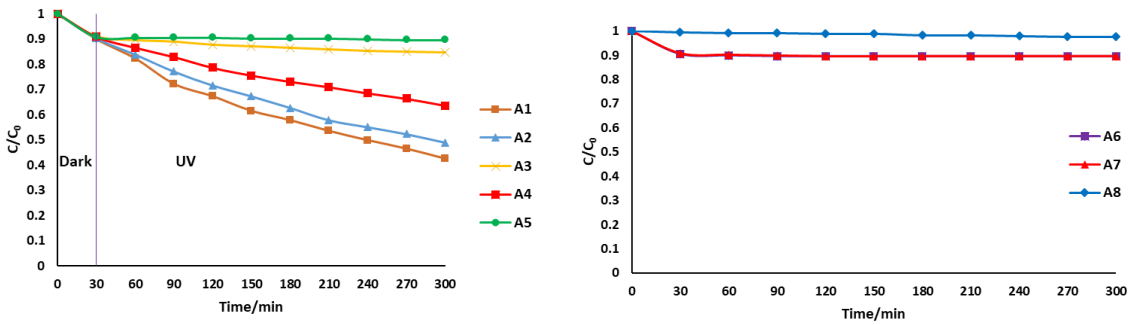

(**a**) (**b**)

Figure 5. Dye concentration over time (**a**) in the presence of UV; over the active layer (A1), through the substrate (A2), reflected (A3), through the substrate but reflection eliminated (A4), uncoated membrane (A5). (**b**) Adsorption by coated membrane (A6), adsorption by uncoated membrane (A7) and photolysis (A8).

Table 3 shows the pseudo first order reaction rates of dye degradation through directing UV over the active layer (A1) and through the substrate (A2). The dye degradation in the other setups does not fit pseudo first order kinetics.

Table 3. Pseudo first order kinetics of the sMO degradation.

Configuration	UV Application Method	k (min^{-1})	R^2
A1	Over active layer	0.0030	0.9869
A2	Through substrate	0.0025	0.9871

With regards to A2, there is the possibility that the apparent dye degradation was simply due to light reflected by the base of the reaction vessel. To remove any doubt, A3 was setup to determine the effect of reflected light on dye degradation, and about 11% degradation in 5 h was observed. This was almost equal to the apparent loss in dye concentration by adsorption to the membrane only (A6), showing that reflection is not a factor in the experiments. The apparent decrease in the degradation in A4 was due to the fact that the entire radiation from the lamp could not be directed onto the top of the membrane substrate where a collimated UV source would be more successful. Both the uncoated (A6) and coated membranes (A7) had the same dye adsorption capacity, which shows that the TiO_2 layer's main role was more to facilitate photocatalytic degradation than adsorption. An uncoated membrane in the presence of UV (A5) resulted in about 11% dye degradation, which shows that the photocatalytic layer plays an important role in the dye degradation. The amount of dye degraded by photolysis was less than 2.5% (A8). The largest contributor to dye degradation was therefore photocatalysis, followed by adsorption.

The rate constant obtained when directing light through the substrate is comparable to other results in the literature in Table 4. In all literature cases, UV was directed over the active layer. The configuration used in this study can therefore give dye degradation rates which are comparable to those in the conventional configuration, while also utilizing the advantages mentioned earlier.

Table 4. Comparison of first order kinetics of directing UV to literature values.

Membrane	Target Compound	k (min^{-1})	R^2	UV Intensity (mW/cm^2)	Reference
TiO_2/PMMA	~0.01 mM MB	0.003	-	1.1	[20]
TiO_2/PES	~0.03 mM MO	0.004	0.998	-	[17]

TiO_2/GO-Psf	~0.2 mM MB	0.004	-	-	[21]
TiO_2/Fibreglass	~0.02 mM MB	0.004	-	-	[11]
TiO_2/SiO_2	~0.01 mM MB	0.006	0.99	5	[22]
TiO_2/Sintered glass	0.01 mM sMO	0.003	0.987	0.45	This work

3.4. Membrane Selectivity and Regeneration after HA Fouling

The BSA rejection of the substrate (measured by TOC) was found to be 11%, while that of the TiO_2 coated membrane was 25%. Although BSA rejection increased slightly after coating the substrate, it is still low, indicating the membrane filtering in the microfiltration range.

Figure 6 shows the relative pressure change over the course of filtration of HA and simulated tap water. At the initial stage of simulated tap water filtration, there are no significant pressure changes due to the absence of foulants. The observed TMP is necessary to overcome the intrinsic membrane resistance. The value of P_0 was 13 ± 2 kPa for the membranes. As soon as the feed is changed to a HA at 30 min, the TMP starts to rise due to fouling on the membrane surface. When there is no cleaning of the membrane that is carried out (B1), there is only a small pressure relief when the system is opened at 60 and 90 min. However, as soon as the filtration is restarted, the TMP quickly rises to values that are higher than before the system opening event. By the end of the 120 min filtration period, the TMP in B1 rises by more than 700% since the start of the filtration process. In contrast, cleaning the membrane by exposing the active layer to UV (B2) resulted in significant restoration of the membrane such that the final TMP is about 500% of the initial. This is also the case with UV exposure through the substrate (B3) and chemical cleaning (B5). Rinsing the membrane in DI water (B4) was the least effective in membrane regeneration. It is suggested that HA molecules penetrate the membrane pores, making it impossible to remove by simple water rinsing [23]; therefore, methods which breakdown the HA molecules would be more effective in mitigating fouling. Each UV cleaning step brings the TMP very close to the initial pressure, and the pressure rise thereafter does not reach the levels seen in the case where no cleaning takes place. UV exposure thus facilitates the

photocatalytic degradation of HA molecules deposited on the membrane, which helps to regenerate the membrane.

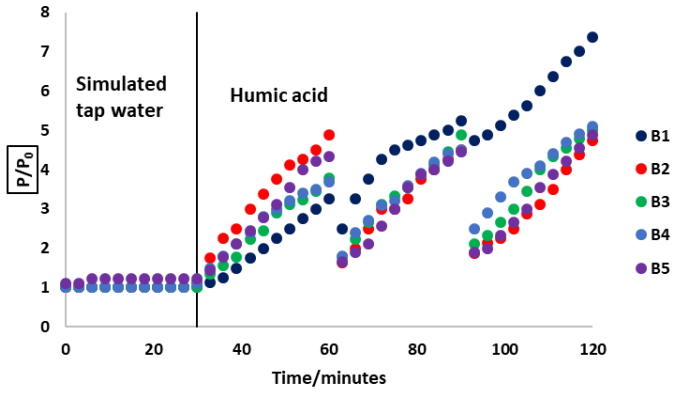

Figure 6. The variation of normalized pressure during filtration and between the cleaning procedures in which no cleaning was employed (B1); UV was applied over the active layer (B2); UV was directed through the substrate (B3); membrane was rinsed in DI water (B4); and membrane was rinsed in chemicals (B5).

Table 5 shows the apparent fouling rates that depict the different rates of foulant buildup on the membrane surface between the two cleaning events. Directing UV over the active layer (B2) resulted in the lowest rate of fouling, as was chemical cleaning (B5). This was closely followed by directing UV through the substrate (B3). Rinsing the membrane in DI water (B4) was the least effective in reducing the fouling rate since it had the closest rate to when no cleaning method was employed (B1).

Table 5. Apparent fouling rate.

Designation	Cleaning Method	Fouling Rate (kPa/min)
B1	No cleaning employed	0.60
B2	UV exposure over the active layer	0.07
B3	UV exposure through the substrate	0.10
B4	Rinsing in DI water	0.23
B5	Rinsing in chemical solutions	0.07

As shown in Table 6, UV exposure on the active layer gives an 84% cleaning efficiency compared to 83% for chemical cleaning and 72% through the substrate for the first cleaning cycle. The second B2 cycle gives decreased cleaning efficiency because the non-reversible fouling layer shields radiation from fully accessing the photocatalytic sites. However, when UV is directed through the substrate in B3, there is only a slight decrease in efficiency, because the radiation path is still relatively free from interfering HA molecules. In long term use, the principle can be useful in maintaining the efficiency of the photocatalytic membrane regeneration process. Since the concept has been proved to work ex-situ, it is important to verify it in situ for longer term fouling mitigation. If a UV source, such as LED lights, is incorporated into the module, such that it can illuminate the photocatalyst through the substrate, continuous photocatalytic degradation of foulants can take place. The filtration process can therefore continue for longer, minimizing or even eliminating any form of physical or chemical cleaning.

The membrane was fabricated on top of a low cost, readily available sintered glass disc substrate for proof of principle testing. However, in considering the potential cost of the membranes for full scale water treatment, a substrate geometry and size suitable for practical applications in filtration is unknown and is the subject of future studies.

Table 6. Cleaning efficiencies of each method.

Designation	Cleaning Method	Cleaning Efficiency %	
		Cycle 1	Cycle 2
B1	No cleaning employed	33	12
B2	UV exposure over the active layer	84	75
B3	UV exposure through the substrate	72	71
B4	Rinsing in DI water	70	57
B5	Rinsing in chemical solutions	83	77

4. Conclusions

A light-conducting photocatalytic membrane was successfully prepared by dip coating TiO_2 onto a sintered glass substrate. The membrane could conduct sufficient UV radiation to facilitate the photocatalytic degradation of sMO. It was shown to be capable of conducting UV for the purposes of mitigating HA fouling ex situ. Directing UV over the active layer showed the best membrane regeneration efficiency in the first cycle, followed by chemical cleaning. However, directing UV through the substrate had the best maintenance of efficiency across two cleaning cycles. The method is therefore of interest for further study during in-situ membrane cleaning over prolonged filtration periods.

Author Contributions: The experimental work was designed and carried out by L.T.N. under the guidance and supervision of M.C.D., S.C., D.N. and B.Z. M.C.D. helped to develop the concept. L.T.N. wrote the manuscript and all authors reviewed and edited it. Conceptualization, L.T.N. and M.C.D.; Formal analysis, L.T.N.; Investigation, L.T.N.; Methodology, L.T.N.; Project administration, L.T.N.; Resources, B.Z.; Supervision, D.N., S.C. and M.C.D.; Validation, L.T.N.; Visualization, L.T.N.; Writing—original draft, L.T.N.; Writing—review & editing, B.Z., D.N., S.C. and M.C.D.

Funding: This research received no external funding.

Acknowledgments: The work was supported by the Victoria University International Postgraduate Scholarships (VUIPRS). The XRD training by Dr. Ikechukwu Anthony Ike is acknowledged. We acknowledge the assistance of Dr. Zongli Xie and Guang

Yang for facilitating porometry measurements at CSIRO, Clayton, Australia. The support from the team in the Victoria University Institute for Sustainable Industries and Liveable Cities (ISILC) and the technical staff in the Victoria University College of Science and Engineering is also acknowledged.

Conflicts of Interest: The authors declare no conflict of interest.

References

1. Distefano, T.; Kelly, S. Are we in deep water? Water scarcity and its limits to economic growth. *Ecol. Econ.* **2017**, *142*, 130–147, doi:10.1016/j.ecolecon.2017.06.019.
2. Alamelu, K.; Jaffar Ali, B.M. TiO_2-Pt composite photocatalyst for photodegradation and chemical reduction of recalcitrant organic pollutants. *J. Environ. Chem. Eng.* **2018**, *6*, 5720–5731, doi:10.1016/j.jece.2018.08.042.
3. Jiang, L.; Choo, K.-H. Photocatalytic mineralization of secondary effluent organic matter with mitigating fouling propensity in a submerged membrane photoreactor. *Chem. Eng. J.* **2016**, *288*, 798–805, doi:10.1016/j.cej.2015.12.060.
4. Madaeni, S.S.; Ghaemi, N. Characterization of self-cleaning RO membranes coated with TiO_2 particles under UV irradiation. *J. Membr. Sci.* **2007**, *303*, 221–233, doi:10.1016/j.memsci.2007.07.017.
5. Geng, Z.; Yang, X.; Boo, C.; Zhu, S.; Lu, Y.; Fan, W.; Huo, M.; Elimelech, M.; Yang, X. Self-cleaning anti-fouling hybrid ultrafiltration membranes via side chain grafting of poly(aryl ether sulfone) and titanium dioxide. *J. Membr. Sci.* **2017**, *529*, 1–10, doi:10.1016/j.memsci.2017.01.043.
6. Guo, B.; Pasco, E.V.; Xagoraraki, I.; Tarabara, V.V. Virus removal and inactivation in a hybrid microfiltration–UV process with a photocatalytic membrane. *Sep. Purif. Technol.* **2015**, *149*, 245–254, doi:10.1016/j.seppur.2015.05.039.
7. Leong, S.; Razmjou, A.; Wang, K.; Hapgood, K.; Zhang, X.; Wang, H. TiO_2 based photocatalytic membranes: A review. *J. Membr. Sci.* **2014**, *472*, 167–184, doi:10.1016/j.memsci.2014.08.016.
8. Starr, B.J.; Tarabara, V.V.; Herrera-Robledo, M.; Zhou, M.; Roualdès, S.; Ayral, A. Coating porous membranes with a photocatalyst: Comparison of LbL self-assembly and plasma-enhanced CVD techniques. *J. Membr. Sci.* **2016**, *514*, 340–349, doi:10.1016/j.memsci.2016.04.050.
9. Li, S.; Hu, J. Transformation products formation of ciprofloxacin in UVA/LED and UVA/LED/TiO_2 systems: Impact of natural organic matter characteristics. *Water Res.* **2018**, *132*, 320–330, doi:10.1016/j.watres.2017.12.065.
10. Khatibnezhad, H.; Sani, M. Preparation and characterization of nanostructured TiO_2 thin film codoped with nitrogen and vanadium on glass surface by sol-gel dip-coating method. *Res. Chem. Intermed.* **2015**, *41*, 7349–7361, doi:10.1007/s11164-014-1816-1.
11. Coto, M.; Troughton, S.C.; Duan, J.; Kumar, R.V.; Clyne, T.W. Development and assessment of photo-catalytic membranes for water purification using solar radiation. *Appl. Surf. Sci.* **2018**, *433*, 101–107, doi:10.1016/j.apsusc.2017.10.027.
12. Dehghani, M.H.; Zarei, A.; Mesdaghinia, A.; Nabizadeh, R.; Alimohammadi, M.; Afsharnia, M.; McKay, G. Production and application of a treated bentonite–chitosan composite for the

efficient removal of humic acid from aqueous solution. *Chem. Eng. Res. Des.* **2018**, *140*, 102–115, doi:10.1016/j.cherd.2018.10.011.

13. Fan, H.; Xiao, K.; Mu, S.; Zhou, Y.; Ma, J.; Wang, X.; Huang, X. Impact of membrane pore morphology on multi-cycle fouling and cleaning of hydrophobic and hydrophilic membranes during MBR operation. *J. Membr. Sci.* **2018**, *556*, 312–320, doi:10.1016/j.memsci.2018.04.014.
14. Hatat-Fraile, M.; Liang, R.; Arlos, M.J.; He, R.X.; Peng, P.; Servos, M.R.; Zhou, Y.N. Concurrent photocatalytic and filtration processes using doped TiO2 coated quartz fiber membranes in a photocatalytic membrane reactor. *Chem. Eng. J.* **2017**, *330*, 531–540, doi:10.1016/j.cej.2017.07.141.
15. Shamaila, S.; Sajjad, A.K.L.; Chen, F.; Zhang, J. Synthesis and characterization of mesoporous-TiO_2 with enhanced photocatalytic activity for the degradation of chloro-phenol. *Mater. Res. Bull.* **2010**, *45*, 1375–1382, doi:10.1016/j.materresbull.2010.06.047.
16. Thamaphat, K.; Limsuwan, P.; Ngotawornchai, B. Phase Characterization of TiO_2 Powder by XRD and TEM. *Nat. Sci.* **2008**, *42*, 357–361.
17. Hir, Z.A.M.; Moradihamedani, P.; Abdullah, A.H.; Mohamed, M.A. Immobilization of TiO_2 into polyethersulfone matrix as hybrid film photocatalyst for effective degradation of methyl orange dye. *Mater. Sci. Semicond. Process.* **2017**, *57*, 157–165, doi:10.1016/j.mssp.2016.10.009.
18. Kaur, R.; Singh, S.; Pandey, O.P. Influence of CdO and gamma irradiation on the infrared absorption spectra of borosilicate glass. *J. Mol. Struct.* **2013**, *1049*, 409–413, doi:10.1016/j.molstruc.2013.06.072.
19. Ebrahimi, E.; Rezvani, M. Optical and structural investigation on sodium borosilicate glasses doped with Cr_2O_3. *Spectrochim. Acta Part A Mol. Biomol. Spectrosc.* **2018**, *190*, 534–538, doi:10.1016/j.saa.2017.09.031.
20. Cantarella, M.; Sanz, R.; Buccheri, M.A.; Romano, L.; Privitera, V. PMMA/TiO_2 nanotubes composites for photocatalytic removal of organic compounds and bacteria from water. *Mater. Sci. Semicond. Process.* **2016**, *42*, 58–61, doi:10.1016/j.mssp.2015.07.053.
21. Gao, Y.; Hu, M.; Mi, B. Membrane surface modification with TiO_2–graphene oxide for enhanced photocatalytic performance. *J. Membr. Sci.* **2014**, *455*, 349–356, doi:10.1016/j.memsci.2014.01.011.
22. Geltmeyer, J.; Teixido, H.; Meire, M.; Van Acker, T.; Deventer, K.; Vanhaecke, F.; Van Hulle, S.; De Buysser, K.; De Clerck, K. TiO_2 functionalized nanofibrous membranes for removal of organic (micro)pollutants from water. *Sep. Purif. Technol.* **2017**, *179*, 533–541, doi:10.1016/j.seppur.2017.02.037.
23. Li, X.; Li, J.; Fang, X.; Bakzhan, K.; Wang, L.; Van der Bruggen, B. A synergetic analysis method for antifouling behavior investigation on PES ultrafiltration membrane with self-assembled TiO_2 nanoparticles. *J. Colloid Interface Sci.* **2016**, *469*, 164–176, doi:10.1016/j.jcis.2016.02.002.

CHAPTER 4: LIGHT CONDUCTING MEMBRANE APPLICATION IN MODEL SOLUTIONS FILTRATION UNDER UV RADIATION

4.1. Chapter Overview

This chapter presents evaluation of the membrane's performance in the treatment of synthetic solutions that mimic water pollutants in water. In this chapter an improved preparation method, morphology and chemical composition of the membrane, fouling mechanisms and fouling indices towards representative water pollutants are also provided. Further results on transmission of UV through the substrate are also presented in this chapter. Fouling from the major natural organic matter (NOM) present in water, namely humics, proteins and polysaccharides was studied. UV radiation to the membrane was supplied by a UV-LED fixed to the membrane module, allowing continuous conditions for photocatalysis and in-situ fouling management. This chapter was published as a research article titled "Light conducting photocatalytic membrane for chemical-free fouling control in water treatment'', by Lavern T. Nyamutswa, Bo Zhu, Stephen F. Collins, Dimuth Navaratna and Mikel C. Duke in the peer reviewed journal "Membranes" (2020), 604, 118018. doi:https://doi.org/10.1016/j.memsci.2020.118018

4.2. Declaration of Co-Authorship and Co-Contribution of the Chapter

VICTORIA UNIVERSITY

THE NEW WAY TO DO UNI

OFFICE FOR RESEARCH TRAINING, QUALITY AND INTEGRITY

DECLARATION OF CO-AUTHORSHIP AND CO-CONTRIBUTION: PAPERS INCORPORATED IN THESIS

This declaration is to be completed for each conjointly authored publication and placed at the beginning of the thesis chapter in which the publication appears.

1. PUBLICATION DETAILS (to be completed by the candidate)

Title of Paper/Journal/Book: **Light conducting photocatalytic membrane for chemical-free fouling control in water treatment**

Surname: **Nyamutswa** First name: **Lavern**

Institute: **Institute for Sustainable Industries and Liveab** Candidate's Contribution (%): **80**

Status:

Accepted and in press: ✓ Date: **22/02/2020**

Published: ✓ Date: **7/03/2020**

2. CANDIDATE DECLARATION

I declare that the publication above meets the requirements to be included in the thesis as outlined in the HDR Policy and related Procedures – policy.vu.edu.au.

[redacted]	30/07/2020
Signature	**Date**

3. CO-AUTHOR(S) DECLARATION

In the case of the above publication, the following authors contributed to the work as follows:

The undersigned certify that:

1. They meet criteria for authorship in that they have participated in the conception, execution or interpretation of at least that part of the publication in their field of expertise;
2. They take public responsibility for their part of the publication, except for the responsible author who accepts overall responsibility for the publication;

PO Box 14428, Melbourne,
Vic 8001, Australia
+61 3 9919 6100

Victoria University ABN 83776954731
CRICOS Provider No. 00124K (Melbourne),
02475D (Sydney), RTO 3113

3. There are no other authors of the publication according to these criteria;

4. Potential conflicts of interest have been disclosed to a) granting bodies, b) the editor or publisher of journals or other publications, and c) the head of the responsible academic unit; and

5. The original data will be held for at least five years from the date indicated below and is stored at the following **location(s)**:

Institute for Sustainable Industries and Liveable Cities, Victoria University, Werribee Campus, Melbourne, Australia

Name(s) of Co-Author(s)	Contribution (%)	Nature of Contribution	Signature	Date
Lavern T. Nyamutswa	80	Concept development and manuscript writing	[redacted]	30/07/2020
Bo Zhu	2	Manuscript review and editing	[redacted]	28/7/2020
Stephen F. Collins	3	Concept development, manuscript review and editing	[redacted]	29 Jul '20
Dimuth Navaratna	5	Concept development, manuscript review and editing	[redacted]	29/07/2020
Mikel C. Duke	10	Concept development, manuscript review and editing	[redacted]	27/7/2020

Updated: September 2019

PO Box 14428, Melbourne,
Vic 8001, Australia
+61 3 9919 6100

Victoria University ABN 83776954731
CRICOS Provider No. 00124K (Melbourne),
02475D (Sydney), RTO 3113

Lavern T. Nyamutswa, Bo Zhu, Stephen F. Collins, Dimuth Navaratna, Mikel C. Duke, Light conducting photocatalytic membrane for chemical-free fouling control in water treatment, Journal of Membrane Science, Volume 604, 2020, https://doi.org/10.1016/j.memsci.2020.118018.

The full-text of this article is subject to copyright restrictions, and cannot be included in the online version of the thesis.

CHAPTER 5: SUNLIGHT-TRANSMITTING PHOTOCATALYTIC MEMBRANE FOR LOW ENERGY AND LOW MAINTENANCE WATER TREATMENT

5.1. Chapter Overview

Chapter 5 presents the performance of the membrane in the treatment of real surface water samples. The membrane's performance under simulated solar radiation (from a solar simulator) is also presented. Evidence of the generation of hydroxyl radicals from the membrane as proof of photocatalytic ability is presented in this chapter. Chapter 5 also presents the effect the membrane has on water contaminants of different molecular weights, as well the potential of the membrane to be applied in low chemical consumption and low energy water treatment. This chapter was submitted as a research article titled "Sunlight-transmitting photocatalytic membrane for low energy and low maintenance water and wastewater treatment'', by Lavern T. Nyamutswa, Blair D. Hanson, Dimuth Navaratna, Stephen F. Collins, Karl G. Linden and Mikel C. Duke in the peer reviewed journal Environmental Science and Technology, on 2 July 2020. It is presented here in the final version submitted to the journal.

5.2. Declaration of Co-Authorship and Co-Contribution of the Chapter

VICTORIA UNIVERSITY

THE NEW WAY TO DO UNI

OFFICE FOR RESEARCH TRAINING, QUALITY AND INTEGRITY

DECLARATION OF CO-AUTHORSHIP AND CO-CONTRIBUTION: PAPERS INCORPORATED IN THESIS

This declaration is to be completed for each conjointly authored publication and placed at the beginning of the thesis chapter in which the publication appears.

1. PUBLICATION DETAILS (to be completed by the candidate)

Title of Paper/Journal/Book: Sunlight-transmitting photocatalytic membrane for low energy and low maintenance water and wastewater treatment

Surname: Nyamutswa First name: Lavern

Institute: Institute for Sustainable Industries and Liveab Candidate's Contribution (%): 70

Status:

Accepted and in press: ☐ Date:

Published: ☐ Date:

2. CANDIDATE DECLARATION

I declare that the publication above meets the requirements to be included in the thesis as outlined in the HDR Policy and related Procedures – policy.vu.edu.au.

Lavern Nyamutswa Digitally signed by Lavern Nyamutswa Date: 2020.07.30 21:04:25 +10'00'	30/07/2020
Signature	**Date**

3. CO-AUTHOR(S) DECLARATION

In the case of the above publication, the following authors contributed to the work as follows:

The undersigned certify that:

1. They meet criteria for authorship in that they have participated in the conception, execution or interpretation of at least that part of the publication in their field of expertise;
2. They take public responsibility for their part of the publication, except for the responsible author who accepts overall responsibility for the publication;

PO Box 14428, Melbourne,
Vic 8001, Australia
+61 3 9919 6100

Victoria University ABN 83776954731
CRICOS Provider No. 00124K (Melbourne),
02475D (Sydney), RTO 3113

3. There are no other authors of the publication according to these criteria;

4. Potential conflicts of interest have been disclosed to a) granting bodies, b) the editor or publisher of journals or other publications, and c) the head of the responsible academic unit; and

5. The original data will be held for at least five years from the date indicated below and is stored at the following **location(s)**:

Institute for Sustainable Industries and Liveable Cities, Victoria University, Werribee Campus, Melbourne, Australia

Name(s) of Co-Author(s)	Contribution (%)	Nature of Contribution	Signature	Date
Lavern T. Nyamutswa	70	Concept development and manuscript writing	[redacted]	30/07/2020
Blair D. Hanson	5	Manuscript writing, review and editing	[redacted]	28/7/2020
Dimuth Navaratna	5	Concept development, manuscript review and editing	[redacted]	30/07/2020
Stephen F. Collins	5	Concept development, manuscript review and editing	[redacted]	29 Jul '20
Karl G. Linden	5	Concept development, manuscript review and editing	[redacted]	29 Jul '20
Mikel C. Duke	10	Concept development, manuscript review and editing	[redacted]	27/7/2020

Updated: September 2019

PO Box 14428, Melbourne,
Vic 8001, Australia
+61 3 9919 6100

Victoria University ABN 83776954731
CRICOS Provider No. 00124K (Melbourne),
02475D (Sydney), RTO 3113

Sunlight-Transmitting Photocatalytic Membrane for Reduced Maintenance Water Treatment
Lavern T. Nyamutswa, Blair Hanson, Dimuth Navaratna, Stephen F. Collins, Karl G. Linden, and Mikel C. Duke, ACS ES&T Water 2021 1 (9), 2001-2011.
https://doi.org/10.1021/acsestwater.1c00073

The full-text of this article is subject to copyright restrictions, and cannot be included in the online version of the thesis.

CHAPTER 6: CONCLUSIONS AND FUTURE DIRECTIONS

Purpose and key conclusions from this thesis

The thesis sought to explore an innovative idea to practically harness photocatalysis and membrane filtration to address potable water supply challenges in remote areas. Membrane filter blockage from fouling, and the need to clean with chemicals, is a widely accepted barrier to sustainable operation and adoption of membrane technology in remote areas, and photocatalysis was proposed as a solution to overcome this barrier. Directing light to a photocatalyst coated on a membrane was identified as another challenge. Light transmitting/distributing substrates were proposed as an innovative solution to this light transmission challenge, leading to the development of light transmitting and distributing photocatalytic membranes that were tested for application in water treatment. This was broken down into four main achievable steps, which were:

(i) identifying a suitable substrate for fabricating a light transmitting membrane through a review of the literature;

(ii) fabricating the membrane and evaluating its physical properties;

(iii) application testing of the membrane with synthetic and real water samples under UV and simulated solar light; and

(iv) translation of research results to show the real reduced chemical consumption and energy in membrane water treatment.

The work in this thesis revealed major findings in seeking to demonstrate the innovative idea. These were suitability of light transmitting porous sintered glass substrates for adoption in photocatalytic membranes, and the potential of the novel membrane to remediate contaminated water while operating with reduced chemical and energy consumption. In the first finding, the porous sintered glass substrate used had light transmittances ranging from 10% to 80% in the wavelength range of 340-400 nm. The ability of the membrane to facilitate photocatalytic reactions in the presence of light was first studied using methyl orange (MO) and a UV lamp with peak emission at 365 nm, as described in Chapter 3. By directing light through the substrate, 52% of MO was degraded in 5 hours in batch experiments, compared to 58% degradation when light was exposed directly over the photocatalytic layer (obstructed only by the

solution). This result was the first major finding of this thesis, providing the fundamental validation that porous glass substrates, which are essential to support the thin membrane coating, additionally possess sufficient properties to transmit light through their porous material to activate the photocatalyst coating. The detection of hydroxyl radicals produced by the membrane through photocatalysis, as described in Chapter 5, was also further confirmation of a practically functional light transmission and distribution property. The pseudo first order reaction rates of dye degradation through directing UV over the active layer and through the substrate were 0.0030 min^{-1} and 0.0025 min^{-1} respectively. The reaction rate obtained when directing light through the substrate was comparable to other results in the literature in conventional setups where UV of higher intensities was directed over the active layer. The configuration used in this study can therefore give desirable photocatalytic response comparable to the conventional configuration, while also utilizing the advantages mentioned earlier. Overall, although an advanced oxidation effect was demonstrated, photocatalysis did not result in significant transformation of organics during filtration, mainly due to the short contact time of 80 ms. This was expected, as higher transformations found in literature are a result of higher contact times, which range from 30 minutes to 8 hours.

Verification of the membrane's performance and suitability for water treatment application was also demonstrated. The suitability of the membrane for rejecting organic water contaminants was reported in Chapter 4, where total organic carbon (TOC) rejection was measured at 37%, 70% and 80% using HA, BSA and SA respectively as model water contaminants. Following on this potential, real surface water treatment was the next logical step, TOC rejection from surface water was measured at 30%, while UV254 removal was 26%. The largest rejection was in turbidity at 94%, which is expected for an MF membrane that is often used to remove particles from waters (including pathogens). Rejection was attributed largely to membrane separation, while photocatalysis contributed to increased hydrophilicity of the membrane surface and reduced resistance from fouling. For surface water, SEC showed that for the coated membrane, rejection was highest for fractions with apparent molecular weights (AMW) of 5-33 kDa, confirming its overall performance as an MF membrane.

The second major finding was the reduced fouling potential from in-situ testing. This was demonstrated by lower transmembrane pressure (TMP) profiles for all filtered

waters during conditions conducive for photocatalytic activation. Firstly, increased hydrophilicity allowed a slight increase in hydrophilic components in the feed to diffuse through the membrane, reducing fouling. Secondly and more importantly, more hydrophobic and hydrophilic organics retained by the membrane were washed off during backwashing, restoring the membrane surface in the process. Water would especially work as a good solvent for washing off hydrophilic components. The improved anti-fouling properties were clearly shown in the fouling indices. During BSA and SA filtration, the hydraulic cleaning efficiency (HCE) was at least 86% in all tests. In surface water treatment, the HCE was at least 95%. These values showed that the fabricated membrane was intrinsically hydrophilic, allowing membrane recovery by simple periodic hydraulic backwashing procedures. The effect of photocatalysis was shown in the lower hydraulically irreversible fouling index (HIFI) values in experiments conducted under UV-LED or simulated solar light. For BSA and SA, photocatalysis led to 2.7-fold and 4.2-fold reductions in the HIFI, respectively, compared to non-photocatalytic filtration. During surface water treatment, photocatalytic conditions reduced the HIFI 8-fold, demonstrating a significant lowering of irreversible fouling and the beneficial effects of solar irradiation in contributing to reduction of the filtration resistance.

To determine the mechanism of fouling occurring on the membrane and how photocatalysis helped to reduce fouling, the resistance-in-series model, SEM imaging and modelling of the carbon retention during surface water treatment were applied. Generally, both surface (cake layer formation) and internal (pore blocking) fouling occurred, but photocatalysis led to a reduction in both fouling mechanisms. This was first reported in Chapter 4, where the photocatalytic processes, facilitated by UV-LED light exposure, led to 3.0-fold reduction in the total filtration resistance (R_t) during BSA filtration and 2.4-fold reduction during SA filtration. Significant reductions in the internal filtration resistance (R_f) for both BSA and SA also occurred. Induced superhydrophilicity also resulted in lowering of the intrinsic membrane resistance (R_m). The observed positive changes to filtration resistance were supported by SEM analysis of the membranes. With light illumination, penetration of membrane pores by the foulants was low, with the formation of a thin cake layer on the membrane surface more dominant. Pore blocking was more pronounced without light. Superhydrophilicity and oxidation were therefore successful in preventing deposition of hydrophobic

organics on the membrane surface, as well as assembly of cohesive fouling layers. In particular, radical facilitated breakdown of protein and polysaccharide complexes that occur in the presence of Ca^{2+} ions contributed to preventing cohesive fouling layer formation.

The third most important finding in this work was the ability of the photocatalytic membrane system to function in simulated partial sunlight. This was the final proof that the membrane can function in real sunlight and can be adopted for real world application. The system showed real potential to operate with reduced cleaning chemical and energy reduction. The clearest evidence of this was shown in the time to clean-in-place (CIP) values in Chapter 5. With solar irradiation, and thus photocatalysis, there was 4.5-fold increase in the time to CIP compared to operating without photocatalysis. A CIP every 2.7 months could therefore be extended to 1 year by using indirect sunlight to clean the membrane instead of chemicals. The result also showed that even the more frequent low intensity cleans such as chemically enhanced backwashes (CEBs) can be completely avoided, and so is the need for coagulants, which can be the highest chemical demand for a high flux membrane filtration system. The system could also lead to a 50% reduction in the filtration pump energy requirements, and energy savings from avoiding the 2.5 kWh/m^3 that is used by artificial UV light by instead using sunlight. Further optimisation for a particular application and improvement in performance from the preliminary practical proof of the working concept is subject of further work, but the present work demonstrates the chemical reduction potential for the major area of need in providing safe water supply for disadvantaged communities with greatly reduced use of cleaning chemicals.

Future work recommendations

Despite the concept validation and measurement of useful practical benefits, several limitations were identified that could further progress the concept's scientific and practical benefits. These were broadly identified around limited light transmission of sintered glass substrates and limited organic compound transformation, as well as the need to use recycled glass to minimise glass manufacturing and disposal environmental impact. In the first area, other materials with higher light transmission properties could be considered. These include polydimethylsiloxane (PDMS), silk

fibroin, freestanding graphene oxide membranes (FSGOMs), thin film porous quartz and regenerated cellulose (RC) membranes. These materials have a combination of up to 90% light transmittances and offer mechanical flexibility. Polylactic acid (PLA) composited with chitosan (CS), can also be considered due to porosity, hydrophilicity, bactericidal properties and 90% transmittance in a wavelength range of 400-700 nm, compared to 10% transmittance at 400 nm for the sintered glass substrate used in the current study. Composites of nylon 6 with single-walled carbon nanotube (SWCNT) with light transmittance of 77.4% at 550 nm could also be considered for visible light active photocatalysts.

The current experimental set up involved illuminating the entire surface of a flat disc membrane, whereas traditional low-pressure membrane systems are typically packaged in hollow fibre elements. The use of flat disc membranes in this thesis was a result of availability of a light transmitting substrate in this geometry, and served the purpose to prove the concept. However future work can be focused on exploring the light transmitting substrates suggested in this thesis (Chapter 2) and fabricating them into more common geometries like hollow-fibre and monolith. As shown in the concept practical setup, the light sources could then be attached to the end of the membrane element, with the light travelling down the element length through the light transmitting substrate. Such hollow-fibre or monolith substrates would allow the membrane to be packed in traditional opaque pressure vessel.

In the second area, higher transformation and degradation of organic compounds can be achieved by increasing the contact time of the compounds and the photocatalyst. This can be achieved by increasing the surface area of the membrane, as well as recirculation of the permeate in a multi-pass filtration system. Higher degradation can also be achieved by using more efficient photocatalysts, such as visible light active TiO_2, instead of Degussa P25 TiO_2. Understanding photocatalyst particle size and quantity optimization are other areas of further work needed to optimize water treatment system, as well as previously reported beneficial changes in surface characteristics, specifically in this type of membrane. In the case where artificial light sources are used, an array of UV-LEDs could be adopted to increase the intensity of light available. The novel system reported in the thesis has potential for water remediation with reduced chemical and energy consumption, and addressing the mentioned limitations would bring it closer to practical use. Manufacture of a porous

glass monolith would allow the design of a dead-end filtration unit resembling commercially available ceramic membranes and their housing, but instead with a window at the top (dead-end) or a transparent housing made of a suitable polymer to allow sunlight to access and illuminate the monolith and the TiO_2 coated internal raw water channels.

APPENDIX 1: PUBLISHED PAPER FOR CHAPTER 3

membranes

MDPI

Article

Proof of Concept for Light Conducting Membrane Substrate for UV-Activated Photocatalysis as an Alternative to Chemical Cleaning

Lavern T. Nyamutswa [1,*], Bo Zhu [1], Dimuth Navaratna [1,2], Stephen Collins [2] and Mikel C. Duke [1]

1 Institute for Sustainable Industries and Liveable Cities, Victoria University, Melbourne 14428, Australia; bo.zhu@vu.edu.au (B.Z.); dimuth.navaratna@vu.edu.au (D.N.); mikel.duke@vu.edu.au (M.C.D.)

2 College of Engineering and Science, Victoria University, Melbourne 14428, Australia; stephen.collins@vu.edu.au

* Correspondence: lavern.nyamutswa@live.vu.edu.au; Tel.: +61-3-9919-8111

Received: 31 October 2018; Accepted: 26 November 2018; Published: 2 December 2018

check for updates

Abstract: Adopting an effective strategy to control fouling is a necessary requirement for all membrane processes used in the water/wastewater treatment industry to operate sustainably. The use of ultraviolet (UV) activated photocatalysis has been shown to be effective in mitigating ceramic membrane fouling by natural organic matter. The widely used configuration in which light is directed through the polluted water to the membrane's active layer suffers from inefficiencies brought about by light absorption by the pollutants and light shielding by the cake layer. To address these limitations, directing light through the substrate, instead of through polluted water, was studied. A UV conducting membrane was prepared by dip coating TiO_2 onto a sintered glass substrate. The substrate could successfully conduct UV from a lamp source, unlike a typical alumina substrate. The prepared membrane was applied in the filtration of a humic acid solution as a model compound to study natural organic matter membrane fouling. Directing UV through the substrate showed only a 1 percentage point decline in the effectiveness of the cleaning method over two cleaning events from 72% to 71%, while directing UV over the photocatalytic layer had a 9 percentage point decline from 84% to 75%. Adapting the UV-through-substrate configuration could be more useful in maintaining membrane functionality during humic acid filtration than the current method being used.

Keywords: Titanium dioxide; photocatalytic membrane; water treatment; membrane fouling

1. Introduction

Water scarcity affects about two-thirds of the world's population for at least a month of every year [1]. Existing water resources of suitable quality are already over-subscribed or rapidly approaching their limits in most parts of the world. To address this gap, conveniently available poorer quality waters may be used, but they first have to be treated to meet quality standards. However, current treatments are beset with several issues, among them high costs, non-effectiveness in removing recalcitrant pollutants such as azo dyes and nitroaromatic compounds [2], and the generation of toxic secondary by-products. Improving accessibility and operational simplicity of treatment technologies would support initiatives to improve wider access to clean water.

Treatment of municipal and industrial wastewater is also becoming an important source of water for industrial and agricultural use [3]. To meet increasingly stringent water quality regulations, natural organic matter, soluble microbial products and micro-pollutants should also be removed from wastewater. Processes that have been used in tertiary water treatment processes include advanced

oxidation, activated carbon adsorption, ion exchange and membrane filtration. Membrane filtration, in particular, is gaining increased use because of its lower energy footprint, compact design, lower chemical consumption and the ease with which it can be maintained and automated [3].

Membrane processes, however, have several issues which limit their use on a wider scale. One such issue is fouling, which reduces membrane separation efficiency, membrane lifespan and can raise energy costs. Maintaining performance and improving the simplicity of operation of membrane systems is necessary to make the technology more widely available to communities worldwide.

The approaches that have been used to reduce membrane fouling include pre-treating the feed, modification of membrane properties, optimisation of operating conditions, as well as optimization of module arrangement and configuration [4]. Although these reduce fouling to some extent, membrane cleaning is always employed in practice. Cleaning can be achieved hydraulically, mechanically, electrically or chemically, with the former being the most common, followed by the latter. More than one of these cleaning methods can also be applied in combination. However, these result in significant downtime and costs associated with loss of productivity, labour, energy as well as procurement, transportation, storage, and disposal of chemicals [4].

In-situ self-cleaning methods are therefore necessary to solve the fouling problem without stopping the water filtration process. One such method is coupling membrane filtration with photocatalysis. The photocatalytic properties of semiconductor photocatalysts such as TiO_2 lead to the photo-induced partial or total decomposition of pollutants present on the surface of the membrane while photo-induced ultra-hydrophilicity leads to elimination of the remaining hydrophobic contaminants through a simple water rinsing operation. Photocatalysis and induced hydrophilicity can occur on the same surface simultaneously to give a "self-cleaning" membrane which leads to savings on cleaning procedures [5,6].

Several configurations have been used to combine filtration with photocatalysis to give an integrated hybrid water treatment process, known as a photocatalytic membrane reactor (PMR). The configurations include a slurry photocatalytic reactor with a membrane submerged in it, a slurry reactor that precedes a membrane filtration unit and a porous photocatalytic membrane in which the photocatalyst is coated onto the membrane substrate [7]. Of these three configurations, the latter is the most interesting for future water treatment because it combines both filtration and photocatalysis in one unit.

A novel configuration in which the feed solution was fed from the uncoated side of the membrane was studied, mainly to independently control the separation and photocatalytic functions of the membrane [6]. Separating the separation and photocatalysis functionalities increases process robustness because failure of one does not necessarily result in the failure of the other [8]. Another advantage cited for this configuration is retention of particulates capable of shielding UV light on the feed side of the membrane, thus making photocatalysis more efficient because the permeated side has more optical transparency than the feed side. This was envisaged to make UV disinfection of highly turbid waters more efficient in terms of UV dosage, though it could come at the expense of increased membrane fouling.

To date, researchers have focused on making photocatalytic membranes for water treatment by coating nano-sized photocatalysts on opaque materials such as ceramics, organic membranes and metals. These membranes lack light transparency, requiring light to be directed through the water being treated to reach the photocatalyst coating on the substrate surface. Directing light this way in complex membrane element designs, such as ceramic monoliths, results in light attenuation before it reaches the photocatalyst coated inside the channels. Organic pollutants present in water can also strongly absorb light which was meant to reach the photocatalyst coating, reducing photocatalytic efficiency [9]. In this study, the potential of replacing these materials with optically transparent sintered glass was investigated. UV light (including solar) can then be conveniently directed through the light-transmitting sintered glass substrate to reach the photocatalyst coated on its surface. The use of sintered glass in this way was not found in the literature. If loss of light through absorption or reflection by the membrane substrate or organic pollutants present in the water being treated are

minimised, it can translate to more efficient use of energy and reduced costs, and long term mitigation of fouling with minimal chemical and physical membrane cleaning. The concept is depicted in Figure 1.

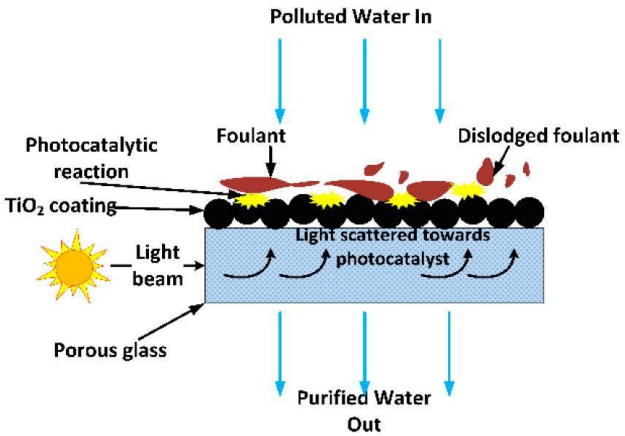

Figure 1. The concept of a light-conducting membrane substrate for practical implementation of a photocatalytic reaction for improved membrane performance.

The key aim of this research study was to verify the concept by coating porous glass membranes with a photocatalyst and observing ex-situ if the photocatalytic reaction can be engaged by directing light through the substrate in comparison to applying the light directly to the photocatalytic layer. The model synthetic dye, screened methyl orange (sMO), was used to observe a practical photocatalytic reaction utilising the well-known commercial catalyst, Aeroxide P25 TiO_2. The model membrane foulant and pollutant, humic acid (HA) was used as a filtration feed solution to study the effect of applying this concept in mitigating membrane fouling.

2. Materials and Methods

2.1. Materials

Humic acid was purchased from Fluka AG Cheische Fabrik., Buchs, Switzerland and used as a representative natural organic matter compound. Titanium dioxide P25 with 99.8% purity and composed of 80% anatase and 20% rutile phases was acquired from Evonik. The TiO_2 had an average particle size of 30 nm and a specific surface area of 50 m^2/g). Bovine Serum Albumin (BSA) of molecular weight 66 kDA was purchased from Sigma Aldrich (St. Louis, MO, USA). Screened methyl orange used as a model dye was purchased from Ajax Chemicals, Australia. Methanol was acquired from Chem-Supply, Australia. Nitric acid was purchased from Merck Pty Limited, Kilsyth, Australia. Acetone (99.9%) was purchased from Sigma-Aldrich, Australia. Sintered glass used as the membrane substrate was acquired from Ningbo Ja-Hely Technology Co., Ltd., Ningbo, China. This was in the form of flat circular discs of 25 mm diameter, 2 mm thickness and G5 porosity grade.

2.2. Apparatus

A panel consisting of 6 × 18 W UVA lamps (A.U.V.S (Ops), Pty. Ltd., Australia) with an emission peak at 365 nm was used to illuminate the membrane outside the module. The UV intensity at 365 nm was measured by a UV irradiance meter from Photoelectric Instrument Factory of Beijing Normal University, Beijing, China. A TPI 665L digital manometer from Accutherm, Melbourne, Australia was used to measure transmembrane pressure (TMP) changes. The membrane was placed in a custom

made filtration module made from stainless steel, giving an effective membrane area of 2.5 cm^2. A programmable Vulcan 3-550PD NEY furnace, (Extech Equipment, Victoria, Australia) was used for heat treating the membrane after coating with TiO_2. A peristaltic pump (Masterflex 7592-45, Cole-Parmer, Vernon Hills, IL, USA) was used to drive the feed through the membrane in dead-end mode. The amount of permeate collected was measured by an electronic balance (FX-3000i WP, A&D Company Ltd., Seoul, South Korea) with real time monitoring software. A sonic bath (Soniclean 500HT, Transtek Systems, Melbourne, Australia) was used to ultrasonically clean the membranes before coating, as well as to remove air bubbles in the coating suspension.

2.3. Preparation of Membranes

The sintered glass discs were first cleaned by washing in acetone, ethanol then water in a sonic bath to remove loose particles and possible contaminants. Each sonic wash was 20 min long. The last wash was followed by deionised water (DI water) rinsing and drying in a fan-forced oven at 80 °C for 3 h. The washed discs were weighed, labelled and stored in an air tight container until use.

To ensure coating on only one side of the membrane, one side was covered with masking tape. The coating suspension was prepared by adding 2 g of Evonik P25 TiO_2 to 60 mL of 70/30% (v/v) water/methanol water acidified to pH 3 with nitric acid. The suspension was sonicated for 20 min followed by magnetic stirring for 2 h before the commencement of coating.

The disc was then dipped into the suspension using a custom made mechanical device and withdrawn at a dipping/withdrawal speed of 2 cm/min. The process was repeated three times. The coated membranes were then air dried over 12 h and the tape carefully removed, followed by heat treatment to 450 °C at a heating rate of 1 °C/min in a programmable muffle furnace. The temperature was held at 450 °C for 2 h, and then cooled to room temperature at 1 °C/min. The membranes were then washed with DI water and oven dried at 80 °C for 5 h. The membranes were weighed before and after coating to determine the amount of TiO_2 that was immobilised on the surface.

2.4. Membrane Characterisation and Chemical Analysis

Fourier transform infrared spectroscopy (FTIR) analysis was used to explore surface functional groups and was performed with a Perkin Elmer Frontier FTIR Spectrometer equipped with an attenuated total reflectance (ATR) accessory. The crystal structure of the photocatalyst after coating was confirmed by powder X-ray diffraction (XRD) using a Rigaku Mini Flex 600 diffractometer operating with CuKα (λ = 1.54060 Å) radiation at 15 mA and 40 kV with a Ni filter. The analysis range was 20°–80° 2θ with 0.02° step and 1.2 s acquisition for steps. The step time was chosen to adequately obtain a good signal to noise ratio in the mean reflections of (1 0 1) and (1 1 0) planes, which are the two main anatase and rutile planes of TiO_2 [10]. The substrate was ground by mortar and pestle before XRD analysis. The pore size of the substrate was determined by capillary flow porometry using a Quantachrome Porometer 3 GZ series. The method involves measuring nitrogen gas flow as a function of TMP through the dry and wetted membrane. The pore size is then calculated using the Washburn equation. The wetting liquid was Porofil from Quantachrome Corp., Boynton Beach, FL, USA. The absorbance of the sMO solution at 642 nm was measured by a UV-Visible-Biochrom Libra 522 UV-visible spectrophotometer. Total organic carbon (TOC) of BSA was determined by a Shimadzu TOC-V CSH analyzer.

2.5. Degradation of Screened Methyl Orange

The developed membranes were tested for photocatalytic activity under several configurations in UV light. The naked UV lamp had an intensity of 2.5 mW/cm^2 at 365 nm and a distance of 10 cm as measured by the UV irradiance meter. The membranes were placed in a beaker with 100 mL 0.01 mM solutions of sMO and the discoloration of the dye monitored by UV-Visible light absorption measurements at 642 nm of 1 mL samples withdrawn by a micropipette at 30 min intervals. The membrane was placed such that only a thin layer of liquid was above the membrane. The first

hour of each experiment was carried out in the dark to allow adsorption of the dye onto the membrane. The degradation experiments carried out are summarised in Table 1.

Table 1. Description of the screened methyl orange (sMO) degradation experiments.

Designation	Description	Purpose
A1	Coated membrane. Coated side facing UV source.	To determine effect of shining UV directly onto active layer.
A2	Coated membrane. Coated side facing away from UV source.	To determine the effect of transmitting light through the substrate.
A3	Coated membrane. Coated side facing away from UV source. Top part of membrane covered with aluminium foil.	To determine whether the apparent photocatalytic activated is due to light reflected from the base of the beaker, rather than light passing through the filter.
A4	Coated membrane. Coated side facing away from UV source. Every area of the beaker blocked except the top part of the membrane.	To focus the light source onto the filter, to determine whether it can transmit light that is sufficient enough to trigger photocatalytic reactions.
A5	Uncoated filter, in the presence of UV light.	To eliminate photocatalytic effect.
A6	Filter coated with P25, without UV light.	To determine adsorption property of coated membrane.
A7	Uncoated filter, without UV light.	To determine adsorption property of uncoated membrane.
A8	UV light only.	To determine the extent of photolysis.

The pseudo first order rate constant of the dye degradation was calculated using the Langmuir-Hinshelwood equation:

$$\ln\left(\frac{C}{C_0}\right) = -kt \quad (1)$$

where C_0 is the initial concentration of dye, C is the concentration in mmol/L at time t (min), and k (min^{-1})is the rate constant [11].

2.6. Filtration of Humic Acid and BSA Rejection Tests

A 20 mg/L HA solution prepared by the appropriate dilution of a previously prepared stock solution was used as the feed. Generally, the concentration range of humic substances in surface and ground water is 20 µg/L–30 mg/L [12]; therefore, 20 mg/L was specifically chosen to fall within the upper region of this range to represent a more challenging wastewater where there is a stronger need for membrane cleaning. To prepare the stock solution, 6 g of HA was mixed in 2 L of deionized water over 2 days by aid of a magnetic stirrer. Suspended solids were removed by vacuum filtration through a 0.45 µm membrane filter (ADVANTEC, Tokyo, Japan). The filtration setup is depicted in Figure 2, and it consisted of a feed tank, a peristaltic pump, membrane module, needle to close the retentate line such that the filtration mode was dead-end, pressure transducer to measure the change in transmembrane pressure (TMP), and a permeate collection tank placed on a balance connected to a data logger. The experiments were carried out at a constant flux of 450 L m^{-2} h^{-1}. The membrane was first compacted with simulated tap water (100 mg/L NaCl solution) for 30 min, followed by filtration of the 20 mg/L HA solution for 30 min. Simulated tap water was used instead of real tap water so that the actual composition of the water was known, controllable and replicable. The membrane was then removed from the module and cleaned by either UV exposure under the lamp for 30 min, chemical cleaning using a 1% NaOH solution and 0.5% NaOCl, or simple rinsing in distilled water. After the cleaning process, the membranes were reloaded onto the module and the membrane recovery

determined by measuring the new TMPs while continuing HA filtration for 30 min, cleaning and another HA filtration cycle. The cleaning methods used are summarised in Table 2.

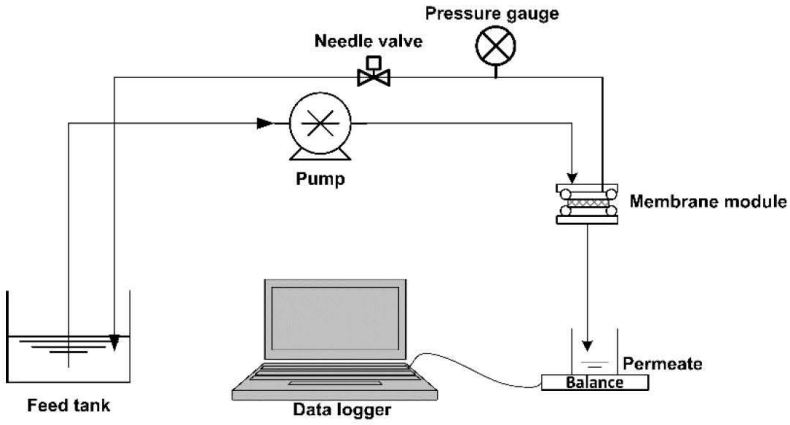

Figure 2. Schematic representation of the filtration setup.

Table 2. Description of the cleaning methods used to regenerate the membrane after fouling.

Designation	Description of Cleaning Method
B1	No cleaning employed
B2	UV exposure over the active layer
B3	UV exposure through the substrate
B4	Rinsing in DI water
B5	Rinsing in NaOH and NaOCl solutions

The apparent fouling rate, r, in kPa/min between two adjacent cleaning events was calculated as:

$$r = \frac{P_{max} - P_{min}}{\Delta t} \tag{2}$$

where P_{max} is the TMP value immediately after the second cleaning event, P_{min} is the TMP value immediately after the first cleaning event, and Δt is the time between these two recorded TMP values.

The efficiency of each cleaning event was calculated as:

$$E = \frac{P_{before} - P_{after}}{P_{before} - P_0} \times 100\% \tag{3}$$

where P_{before} and P_{after} are the TMP values immediately before and after the cleaning event, and P_0 is the pressure required to overcome the intrinsic membrane resistance [13].

To determine the selectivity of the substrate and prepared membrane, a 50 mg/L BSA solution was prepared by appropriate dilution of a 1 mg/mL BSA stock solution containing 1 mM $CaCl_2$ and 7 mM NaCl in DI water. The BSA solution was then filtered through the uncoated substrate as well as the prepared membrane. The change in TOC was measured and the rejection, R, is calculated by

$$R = 1 - \frac{C_p}{C_f} \times 100\% \tag{4}$$

where C_p and C_f are the TOC concentrations in the permeate and feed, respectively.

3. Results and Discussion

3.1. Membrane Characterisation

The average pore size of the substrate as measured by porometry was 1.4 μm. After coating with TiO_2, the normalized weight of the coating was measured on the membranes to be 4 ± 0.2 mg/cm^2. The results of the XRD analysis of the photocatalyst and substrate are shown in Figure 3.

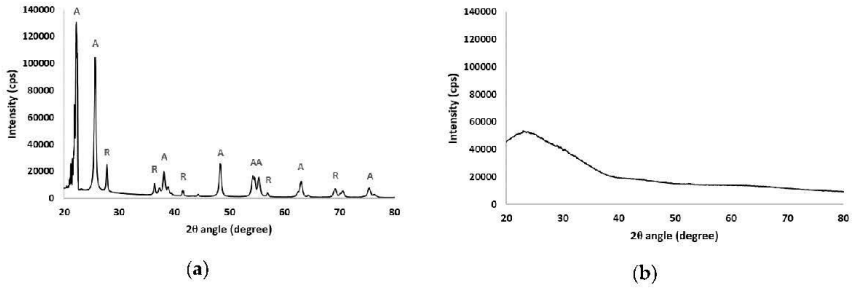

Figure 3. The X-ray diffraction (XRD) patterns of the (**a**) TiO_2 photocatalyst; (**b**) the substrate with markers to indicate the Bragg peaks associated with the anatase (A) and rutile (R) phases.

The diffraction pattern of the TiO_2 immobilized on the membranes shows that the anatase phase is predominant, while the rutile phase is also present [14]. Typical anatase peaks include 25.7° (1 0 1), 38.1° (0 0 4), 48.5° (2 0 0), 54.3° (1 0 5), 55.3° (2 1 1) and 63.0° (1 1 8) [15,16], while rutile peaks appeared at 27.8° (1 1 0) [17], 36.4° (1 0 1), 41.6° (1 1 1), 57.1° (2 2 0) and 69.3° (3 0 1) [14]. The substrate is amorphous, therefore no distinct crystalline phases were detected.

Figure 4 shows the Fourier Transform Infrared (FT-IR) spectrum of the sintered glass substrate and the P25 photocatalyst.

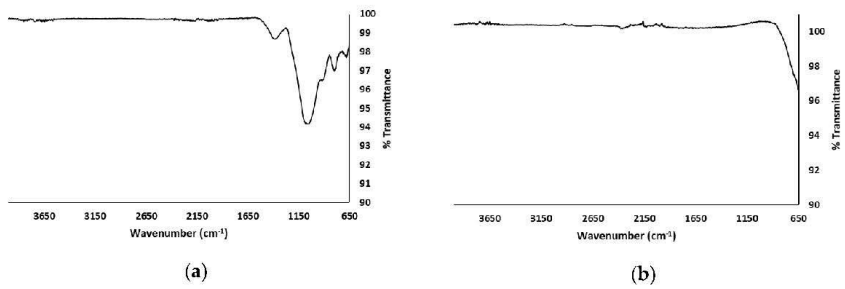

Figure 4. Fourier Transform Infrared (FT-IR) spectrum of the: (**a**) sintered glass substrate and; (**b**) P25 powder.

Borosilicate glass is a composite of the three network forming units whose proportions depend on each particular type of glass. The units are trigonally coordinated boron (BO_3), tetrahedrally coordinated boron (BO_4), and tetrahedral SiO_4 structural units. It can also consist of network modifiers such as alkali and or alkaline earth metal oxides. The peak appearing at 680 cm^{-1} is assigned to the bending vibrations of Si–O–B bridges. The peak at 920 cm^{-1} is due to the stretching vibrations of B–O bonds in tetrahedral BO_4 units. The band between 1000–1120 cm^{-1} is thought to arise from overlapping contributions of silicate and borate groups containing BO_3 and BO_4 units. The absorption band which peaks at 1379 cm^{-1} is attributed to the B–O stretching vibrations of polymerized BO_3 units. Broad bands which normally appear from 2200 cm^{-1} and extend beyond due to OH, water

and hydroxyl groups, were not observed, mainly due to the heating process which drives out water. The barely noticeable peaks in this region are attributed to the stretching vibrations of O–H bonds which are formed at non-bridging oxygen sites [18,19]. FT-IR thus confirmed that the substrate consists of the borosilicate glass functional units. For the P25 samples, no significant peaks were observed.

3.2. UV Intensity

The intensity of the UV radiation at 365 nm passing through the membrane substrate was measured at 0.45 mW/cm^2 at a distance of 10 cm from the light source. In contrast, 0.00 mW/cm^2 was detected from a similar substrate with the same dimensions made from α-Al_2O_3. The sintered glass substrate is therefore better at conducting light than typical alumina substrates commonly used to make ceramic membranes.

3.3. Degradation of Screened Methyl Orange

Figure 5 shows relative changes of dye concentration with time for the various batch experiment setups. When light was directed onto the coated surface, about 58% of the dye had been degraded after 5 h (A1). This configuration can work well in cases of low turbidity waters, or low concentration dyes where there is minimal absorption of radiation by organic molecules or scattering and attenuation of radiation by minute particles present in the water. It is also of interest to note that the depth of the liquid above the coated layer was just 2 mm, therefore, no significant absorption of radiation by organic molecules would be expected. To address these limitations, UV directed through the substrate was investigated. After 5 h, the dye degradation percentage was 52% (A2). Although lower than when the UV was directed to the active layer, this configuration can be useful in turbid waters or high concentration organic solutions as mentioned before. The kinetics of screened methyl orange degradation thus showed that UV light could be successfully directed through the substrate to initiate photocatalytic reactions on the coated surface.

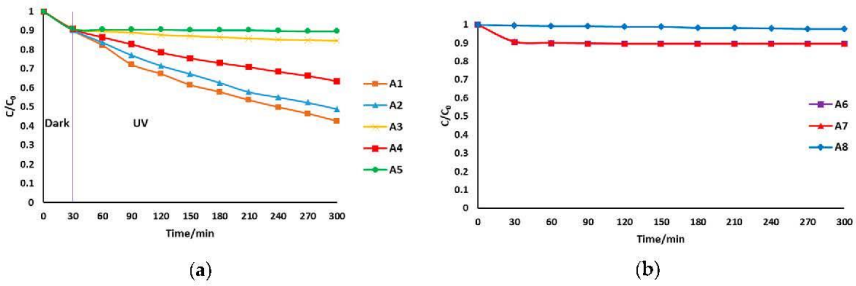

Figure 5. Dye concentration over time (**a**) in the presence of ultraviolet (UV); over the active layer (A1), through the substrate (A2), reflected (A3), through the substrate but reflection eliminated (A4), uncoated membrane (A5). (**b**) Adsorption by coated membrane (A6), adsorption by uncoated membrane (A7) and photolysis (A8).

Table 3 shows the pseudo first order reaction rates of dye degradation through directing UV over the active layer (A1) and through the substrate (A2). The dye degradation in the other setups does not fit pseudo first order kinetics.

Table 3. Pseudo first order kinetics of the sMO degradation.

Configuration	UV Application Method	k (min^{-1})	R^2
A1	Over active layer	0.0030	0.9869
A2	Through substrate	0.0025	0.9871

With regards to A2, there is the possibility that the apparent dye degradation was simply due to light reflected by the base of the reaction vessel. To remove any doubt, A3 was setup to determine the effect of reflected light on dye degradation, and about 11% degradation in 5 h was observed. This was almost equal to the apparent loss in dye concentration by adsorption to the membrane only (A6), showing that reflection is not a factor in the experiments. The apparent decrease in the degradation in A4 was due to the fact that the entire radiation from the lamp could not be directed onto the top of the membrane substrate where a collimated UV source would be more successful. Both the uncoated (A6) and coated membranes (A7) had the same dye adsorption capacity, which shows that the TiO_2 layer's main role was more to facilitate photocatalytic degradation than adsorption. An uncoated membrane in the presence of UV (A5) resulted in about 11% dye degradation, which shows that the photocatalytic layer plays an important role in the dye degradation. The amount of dye degraded by photolysis was less than 2.5% (A8). The largest contributor to dye degradation was therefore photocatalysis, followed by adsorption.

The rate constant obtained when directing light through the substrate is comparable to other results in the literature in Table 4. In all literature cases, UV was directed over the active layer. The configuration used in this study can therefore give dye degradation rates which are comparable to those in the conventional configuration, while also utilizing the advantages mentioned earlier.

Table 4. Comparison of first order kinetics of directing UV to literature values.

Membrane	Target Compound	k (min^{-1})	R^2	UV Intensity (mW/cm^2)	Reference
TiO_2/PMMA	~0.01 mM MB	0.003	-	1.1	[20]
TiO_2/PES	~0.03 mM MO	0.004	0.99849	-	[17]
TiO_2/GO-Psf	~0.2 mM MB	0.004	-	-	[21]
TiO_2/Fibreglass	~0.02 mM MB	0.004	-	-	[11]
TiO_2/SiO_2	~0.01 mM MB	0.006	0.99	5	[22]
TiO_2/Sintered glass	0.01 mM sMO	0.003	0.9871	0.45	This work

3.4. Membrane Selectivity and Regeneration after HA Fouling

The BSA rejection of the substrate (measured by TOC) was found to be 11%, while that of the TiO_2 coated membrane was 25%. Although BSA rejection increased slightly after coating the substrate, it is still low, indicating the membrane filtering in the microfiltration range.

Figure 6 shows the relative pressure change over the course of filtration of HA and simulated tap water. At the initial stage of simulated tap water filtration, there are no significant pressure changes due to the absence of foulants. The observed TMP is necessary to overcome the intrinsic membrane resistance. The value of P_0 was 13 ± 2 kPa for the membranes. As soon as the feed is changed to a HA at 30 min, the TMP starts to rise due to fouling on the membrane surface. When there is no cleaning of the membrane that is carried out (B1), there is only a small pressure relief when the system is opened at 60 and 90 min. However, as soon as the filtration is restarted, the TMP quickly rises to values that are higher than before the system opening event. By the end of the 120 min filtration period, the TMP in B1 rises by more than 700% since the start of the filtration process. In contrast, cleaning the membrane by exposing the active layer to UV (B2) resulted in significant restoration of the membrane such that the final TMP is about 500% of the initial. This is also the case with UV exposure through the substrate (B3) and chemical cleaning (B5). Rinsing the membrane in DI water (B4) was the least effective in membrane regeneration. It is suggested that HA molecules penetrate the membrane pores, making it impossible to remove by simple water rinsing [23]; therefore, methods which breakdown the HA molecules would be more effective in mitigating fouling. Each UV cleaning step brings the TMP very close to the initial pressure, and the pressure rise thereafter does not reach the levels seen in the case where no cleaning takes place. UV exposure thus facilitates the photocatalytic degradation of HA molecules deposited on the membrane, which helps to regenerate the membrane.

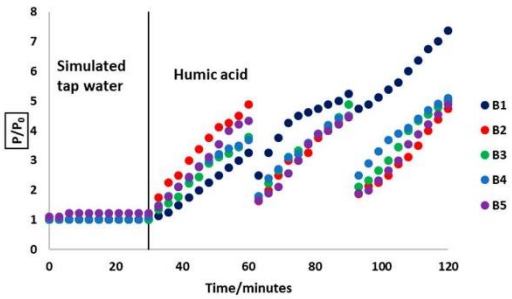

Figure 6. The variation of normalized pressure during filtration and between the cleaning procedures in which no cleaning was employed (B1); UV was applied over the active layer (B2); UV was directed through the substrate (B3); membrane was rinsed in DI water (B4); and membrane was rinsed in chemicals (B5).

Table 5 shows the apparent fouling rates that depict the different rates of foulant buildup on the membrane surface between the two cleaning events. Directing UV over the active layer (B2) resulted in the lowest rate of fouling, as was chemical cleaning (B5). This was closely followed by directing UV through the substrate (B3). Rinsing the membrane in DI water (B4) was the least effective in reducing the fouling rate since it had the closest rate to when no cleaning method was employed (B1).

Table 5. Apparent fouling rate.

Designation	Cleaning Method	Fouling Rate (kPa/min)
B1	No cleaning employed	0.60
B2	UV exposure over the active layer	0.07
B3	UV exposure through the substrate	0.10
B4	Rinsing in DI water	0.23
B5	Rinsing in chemical solutions	0.07

As shown in Table 6, UV exposure on the active layer gives an 84% cleaning efficiency compared to 83% for chemical cleaning and 72% through the substrate for the first cleaning cycle. The second B2 cycle gives decreased cleaning efficiency because the non-reversible fouling layer shields radiation from fully accessing the photocatalytic sites. However, when UV is directed through the substrate in B3, there is only a slight decrease in efficiency, because the radiation path is still relatively free from interfering HA molecules. In long term use, the principle can be useful in maintaining the efficiency of the photocatalytic membrane regeneration process. Since the concept has been proved to work ex-situ, it is important to verify it in situ for longer term fouling mitigation. If a UV source, such as LED lights, is incorporated into the module, such that it can illuminate the photocatalyst through the substrate, continuous photocatalytic degradation of foulants can take place. The filtration process can therefore continue for longer, minimizing or even eliminating any form of physical or chemical cleaning.

Table 6. Cleaning efficiencies of each method.

Designation	Cleaning Method	Cleaning Efficiency %	
		Cycle 1	Cycle 2
B1	No cleaning employed	33	12
B2	UV exposure over the active layer	84	75
B3	UV exposure through the substrate	72	71
B4	Rinsing in DI water	70	57
B5	Rinsing in chemical solutions	83	77

The membrane was fabricated on top of a low cost, readily available sintered glass disc substrate for proof of principle testing. However, in considering the potential cost of the membranes for full scale water treatment, a substrate geometry and size suitable for practical applications in filtration is unknown and is the subject of future studies.

4. Conclusions

A light-conducting photocatalytic membrane was successfully prepared by dip coating TiO_2 onto a sintered glass substrate. The membrane could conduct sufficient UV radiation to facilitate the photocatalytic degradation of sMO. It was shown to be capable of conducting UV for the purposes of mitigating HA fouling ex situ. Directing UV over the active layer showed the best membrane regeneration efficiency in the first cycle, followed by chemical cleaning. However, directing UV through the substrate had the best maintenance of efficiency across two cleaning cycles. The method is therefore of interest for further study during in-situ membrane cleaning over prolonged filtration periods.

Author Contributions: The experimental work was designed and carried out by L.T.N. under the guidance and supervision of M.C.D., S.C., D.N. and B.Z. M.C.D. helped to develop the concept. L.T.N. wrote the manuscript and all authors reviewed and edited it. Conceptualization, L.T.N. and M.C.D.; Formal analysis, L.T.N.; Investigation, L.T.N.; Methodology, L.T.N.; Project administration, L.T.N.; Resources, B.Z.; Supervision, D.N., S.C. and M.C.D.; Validation, L.T.N.; Visualization, L.T.N.; Writing—original draft, L.T.N.; Writing—review & editing, B.Z., D.N., S.C. and M.C.D.

Funding: This research received no external funding.

Acknowledgments: The work was supported by the Victoria University International Postgraduate Scholarships (VUIPRS). The XRD training by Dr. Ikechukwu Anthony Ike is acknowledged. We acknowledge the assistance of Dr. Zongli Xie and Guang Yang for facilitating porometry measurements at CSIRO, Clayton, Australia. The support from the team in the Victoria University Institute for Sustainable Industries and Liveable Cities (ISILC) and the technical staff in the Victoria University College of Science and Engineering is also acknowledged.

Conflicts of Interest: The authors declare no conflict of interest.

References

1. Distefano, T.; Kelly, S. Are we in deep water? Water scarcity and its limits to economic growth. *Ecol. Econ.* **2017**, *142*, 130–147. [CrossRef]
2. Alamelu, K.; Jaffar Ali, B.M. TiO_2-Pt composite photocatalyst for photodegradation and chemical reduction of recalcitrant organic pollutants. *J. Environ. Chem. Eng.* **2018**, *6*, 5720–5731. [CrossRef]
3. Jiang, L.; Choo, K.-H. Photocatalytic mineralization of secondary effluent organic matter with mitigating fouling propensity in a submerged membrane photoreactor. *Chem. Eng. J.* **2016**, *288*, 798–805. [CrossRef]
4. Madaeni, S.S.; Ghaemi, N. Characterization of self-cleaning RO membranes coated with TiO_2 particles under UV irradiation. *J. Membr. Sci.* **2007**, *303*, 221–233. [CrossRef]
5. Geng, Z.; Yang, X.; Boo, C.; Zhu, S.; Lu, Y.; Fan, W.; Huo, M.; Elimelech, M.; Yang, X. Self-cleaning anti-fouling hybrid ultrafiltration membranes via side chain grafting of poly(aryl ether sulfone) and titanium dioxide. *J. Membr. Sci.* **2017**, *529*, 1–10. [CrossRef]
6. Guo, B.; Pasco, E.V.; Xagoraraki, I.; Tarabara, V.V. Virus removal and inactivation in a hybrid microfiltration–UV process with a photocatalytic membrane. *Sep. Purif. Technol.* **2015**, *149*, 245–254. [CrossRef]
7. Leong, S.; Razmjou, A.; Wang, K.; Hapgood, K.; Zhang, X.; Wang, H. TiO_2 based photocatalytic membranes: A review. *J. Membr. Sci.* **2014**, *472*, 167–184. [CrossRef]
8. Starr, B.J.; Tarabara, V.V.; Herrera-Robledo, M.; Zhou, M.; Roualdès, S.; Ayral, A. Coating porous membranes with a photocatalyst: Comparison of LbL self-assembly and plasma-enhanced CVD techniques. *J. Membr. Sci.* **2016**, *514*, 340–349. [CrossRef]
9. Li, S.; Hu, J. Transformation products formation of ciprofloxacin in UVA/LED and UVA/LED/TiO_2 systems: Impact of natural organic matter characteristics. *Water Res.* **2018**, *132*, 320–330. [CrossRef]
10. Khatibnezhad, H.; Sani, M. Preparation and characterization of nanostructured TiO_2 thin film codoped with nitrogen and vanadium on glass surface by sol-gel dip-coating method. *Res. Chem. Intermed.* **2015**, *41*, 7349–7361. [CrossRef]

11. Coto, M.; Troughton, S.C.; Duan, J.; Kumar, R.V.; Clyne, T.W. Development and assessment of photo-catalytic membranes for water purification using solar radiation. *Appl. Surf. Sci.* **2018**, *433*, 101–107. [CrossRef]
12. Dehghani, M.H.; Zarei, A.; Mesdaghinia, A.; Nabizadeh, R.; Alimohammadi, M.; Afsharnia, M.; McKay, G. Production and application of a treated bentonite–chitosan composite for the efficient removal of humic acid from aqueous solution. *Chem. Eng. Res. Des.* **2018**, *140*, 102–115. [CrossRef]
13. Fan, H.; Xiao, K.; Mu, S.; Zhou, Y.; Ma, J.; Wang, X.; Huang, X. Impact of membrane pore morphology on multi-cycle fouling and cleaning of hydrophobic and hydrophilic membranes during MBR operation. *J. Membr. Sci.* **2018**, *556*, 312–320. [CrossRef]
14. Hatat-Fraile, M.; Liang, R.; Arlos, M.J.; He, R.X.; Peng, P.; Servos, M.R.; Zhou, Y.N. Concurrent photocatalytic and filtration processes using doped TiO_2 coated quartz fiber membranes in a photocatalytic membrane reactor. *Chem. Eng. J.* **2017**, *330*, 531–540. [CrossRef]
15. Shamaila, S.; Sajjad, A.K.L.; Chen, F.; Zhang, J. Synthesis and characterization of mesoporous-TiO_2 with enhanced photocatalytic activity for the degradation of chloro-phenol. *Mater. Res. Bull.* **2010**, *45*, 1375–1382. [CrossRef]
16. Thamaphat, K.; Limsuwan, P.; Ngotawornchai, B. Phase Characterization of TiO_2 Powder by XRD and TEM. *Nat. Sci.* **2008**, *42*, 357–361.
17. Hir, Z.A.M.; Moradihamedani, P.; Abdullah, A.H.; Mohamed, M.A. Immobilization of TiO_2 into polyethersulfone matrix as hybrid film photocatalyst for effective degradation of methyl orange dye. *Mater. Sci. Semicond. Process.* **2017**, *57*, 157–165. [CrossRef]
18. Kaur, R.; Singh, S.; Pandey, O.P. Influence of CdO and gamma irradiation on the infrared absorption spectra of borosilicate glass. *J. Mol. Struct.* **2013**, *1049*, 409–413. [CrossRef]
19. Ebrahimi, E.; Rezvani, M. Optical and structural investigation on sodium borosilicate glasses doped with Cr_2O_3. *Spectrochim. Acta Part A Mol. Biomol. Spectrosc.* **2018**, *190*, 534–538. [CrossRef]
20. Cantarella, M.; Sanz, R.; Buccheri, M.A.; Romano, L.; Privitera, V. PMMA/TiO_2 nanotubes composites for photocatalytic removal of organic compounds and bacteria from water. *Mater. Sci. Semicond. Process.* **2016**, *42*, 58–61. [CrossRef]
21. Gao, Y.; Hu, M.; Mi, B. Membrane surface modification with TiO_2–graphene oxide for enhanced photocatalytic performance. *J. Membr. Sci.* **2014**, *455*, 349–356. [CrossRef]
22. Geltmeyer, J.; Teixido, H.; Meire, M.; Van Acker, T.; Deventer, K.; Vanhaecke, F.; Van Hulle, S.; De Buysser, K.; De Clerck, K. TiO_2 functionalized nanofibrous membranes for removal of organic (micro)pollutants from water. *Sep. Purif. Technol.* **2017**, *179*, 533–541. [CrossRef]
23. Li, X.; Li, J.; Fang, X.; Bakzhan, K.; Wang, L.; Van der Bruggen, B. A synergetic analysis method for antifouling behavior investigation on PES ultrafiltration membrane with self-assembled TiO_2 nanoparticles. *J. Colloid Interface Sci.* **2016**, *469*, 164–176. [CrossRef] [PubMed]

© 2018 by the authors. Licensee MDPI, Basel, Switzerland. This article is an open access article distributed under the terms and conditions of the Creative Commons Attribution (CC BY) license (http://creativecommons.org/licenses/by/4.0/).

APPENDIX 2: PUBLISHED PAPER FOR CHAPTER 4

Journal of Membrane Science 604 (2020) 118018

Contents lists available at ScienceDirect

Journal of Membrane Science

journal homepage: http://www.elsevier.com/locate/memsci

Light conducting photocatalytic membrane for chemical-free fouling control in water treatment

Lavern T. Nyamutswa [a], Bo Zhu [a], Stephen F. Collins [b], Dimuth Navaratna [a,b], Mikel C. Duke [a,*]

[a] Institute for Sustainable Industries and Liveable Cities, Victoria University, Melbourne, Australia
[b] College of Engineering and Science, Victoria University, Melbourne, Australia

ARTICLE INFO

Keywords:
Membrane fouling
Photocatalytic membrane
Self-cleaning
Water treatment

ABSTRACT

This work shows for the first time the convenient *in situ* UV illumination of a titanium dioxide (TiO_2) photocatalytic membrane via a sintered porous glass substrate for effective fouling reduction during water treatment. By directing light through the light conducting glass substrate, this concept overcomes the current challenge of photocatalytic membranes that direct light through turbid, light obstructing feed waters. Fouling was tested by filtering model solutions of humic acid (HA), bovine serum albumin (BSA) or sodium alginate (SA). Photocatalysis initiated by simply directing light via the permeate side through the porous glass substrate led to significant reductions in trans-membrane pressure (TMP) rise rates between backwashes and all model organic fouling compounds. Specifically, the UV-light exposed membranes showed a 3.0-fold and 2.4-fold reduction in total filtration resistance for BSA and SA solutions, respectively, which also showed 2.7-fold and 4.2-fold reductions in the irreversible fouling indices. Analysis by SEM coupled with fouling modelling showed the beneficial anti-fouling effects stemmed from reduced intrusion of organic material inside the TiO_2 membrane pores, as well as reduced cake layer resistance. The novel, convenient light conducting photocatalytic membranes concept could be used for sustainable, low-chemical membrane filtration of polluted water.

1. Introduction

Membrane filtration processes are an attractive solution to pathogen and contaminant removal in water because of their proven effectiveness even at low contaminant concentrations [1] to meet water quality standards and guidelines [2,3]. However, since membranes only provide a barrier for separation of contaminants from water, disposing of the separated waste generated from the process becomes a new challenge. Membrane fouling is also a major drawback which reduces separation efficiency, permeate flux [4], membrane lifespan [5] and increases transmembrane pressure (TMP) required to maintain flux. Membrane fouling also necessitates more frequent chemical cleaning of the membrane [6]. Adopting a method to minimise or reverse membrane fouling is the reality of all membrane processes. Modern research studies could contribute to minimisation and control of membrane fouling, allowing the wider adoption of membrane technology in the water treatment industry.

Membrane anti-fouling techniques such as chemical, hydraulic, physical or electrical cleaning of the membrane pose undesirable elements to the process such as downtime, increased running costs and inflicting damage to the membrane. Chemical cleaning in particular gives rise to the need for purchasing of chemicals, transportation and safe storage, followed by correct use and handling, which requires some level of expertise, and their eventual safe disposal. All these come at a significant cost which increases the price of treated water. In some communities such as rural and remote areas, membrane chemical cleaning, and thus membrane water treatment, is not a viable option because of a lack of the required resources.

To address these challenges, photocatalysis could be adopted to improve the filtration performance of membranes as an *in-situ* method of fouling management. By immobilising heterogeneous semiconductor photocatalysts such as titanium dioxide (TiO_2) on the membrane surface, the separation function of membranes and the oxidative degradation ability of photocatalysts could be combined into one unit to give a superior hybrid membrane material [7]. As the membrane separates the targeted water contaminants, the photocatalyst degrades them into non-harmful, smaller molecules [8], which has a double-edged positive effect. Firstly, the degradation prevents accumulation of the contaminants on the membrane surface and hence, contributes to resolving the excessive fouling of the membrane and enable high flux/low pressure

* Corresponding author.
E-mail address: mikel.duke@vu.edu.au (M.C. Duke).

https://doi.org/10.1016/j.memsci.2020.118018
Received 17 December 2019; Received in revised form 4 February 2020; Accepted 22 February 2020
Available online 7 March 2020
0376-7388/© 2020 Elsevier B.V. All rights reserved.

performance. Secondly, by preventing the accumulation of foulants on the membrane, the secondary waste disposal problem from using maintenance cleaning chemicals would be avoided. Such hybrid membranes are aptly dubbed "self-cleaning", in that they continuously regenerate themselves without the need to apply some external cleaning method [5].

Also occurring simultaneously with oxidative degradation to reduce membrane fouling is induced super-hydrophilicity. In this phenomenon, radiation energy provided by an energy source, such as a UV lamp or sunlight, results in the creation of electron-hole pairs on the TiO_2 photocatalyst coated membrane surface. The photo-generated hole then weakens the bond between titanium and the lattice oxygen atom, resulting in it being broken by water adsorbed to the membrane surface to form new Ti–OH bonds [9]. These new hydroxyl groups on the membrane surface induce super-hydrophilicity, which prevents hydrophobic compounds from attaching to the membrane, thus keeping it free from foulants.

Photocatalytic membrane technology, however, also consists of a significant number of challenges. To start with, for the photocatalytic process to be activated, light of the correct wavelength needs to be supplied to the membrane surface at sufficient intensities [10]. One of the main challenges which is of interest in membrane photocatalysis is how to supply this light to the photocatalyst. Ever since the photocatalytic membrane was developed, the traditional approach to deliver light to the membrane was to transmit light through the contaminated water being treated. This approach is a recognised operational challenge in photocatalytic membrane technology, because of the high propensity of light to be absorbed and scattered by the water contaminants before the light rays reach the photocatalyst coated active layer of the membrane. This becomes an even more significant challenge in turbid waters where such light attenuation considerably reduces the efficiency of the photocatalytic process [11].

Having recognised this challenge, Starr et al. [11] adopted a novel approach of immobilising the photocatalyst onto the membrane's substrate support side instead of the functional active layer, as shown in Fig. S1. The main motivation in this approach was to deliver light through the permeate, which is less turbid, and therefore, results in less light scattering. Even though this method combines the separation ability of a membrane and degradation function of photocatalysis, the processes occur on different surfaces, and hence the anti-fouling ability of photocatalysis does not exist in this membrane separation configuration.

Horovitz et al. [12] also attempted an alternative method of delivering light by directing it from the permeate stream, with the membrane prepared in the traditional way of immobilising the photocatalyst on the membrane separation layer. In this approach, water flows from the substrate, non-functional side of the membrane, meaning that it can reach the photocatalytic layer when it is still significantly contaminated. The schematic of their approach is shown in Fig. S2. While both cases showed potential by harnessing the cleaner permeate side to better facilitate the introduction of UV light to the membrane, they still do not conform to the traditional well-known format of high performance membranes involving raw water being fed directly to the selective layer with inbuilt anti-fouling functionality.

In this study, we proposed a novel alternative approach to overcome the challenges of directing light from the source to the photocatalyst coated active layer of the membrane. This concept, previously demonstrated and validated by our research group in *ex-situ* tests [13], directs light to the photocatalytic layer through a light conducting, low cost sintered porous glass substrate. By adopting this configuration in which light is directed from the end of an element through the membrane substrate, the nature of water being treated becomes a less significant factor in determining the efficiency of the photocatalytic process than in current configurations. The previous results confirmed that light could be directed successfully through the substrate to achieve a photocatalytic effect on the membrane surface. The preliminary experiments also showed that the configuration could be adopted for *ex-situ* control of membrane fouling. However, an *in-situ* demonstration within the industry-standard pressurised dead-end membrane filtration (with backwashing) format is clearly needed for the practical implementation of this concept. The working principle is depicted in Fig. 1. In this article, this novel approach is demonstrated for the first time as an effective strategy for *in-situ* control of membrane fouling.

The impact of organics on membrane performance was considered as the basis for measuring beneficial effects from the photocatalytic action. Model solutions of typical organic water contaminants were filtered through the membrane to observe anti-fouling and separation behaviour. In this study, three types of organic compounds found in water were used. These are humic acid (HA), as a representative of humic substances, sodium alginate (SA), representing polysaccharides and bovine serum albumin (BSA), a common water-borne protein. Apart from being undesirable water contaminants [14] these three groups of organic compounds were specifically chosen because they are known to be chiefly responsible for irreversible fouling in membrane water treatment [15].

2. Experimental

2.1. Materials

Analytical grade chemicals were used in the experiments. NaOH (Fischer Scientific, Loughborough, UK) and NaOCl (Sigma Aldrich, St. Louis, MO, USA) were used to prepare solutions for chemical cleaning of membrane substrates.

NaCl (Ajax Finechem, Scoresby, Australia) and $CaCl_2$ (Sigma Aldrich, St. Louis, MO, USA) were used to add ions to synthetic water contaminant solutions. Ions were added to synthetic contaminated water to mimic the ionic load in surface/ground water. HA (Fluka AG Cheische Fabrik., Buchs, Switzerland) was used as a representative natural organic matter (NOM) water contaminant. BSA (Sigma Aldrich, St. Louis, MO, USA) of average molecular weight 66 kDa was used as a representative protein water contaminant. SA (Ajax Chemicals, Melbourne, Australia) was used as a representative polysaccharide water contaminant as well as a binder in the preparation of membranes.

P25 TiO_2 nanoparticles with 99.8% purity and a composition of 80% anatase and 20% rutile phases, average particle size of 30 nm and a specific surface area of 50 m^2/g were acquired from Degussa AG, Frankfurt, Germany. When dispersed in water, the hydrodynamic size of P25 particles is known to increase from a few nanometres up to 300 nm [16,17]. Sintered glass discs of 25 mm diameter, 2 mm thickness and G5 porosity were sourced from Ningbo Ja-Hely Technology Co., Ltd., Ningbo, China.

2.2. Apparatus and equipment

A sonic bath (Soniclean 500HT, Transtek Systems, Melbourne, Australia) was used to enhance membrane cleaning before the TiO_2 coating was applied, as well as for removing air bubbles and breaking aggregates in the coating suspension. A fan forced oven (S.E.M Equipment, Australia) was used for drying wet membranes after dip coating. A programmable Vulcan 3-550PD NEY furnace (Extech Equipment, Victoria, Australia) was used for sintering the membranes after coating and drying. During filtration, the membrane was placed between two rubber O-rings in a custom-made stainless steel filtration module, to give an effective membrane area of 2.5 cm^2. A 1.2 W, 365 nm ultraviolet light emitting diode (UV-LED) acquired from DigiKey Electronics, Minnesota, USA was placed underneath the module for delivering UV radiation through the membrane substrate to the TiO_2 layer. The spectral output and radiation pattern data of the LED were obtained from the product data sheet [18]. The LED has a narrow emission bandwidth and a spectral line half width of 15 nm, with the maximum power output occurring at 365 nm. The LED therefore emits most of its power in the

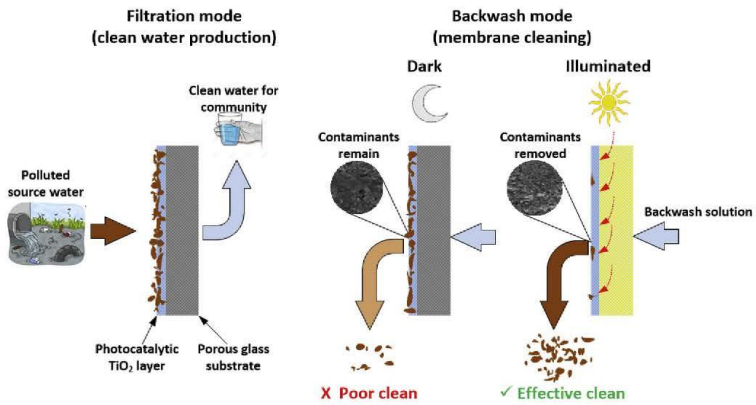

Fig. 1. Chemical-free fouling management by illuminating light-conducting photocatalytic membrane with a light source.

wavelength band of interest for activating TiO_2 [19]. The beam angle of about 45° and a distance of 2 cm between the LED and the membrane allows the radiation to be spread more evenly throughout the membrane. To prevent the LED from overheating, it was connected to a microcontroller board (Arduino, Ivrea, Italy) to enable pulse width modulation. For each pulse period of 2.04 ms, the LED ON time was set at 15% of period duration, allowing cooling for 85% of the period duration. The voltage across the LED was 2.2 V and the current was reduced to 260 mA, from 300 mA. Reducing the power at which the LED operates also assists in lowering the operating temperature and prolonging the life of the LED. A quartz window was fixed in a hole made in the steel module to allow UV from the LED to pass through. The UV intensity emitted by the LED was measured by a UV irradiance meter (Photoelectric Instrument Factory of Beijing Normal University, Beijing).

Changes in TMP during filtration were recorded using a TPI 665L digital manometer from Accutherm, Melbourne, Australia. Changes in the temperature of the module were monitored through an Ulirvision TI384 infrared camera from OneTemp Pty. Ltd., Melbourne, Australia. The feed was driven through the filtration system by a QG20 positive displacement pump (Fluid Monitoring Inc., Syosset, USA). An electronic balance (FX-3000i WP, A&D Company Ltd., Seoul, South Korea) with real time monitoring software was used to measure the amount of permeate (membrane filtrate) during the experiments. Total organic carbon (TOC) of test solutions was determined from a Shimadzu TOC-V CSH analyser. A UV–visible light spectrophotometer (HACH DR5000, USA) was used to measure specific absorbance at a wavelength of 254 nm (UV254).

2.3. Preparation of coating suspension

5 g of P25 TiO_2 powder was mixed with 60 mL deionised (DI) water for 30 min using a CAT Unidrive X1000 homogenizer operated at a speed of 8500 revolutions per minute (rpm). This part of coating suspension was labelled "Part A", and it was sonicated for 20 min while preparing the Part B of the coating suspension. Part B was prepared by mixing 0.4 g of sodium alginate (SA) with 60 mL of deionised (DI) water for 30 min using the homogenizer. Care was taken to add alginate powder to water at a very slow rate to prevent it from sticking to the homogenizer blades. Part B was then added to Part A in little quantities while mixing the two parts of coating suspension with the help of the homogenizer. The mixture was further homogenized for 30 min at a speed of 15 000 rpm, followed by the sonication process for 30 min. The prepared coating suspension was transferred into a 200 mL beaker and magnetically stirred for 2 h prior to coating to maintain homogeneity.

2.4. Preparation of photocatalytic membranes

Each of the membrane substrates was sonically cleaned with a succession of 1% NaOH solution, 0.5% NaOCl and DI water for 20 min and then dried at 80 °C for 3 h in a fan-forced oven. The membranes were weighed and covered with autoclave tape on the non-functional side on which a TiO_2 coating was not required. A custom made mechanical device was used to dip and withdraw the membrane at a speed of 2 cm/min. The membrane was kept in the suspension for 3 min before withdrawing it. After the coating procedure, the membrane was air dried for 12 h and the autoclave tape was removed before it was heated to 450 °C at a rate of 1 °C/min in a programmable muffle furnace. The temperature was maintained at 450 °C for 2 h, followed by cooling to room temperature at a rate of 1 °C/min. After this heat treatment process, the membranes were washed with DI water and oven dried at 80 °C for 2 h.

2.5. Characterisation of membranes

The topographical features and elemental composition of the membranes were analysed by a Field Emission Scanning Electron Microscope (FESEM) and an Energy Dispersive Spectroscope (EDS), respectively. First, the samples were mounted on aluminium stubs with double-sided conductive carbon tape and sputter coated (60 mA for 50 s) with an approximately 4 nm thick iridium coating using a Cressington 208HRD sputter coater. The conducting coating assists in preventing charge accumulation and obtaining clear images. After applying the coating, the samples were imaged using a Zeiss Merlin Gemini 2 FESEM instrument operated in the secondary electron (SE) mode and an accelerating voltage of 5 kV. For element identification, the accelerating voltage was set at 15 kV and an EDS detector (80 mm^2 X-Max) equipped with AZTEC software (Oxford Instruments Pty Ltd) was used.

The pore size of the substrate and membrane were determined via capillary flow porometry using a Quantachrome Porometer 3 GZ series from Quantachrome Corp., Boynton Beach, FL, USA. The instrument measures the flow of nitrogen gas through the dry and wet (using a wetting liquid) membrane samples as a function of TMP and then calculates the pore size using the Washburn equation. Porofil™ from Quantachrome Corp., Boynton Beach, FL, USA was used as the wetting liquid in this study.

2.6. Filtration experiments

The membrane filtration setup which was used in this study is depicted in the schematic diagram in Fig. 2. The filtration setup includes a feed tank, a positive displacement pump, membrane module, 5 solenoid valves connected to a logic controller, a pressurised tank for backwashing, a digital manometer, a retentate collection tank, a permeate collection tank placed on an electronic balance and 2 data loggers to record pressure and permeate volume. To ensure safety from UV radiation, the module was housed in a metal box on which a switch deactivated by opening the box's door was installed. Filtration was carried out in the dead-end mode at constant flux. Backwashing and filtration mode were determined by programmed opening or closing of the appropriate valves, labelled V-1 to V-5.

2.6.1. Experiments with HA

Membrane filtration experiments with HA solutions were carried out at a constant permeate flux of 450 L/(m^{2}h). The membrane was initially compacted with 20 mg/L NaCl solution for 1 h to give a steady state pressure, followed by a 20 mg/L HA [12] and 100 mg/L NaCl solution. NaCl was added to DI water since surface and ground water systems always contain some salts. Filtration was conducted in a dead end mode in which the UV-LED was either switched ON (light) or OFF (dark) to induce the effects of photocatalysis and super-hydrophilicity to alter membrane fouling, which was measured in our work through the variation of TMP. Uncoated sintered glass substrates were also used in these experiments and considered for control experiments purposes.

2.6.2. Experiments with BSA and SA

Membranes were compacted with 100 mg/L NaCl solution for 1 h followed by a 50 mg/L solution of BSA, which also contained 5 mg/L $CaCl_2$ and 20 mg/L NaCl. Backwashing of the membrane was achieved by opening appropriate valves to allow 100 mg/L NaCl to flush the membrane from the permeate side at 1 h intervals. Backwash duration was 1 min and the pressure was set at 200 kPa. Filtration was conducted in a dead end mode in which the UV-LED was either switched ON (light) or OFF (dark). The same procedure was followed for 20 mg/L SA containing 5 mg/L $CaCl_2$ and 20 mg/L NaCl. The operating flux was set at 70 L/(m^{2}h) for SA and 100 L/(m^{2}h) for BSA. These were chosen to be above the critical flux to demonstrate a positive effect from the action of the photocatalysis as compared to when no light is applied.

2.7. Evaluation of membrane cleaning efficiency

The cleaning efficiency of the photocatalytic membranes was evaluated through the recorded trend of TMP, the hydraulic cleaning efficiency (HCE) and the hydraulically irreversible fouling index (HIFI).

HCE was determined from Equation (1), which calculates the fouling reversibility after each filtration cycle n [20]:

$$HCE = \sum_{n=1}^{k} \frac{HCE(n)}{k} = \frac{P_f^n - P_{ini}^{n+1}}{P_f^n - P_{ini}^n} \quad (1)$$

where P_{ini}^n and P_f^n are the initial and final TMP values of cycle n respectively, and P_{ini}^{n+1} is the initial TMP value of cycle n+1.

The HIFI, an indication of fouling which could not be reversed by backwashing and/or the photocatalytic effect, was calculated using Equation (2) [13]:

$$1/J_s' = 1 + (HIFI)V_s \quad (2)$$

where J_s' is the normalised specific flux, which is replaced by $(J/P_{ini})/(J/P_0) = P_0/P_{ini}$ when the filtration is carried out under constant flux. P_0 (kPa) is the TMP of fresh membrane, and P_{ini} is the initial TMP after each backwashing event, and V_s (L/m^2) is the total volume of filtrate per unit membrane area.

The HIFI fouling index model is not attributed to a specific fouling mechanism, therefore it could be used for all fouling mechanisms such as pore narrowing/blocking and cake formation, or a combination of both [20].

If the plot of $(1/J_s')$ versus (V) is linear, i.e. the rate of increase in filtration resistance is linearly proportional to V, the HIFI can be quantified using linear regression. In instances where a linear function cannot be obtained, a 2 point method can be used to determine the HIFI. In this case, instead of using all performance data, the first and the last points are used to calculate the average rate of increase in filtration resistance [20].

2.8. Fouling mechanism

Fouling of the membrane can occur either through pore blocking or the formation of a cake layer on the surface of the membrane, leading to filtration resistance. The mechanism of fouling that occurred was determined from observing SEM images of the membranes as well as applying the resistance-in-series model.

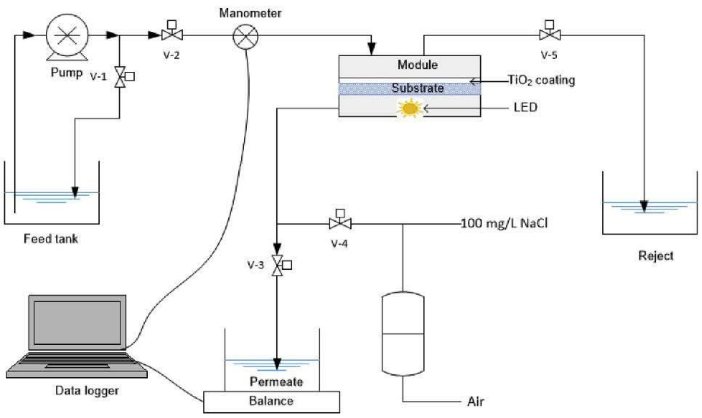

Fig. 2. Schematic diagram of the filtration system used in this study.

The resistance-in-series model [21] was used to analyse and calculate the total membrane resistance (R_t), which has contributions from the intrinsic membrane resistance (R_m), resistance due to pore blocking (R_p) and resistance due to cake formation (R_c).

$$R_t = R_m + R_p + R_c \tag{3}$$

R_m and R_p make up the internal membrane resistance, R_f.

$$R_f = R_m + R_p \tag{4}$$

At constant flux, J, the resistance can be determined from Equation (5),

$$J = \frac{P}{\mu R} \tag{5}$$

where P is the TMP (Pa), μ is the solution viscosity (Pa.s) and R is either R_t, R_m or R_f, depending on the experimental conditions.

R_t can be estimated from Equation (5) by finding J and P from the filtration experiments of either using BSA or SA solution at constant flux. In this study, J and P measurements were taken at 6 h. R_m was also obtained from Equation (5) after obtaining the results from the pure water filtration experiments. To obtain R_f, Equation (5) was applied after gently wiping the BSA or SA fouled membrane with a wet sponge and rinsing it with water to remove the cake layer, then filtering pure water through it. R_p was then calculated from Equation (4), and R_c from Equation (3) [22].

3. Results and discussion

3.1. Membrane morphology and composition

The bare sintered porous glass substrate which was used in this study was composed of micro-sized particles as seen from the SEM image shown in Fig. 3(a). The coating procedure described in Section 2.4 resulted in the achievement of complete coverage of the substrate surface with TiO_2 nano-sized particles, as shown in Fig. 3(b) and (c). The thickness of the TiO_2 layer was about 15 μm, as shown in Fig. 3 (c). A set of EDS analyses were also conducted to confirm the effectiveness of the TiO_2 coating procedure adopted in this study. From the EDS results illustrated in Fig. 3(d), a 53.5 wt% of Ti on the functional side of the membrane and just 0.2 wt% silicon shows the effectiveness of the coating method in covering the surface with TiO_2, to the extent that the minor elements Na and Al, which make up borosilicate glass, were not detected. Detection of 0.2 wt% Si on the coated side could also be a result of electron penetration into the underlying substrate. The bare side of the membrane had a composition of 51.6 wt% O, 35.1 wt% Si, 2.6 wt% Na and 1.1 wt% Al, confirming its silicate properties [23].

The membrane pore size data of the membrane determined by capillary flow porometry is shown in Table 1. The average pore size of the P25 coated membrane was 0.53 μm, which is about a third of that of the bare porous glass substrate. The coated membrane is therefore in the MF range, meaning fouling would be expected. Despite the relatively larger pore sizes of MF membranes of more than 0.1 μm, rapid fouling by HA as high as 90% flux decline in 5 min for 100 mg/L HA and 50% flux decline in 5 min for 10 mg/L HA has been reported for MF membranes of 1.9 μm pore size [24]. Fouling is not only determined by the membrane pore size but other factors such as the operating flux or pressure, solution pH, electrostatic interaction of HA with the membrane surface and

Table 1
Pore size data of the membrane determined by capillary flow porometry.

Material	Mean pore size (μm)	Minimum pore size (μm)	Maximum pore size (μm)
Bare substrate	1.4	0.58	2.0
P25 coated membrane	0.53	0.18	1.0

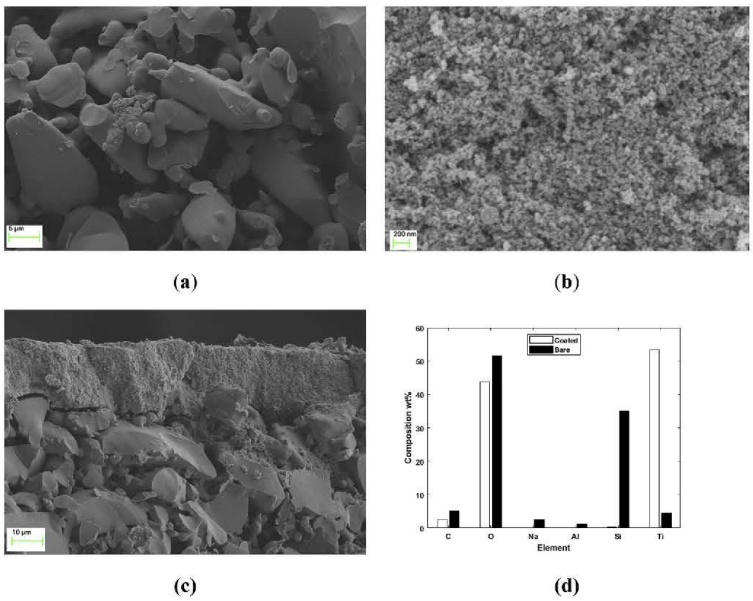

Fig. 3. SEM images of the uncoated membrane (substrate) surface (a), TiO_2 coated membrane surface (b) and membrane cross section (c), and EDS determined elemental composition of the coated and bare side of the membrane (d).

concentration. In conclusion, the MF property of the P25 coated porous glass membrane indicates its suitability for fouling investigation in this study.

The water permeability of the bare and P25 coated membrane was measured at a constant flux of 450 L/(m^2h) and a temperature of 24 °C. Table 2 shows the water permeability results for bare substrate and P25 coated membranes. The reduced pore size of the membrane was also apparent in the reduced pure water permeability of the coated membrane when compared to the bare substrate.

3.2. Light transmittance through the substrate

The light intensity of the UV-LED, measured from a distance of 2 cm, was 12 mW/cm^2. The membranes were wetted with water before intensity measurements to mimic filtration conditions. Measured through the bare substrate, the intensity was 0.45 mW/cm^2, and 0.10 mW/cm^2 through the coated membrane. The reduced transmittance on the coated membrane is due to the fact that some of the light is absorbed by the photocatalyst coating.

From these figures, it is apparent that the substrate absorbs most of the light energy. However, it has been shown that the light that transmits through the substrate is sufficient to facilitate photocatalytic reactions on the membrane surface [13]. Moreover, the intensity of 0.45 mW/cm^2 transmitted through the wet glass substrate is comparable to that applied in other studies that used the traditional light directing configuration. For example, 0.3 mW/cm^2 from visible light LEDs illuminating a nitrogen-doped titania-alumina membrane led to a 57% removal of methylene blue [25] and 0.39 mW/cm^2 from 365 nm LEDs illuminating titania self-assembled on porous TiO_2 sheets led to successful removal of selected estrogens [26]. In future studies, substrates with higher light transmittances could be investigated. A few examples include polylactic acid (PLA) [27], silk fibroin [28], cellulose [29–31], single-walled carbon nanotubes (SWCNTs) [32–34] and free standing graphene oxide [35].

3.3. Filtration of synthetic water containing HA

Fig. 4 shows the TMP profiles under different UV lighting scenarios while filtering HA solution. Fig. 4(a) shows the continuous UV ON and OFF TMP profiles in 6 h of filtration, where only a slight increase in TMP was recorded during the filtration with HA solution when the membrane was illuminated with UV. However, TMP rapidly increased when conducting the experiment without UV illumination. Absence of fouling could be a result of two factors, namely degradation of HA and/or induced hydrophilicity, as discovered by Chen and Poon [9]. However, the bulk degradation was very low as concluded from UV_{254} absorbance and TOC tests. Only a 37% decrease in the UV_{254} absorbance and an insignificant decrease in TOC of permeate stream was recorded during UV illumination. This would be expected because the low contact times with the photocatalyst could not lead to complete mineralisation of HA, or any significant degradation. Hence, the observed anti-fouling behaviour could instead be due to the induced hydrophilicity that occurs on the surface of the TiO_2 coated photocatalytic membrane [4,9]. The hydration layer induced on the membrane surface would prevent HA from attaching to the membrane surface. HAs are known to have a high propensity of irreversibly fouling MF TiO_2 ceramic membranes [36], therefore fouling mitigation by the photocatalytic layer was quite remarkable. When the UV-LED was OFF, the induced beneficial phenomena did not occur, hence the observed TMP rise and fouling mainly due to contact of HA with the membrane, leading to pore blocking [37].

Table 2
Water permeability of the bare substrate and coated membrane measured at a flux of 450 L/(m^2h) and 24 °C.

Material	Pressure (kPa)	Permeability [L/(m^2hPa)]
Bare substrate	4.5 ± 1	0.10 ± 0.01
P25 coated membrane	15 ± 2	0.030 ± 0.002

Fig. 4(b) shows the case where UV ON or OFF status is alternated every two hours. In this test, when the UV was initially ON, a very low rate of increase of fouling during the first two hours occurred, being consistent with the continuous test in Fig. 4(a). In the next 2 h when the UV was OFF, fouling of membrane began to increase at a higher rate, but it significantly slowed again when UV illumination was recommenced for the last two hours. Due to low HA degradation and the fact that the irreversible internal fouling is common in MF membranes when HA is present [37], there was no significant membrane recovery when the LED was switched back to ON, but the beneficial effect of UV light on the TiO_2 surface was enough to prevent further accumulation of HA on the membrane surface.

When the filtration run commenced without UV illumination, TMP rise was very similar to the continuous test in Fig. 4(a) until UV illumination began after 2 h. When illumination began, some recovery of the initial TMP occurred until the TMP rise appeared to cease. The observed recovery in TMP then stops when the rate of degradation becomes less than the rate of deposition, resulting in constant TMP. When there was no UV exposure in the last two hours, a sharp rise in TMP was recorded, demonstrating a higher rate of fouling which interestingly reached the similar TMP value after six hours when no light was used at all (Fig. 4(a)). This strongly suggests that the accumulated organics over the six hour dead-end filtration with no backwash reassembles into a fouling layer of similar flow resistance as that which was made in the absence of photocatalytic activity. The photocatalytic activity appears to inhibit formation of a cohesive fouling layer. The results of this experiment confirmed the effectiveness of continuous UV exposure on to the membrane for controlling HA fouling. Providing UV illumination throughout the filtration run is therefore the most effective way of preventing HA fouling.

The findings of a previous study conducted by Zhu et al. [4] for assessing the mitigation of membrane fouling when UV illumination is present match with the results obtained in our study. They found that photocatalytically partially oxidized humic acid (OHA) reduces the fouling propensity of polyvinylidene fluoride (PVDF) ultrafiltration membranes better compared to purified humic acid (PHA). Over a filtration duration of 140 min, the OHA experiment had a flux 21.3% higher than the PHA experiment. Photocatalytic oxidation facilitated the decomposition of PHA into smaller, more hydrophilic fragments. OHA became softer, weakening its adherence to the membrane and OHA-OHA interactions. Hence, in the study reported in this paper, even though mineralisation of HA did not occur, photocatalysis does change its structure, leading to less adherence to the membrane and less fouling.

3.4. Filtration of synthetic water containing BSA

Fig. 5 shows the SEM surface images of membranes fouled under different test conditions while filtering BSA solution as well as the TMP profiles and fouling layer elemental composition. Fig. S3 shows a membrane cross section after filtration of BSA. There was no noticeable change in the TiO_2 layer thickness after the filtration processes. However a denser coating of about 1 μm can be seen that is likely to be the organic fouling material on the membrane surface. The SEM image shown in Fig. 5 (a) shows that filtration of BSA solution with UV exposure resulted in the foulant being retained in the form of flakes on the membrane surface, leading to a 70% removal of TOC. It was found that the fouling could be easily reversed by backwashing, as the BSA flakes were loosely deposited on the membrane, resulting in better membrane restoration, as shown in Fig. 5 (b). Without UV illumination, the foulant tended to penetrate pores rather than being retained on the membrane surface, as shown in Fig. 5 (c). This led to poor restoration of the membrane after backwashing, as shown in Fig. 5 (d). As seen in Fig. 5(f), an increase of the amount of carbon deposited on the

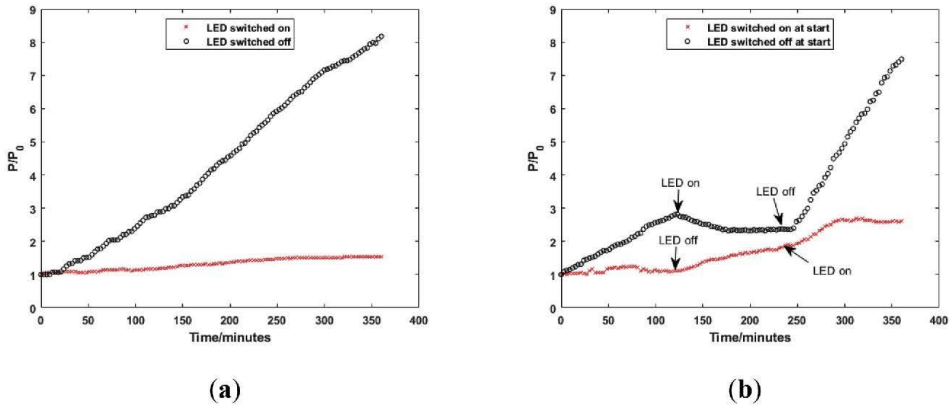

Fig. 4. Normalised pressure-time profiles for HA filtration: (a) without a change of the UV-LED status and (b) when the status of the UV-LED is changed every 2 h. P is the TMP at the selected time interval and P_0 (9.0 kPa) is the initial TMP.

membrane from 2.5 wt% to 35.6 wt% indicates that the fouling of membrane was primarily due to organic fouling. The P25 TiO_2 coated surface largely prevented fouling of the membrane, and backwashing significantly led to TMP recovery for both the photocatalytic and non-photocatalytic processes, as shown in Fig. 5(e). The photocatalytic process kept the operating TMP low ($P/P_0 < 10$) throughout the filtration period, compared to the TMP during the non-photocatalytic process when there was no UV ($P/P_0 < 35$). These observations could be attributed to effects of photocatalytic alteration of the protein structure as described by Xu et al. [38] as well as induced super-hydrophilicity [9], which potentially maintained a chemisorbed layer of water on the membrane surface for as long as the UV radiation was present.

3.5. Filtration of synthetic water containing SA

Fig. 6 shows the SEM surface images of membranes fouled under different test conditions while filtering SA solution as well as the TMP profiles and fouling layer elemental composition. Unlike BSA, the SEM image depicted in Fig. 6(a) shows that SA was retained on the membrane surface in the form of a continuous layer during the experiments with UV exposure. Because of the chemical nature of SA as a binder, it forms complex cross-linked structures [22], preventing the complete recovery of the membrane from backwashing. Because of its larger molecular size compared to HA and BSA, an 80% reduction of TOC in the permeate stream relative to the feed was achieved. TMP profiles in Fig. 6(e) show that the photocatalytic processes were still effective in keeping the operating TMP lower compared to when UV illumination was not provided. Based on elemental analysis in Fig. 6(f), the deposited SA layer was thin, since the fouled membrane still showed a 40.1 wt% composition of Ti, down from 53.5 wt% of Ti in the clean membrane. Because of the thinness of the SA layer, electrons from EDS analysis could still penetrate it to be able to reach the titania layer beneath it. Just like with BSA, induced beneficial effects of UV light on the TiO_2 surface led to a prevention of pore blocking, which led to better membrane restoration compared to the non-illuminated experiment. Without UV illumination, significant penetration of the foulant into the pores occurred, leading to poor membrane restoration, as seen in Fig. 6(d).

As shown in Fig. 6 (e), UV illumination had the overall trend of decreasing both reversible and irreversible fouling since TMP rise between backwash events decreased, and the TMP returned close to the original values, respectively. However, as more fouling occurs over time, the positive effect of UV illumination also diminishes, leading to increasing fouling, as depicted by the steeper slopes of normalised pressure. Further refinement of the process could see increased backwash frequency or reduced fluxes, but regardless, there does appear to be a gradual irreversible rise in TMP even with photocatalytic action to mitigate fouling, implying the eventual (but significantly less frequent) need for a chemical clean.

The TMP behaviour indicating fouling may also be explained by the choice of an experimentally convenient backwash solution (normally permeate is used as a backwash), being higher in NaCl concentration (100 mg/L versus 20 mg/L in the feed), and not having any Ca^{2+} ions. Ca^{2+} ions and other divalent ions are known to play an important role in SA fouling, because they preferentially bind to carboxylic groups on alginate to form a highly fouling egg-box-shaped gel network [20,39]. An important step for reversing alginate fouling is therefore breaking the calcium-alginate complex. Na^+ ions that were present in the more concentrated backwash solution (100 mg/L NaCl) can play this role, which can break up the cross-linked alginate complex by ion exchange. Presence of Na^+ ions in the backwash solution can therefore explain the high recoveries obtained through hydraulic backwashing, even without UV illumination. Regardless of whether the relatively Na^+ rich and Ca^{2+} lean backwash solution played a role on the fouling behaviour evident as TMP, its use was consistent across all experiments (both BSA and SA), and differences can still be attributed to the impact of UV light on the TiO_2 membrane surface.

3.6. Fouling indices

The fouling indices, namely hydraulic cleaning efficiency (HCE) and hydraulically irreversible fouling index (HIFI), calculated from Equation 1 (HCE) and Equation 2 (HIFI), for BSA and SA filtration are shown in Fig. 7. The HCE of the membrane was recorded above 86% for both BSA and SA. This HCE was high regardless of the state of the UV-LED, showing that the membrane was largely effective in minimising organic fouling, due to the TiO_2 coating which renders it intrinsically hydrophilic. This is consistent with other ceramic membranes due to their hydrophilic nature [40,41]. Most significantly, the photocatalytic processes kept hydraulically irreversible fouling low, as seen by the HIFI values in Fig. 7(b). For BSA and SA, the photocatalytic membrane filtration processes resulted in a reduction of HIFI by 2.7-fold and 4.2-fold respectively, compared to when conducting the experiments in UV-LED OFF mode. In comparison, as shown in Fig. 7 (b), the HIFI values from natural surface water filtration through commercial single channel tubular ceramic membranes with pore sizes of 0.14 μm 0.20 μm had corresponding HIFI values of 0.0252 m^2/L (Lit 1) and 0.0297 m^2/L

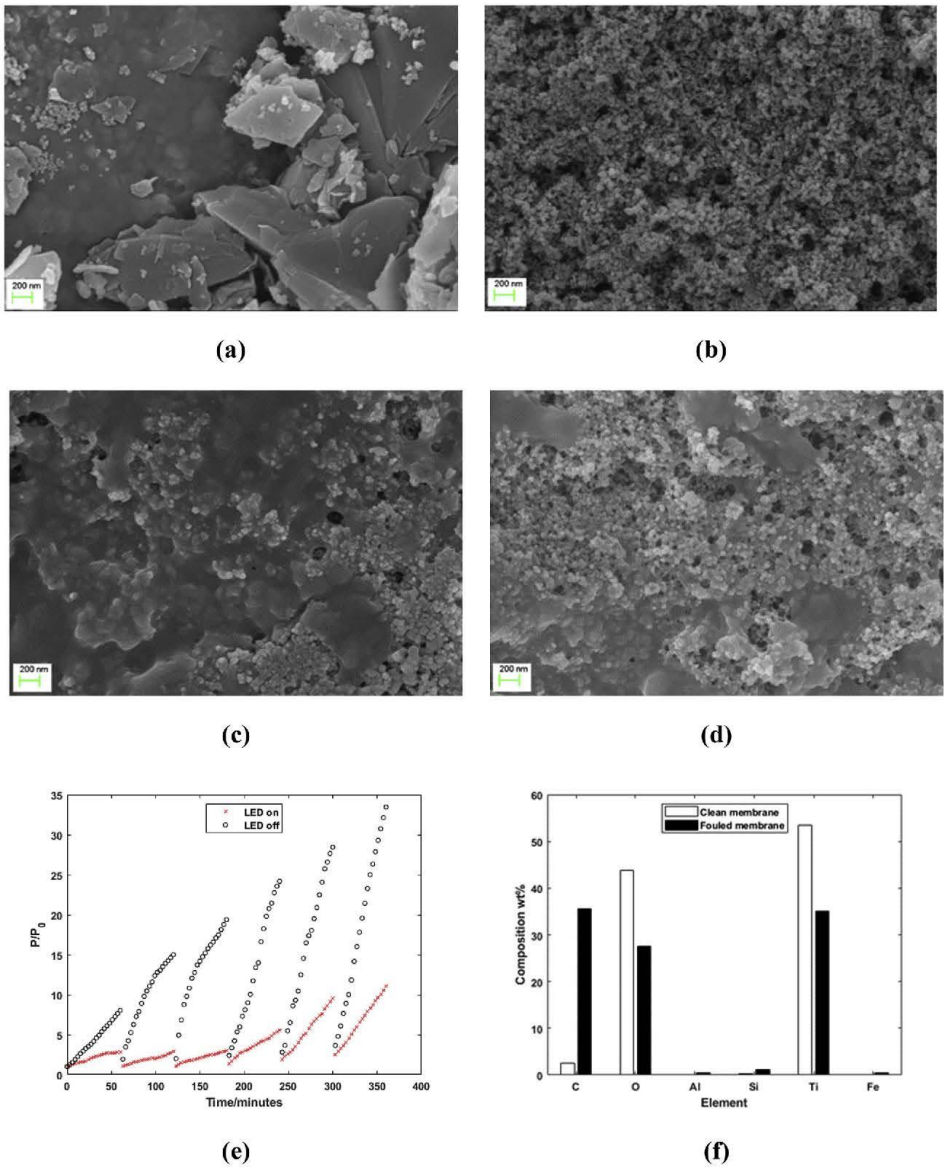

Fig. 5. SEM surface images of the membrane after BSA filtration, LED on (a) before backwash (b) after backwash, and LED off (c) before backwash (d) after backwash, (e) the normalised pressure-time profiles of the filtration run and (f) elemental composition of the clean and BSA fouled membrane surface. P is the TMP at the selected time interval and P_0 (6.5 kPa) is the initial TMP.

(Lit 2), respectively [36].

3.7. Fouling mechanism

The nature of the fouling that occurred on the membrane was evaluated using the resistance-in-series model, described in Section 2.8, as well as SEM images obtained for the membranes. The filtration resistance values for BSA and SA are shown in Fig. 8(a) and (b) respectively. In general (regardless of UV light), the total filtration resistance (R_t) in filtering BSA solution was much greater than for SA solution, correlating to the TMP profile differences in Figs. 5 and 6 where BSA showed faster TMP rise rates than SA. This could be simply due to the higher

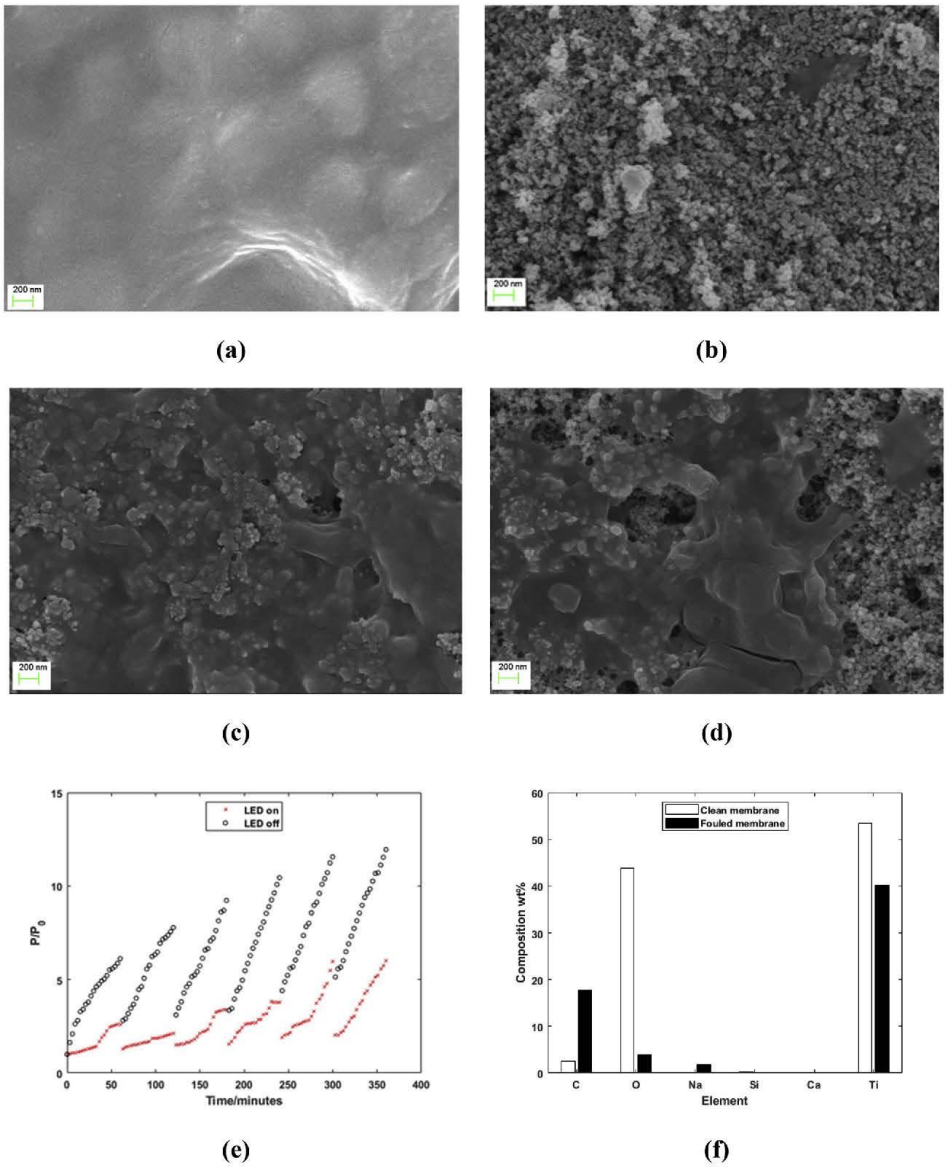

Fig. 6. SEM surface images of the membrane after SA filtration, LED on (a) before backwash (b) after backwash, and LED off (c) before backwash (d) after backwash, (e) the normalised pressure-time profiles of the filtration run and (f) elemental composition of the clean and BSA fouled membrane surface. P is the TMP at the selected time interval and P_0 (3.2 kPa) is the initial TMP.

concentration of BSA (50 mg/L vs 20 mg/L for SA), and/or that BSA solution filtration flux was higher (100 L/(m^{2}h) versus 70 L/(m^{2}h) for SA), selected for testing under sustainable performance conditions. The influence of UV on the fouling will therefore be analysed separately for BSA and SA solution filtration.

Considering the effect of UV-light, the results indicate that UV light directed to the photocatalytic coating on the membranes led to measureable beneficial effects to reducing membrane filtration resistance. Generally, both internal (pore blocking) and surface (cake layer formation) fouling occurred. Pore blocking and constriction is expected in MF membranes due to the presence of large pore sizes [37]. The photocatalytic processes, facilitated by the UV-LED light exposure resulted

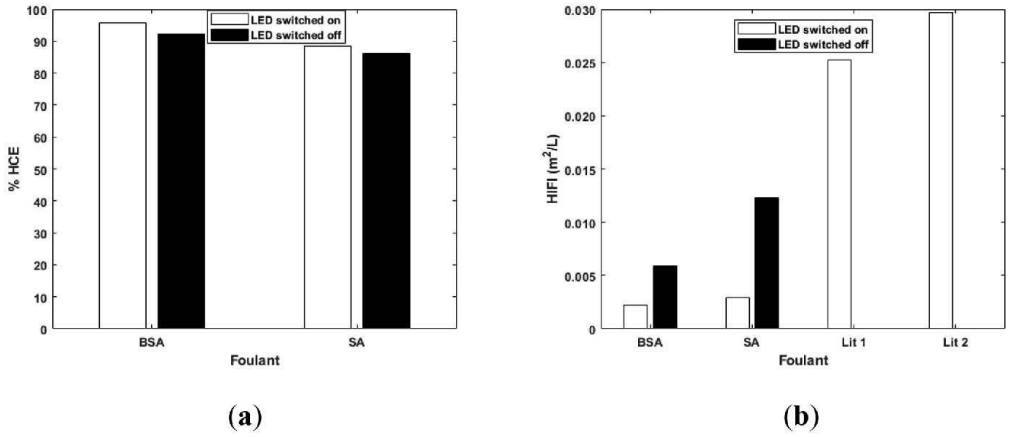

Fig. 7. The fouling indices calculated for the filtration of BSA and SA (a) HCE values in this study and (b) the HIFI in this study and two selected literature values (Lit 1 and Lit 2) [36].

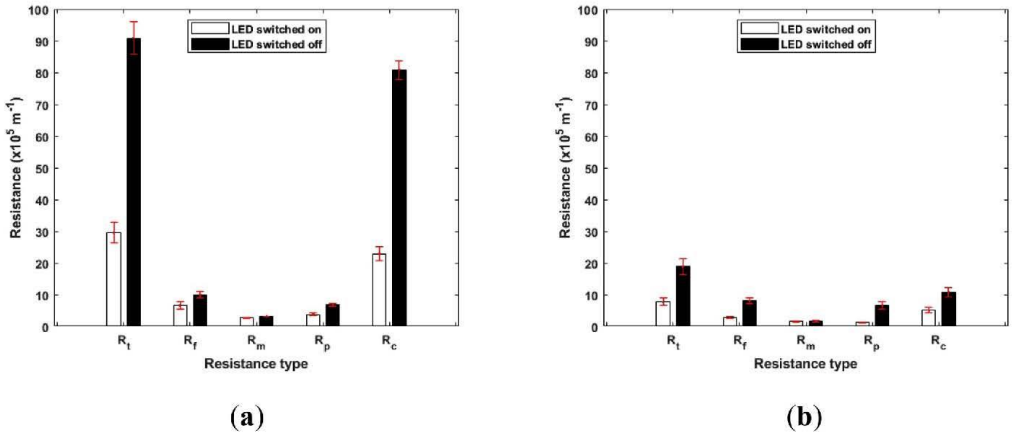

Fig. 8. Filtration resistance values for the filtration of (a) BSA and (b) SA.

in a 3.0-fold reduction in the total filtration resistance (R_t) during BSA filtration and a 2.4-fold reduction during SA filtration. A significant reduction in the internal filtration resistance (R_f) for both BSA and SA was also recorded. The photocatalytic effect on the membrane also slightly decreased the intrinsic membrane resistance (R_m). Generally, it was found that UV-LED illumination leads to reduced pore blocking and cake layer formation during photocatalytic membrane filtration. All these observations were supported by SEM analysis of the membranes.

SEM analysis of the membranes at selected events during the filtration process supported the conclusions that were made from the resistance-in-series model. With UV illumination, the foulants tended to form a cake layer on the membrane surface rather than penetrate the pores. Without UV, penetration of the pores occurred, resulting in an increase in pore blocking resistance, R_p. These observations can be explained by the effect of induced hydrophilicity that occurs in the presence of UV [9]. Enhanced hydrophilicity of the membrane surface also lowers the intrinsic resistance of the membrane, R_m, while also preventing direct adsorption of the hydrophobic BSA and SA and assembly of a cohesive fouling layer. This has the net result of decreasing the observed internal filtration resistance of the membrane.

Reduction of the total filtration resistance could be explained by changes in the intermolecular interactions that occur due to photocatalytic processes facilitated by UV radiation. Polysaccharides are known to gel due to intermolecular cross-linking of the polysaccharide chains [15], while the carboxylic groups (–COOH) in proteins enable them to chemically bind to Ca^{2+} ions present in water, resulting in observed MF membrane fouling [37]. The crosslinking can result in the formation of complex networks which increase the effective size and dimensions of the biopolymers. However, under UV illumination, new species in the form of photo-generated electrons and holes can interfere with the crosslinking interactions. The redox potential of the electron-hole pair is greater than the competing species, therefore the hole, for example, can oxidise the carboxylic group, initiating the formation of reactive radical species which effectively lead to

decomposition of biopolymer chains. Although this may not be enough to result in complete mineralisation of the organics, it is enough to prevent the formation of cross-linked complexes which increase the fouling propensity (hydraulic resistance to water flux) of the biopolymers. This could be the reason why BSA appears as flakes on the membrane surface on the SEM image. BSA (66 kDa), being of lower molecular weight than SA (120–190 kDa), would be expected to be affected more by the size reducing effect of the photocatalytic reactions.

3.8. Investigating possible thermal effects

A test was conducted to rule out the possibility that beneficial low-fouling effects could have instead been caused simply by temperature increases due to the UV-LED. Fig. 9 (a) shows a thermal camera image of the membrane module with LED fitting coming from the bottom (LED fitting recorded highest temperature, indicated by the red colour). Inlet and backwash reject tubing can be seen entering the top of the module, while the permeate tubing can be seen at the lower part of the image. Line "L1" in Fig. 9 (a) passes across the horizontal point where the membrane is housed in the stainless steel module. The temperature profile along this line is shown in Fig. 9 (b). As shown in Fig. 9 (a) and 9 (b), it was found that the temperature difference between the ambient temperature and the reactor chamber of the membrane module was only 3 °C. The LED had a heat sink which was isolated from the main module components, and hence, there was no adverse temperature increase caused by overheating of the LED which could have led to thermal energy transfer to the reactor. It is therefore unlikely that thermally induced structure changes or reactions could be the reason for the anti-fouling effects observed during the experiments reported in this article.

To further demonstrate that UV light energy was responsible for the observed low-fouling beneficial effects, another membrane filtration trial was conducted using a HA synthetic solution. The filtration process was carried out in the LED ON mode, but with the light blocked by aluminium foil. This was done to recreate the thermal conditions induced by the LED but not the conditions necessary for photocatalysis to take place. As shown in Fig. 9 (c), the TMP rise was comparable to when the LED is OFF. The recreated thermal conditions were therefore not enough to explain the low-fouling effects reported earlier in this paper.

To add to these findings, future studies will look at the effect of parameters such as pH, ionic strength, contaminant concentration and flux on the membrane's anti-fouling behaviour. Also testing the membrane with real water samples and sunlight is the next logical step. The induced super-hydrophilicity implied from the literature could also be tested, for example by water contact angle method.

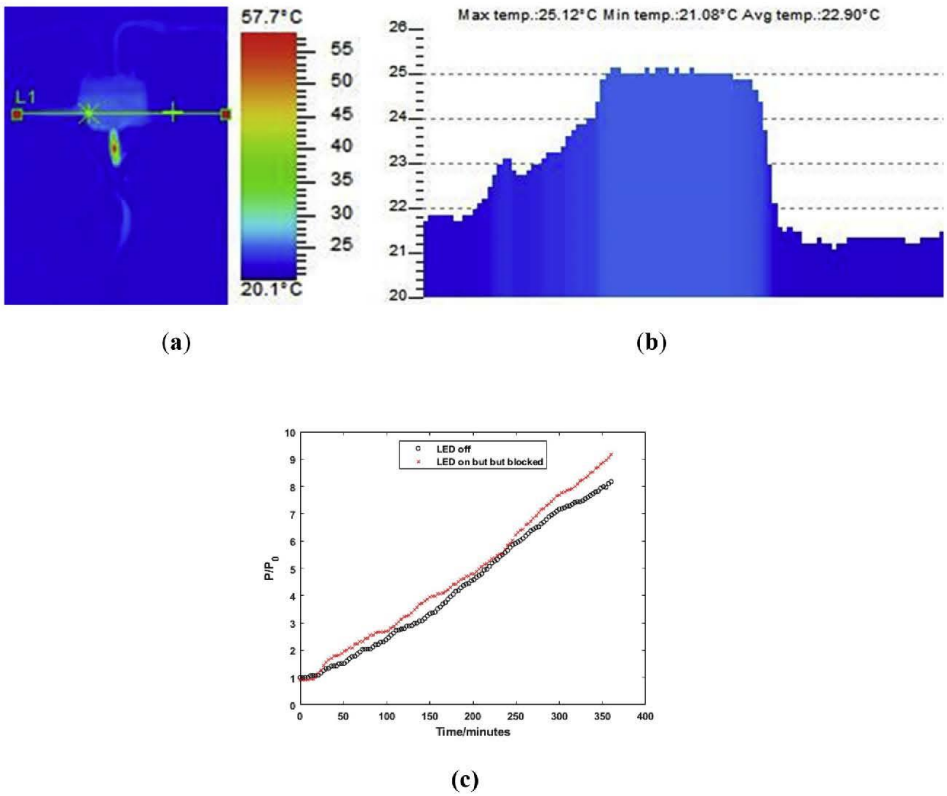

Fig. 9. (a) Temperature profile of the module and surroundings, (b) temperature along the axis which passes through the reactor chamber and (c) normalised pressure-time profile of the non-photocatalytic filtration of HA. P is the TMP at the selected time interval and P_0 (9.0 kPa) is the initial TMP.

4. Conclusion

In this work, a light conducting photocatalytic membrane was fabricated and tested for application in water treatment. The light conducting substrate offered a new route through which light can be provided to the photocatalytic layer. The photocatalytic processes provided a continuous means for mitigating organic fouling during filtration, resulting in low rates of reversible and irreversible fouling of the membrane. The light conducting substrate can allow simplified integration of light sources into photocatalytic membranes, where light can be directed from the end of the membrane element and transmitted through its length. The concept could offer a sustainable, low maintenance technology that produces purified water for marginalised communities, which maintains its operation by simply exposing it to the sun.

Declaration of competing interest

The authors declare that they have no known competing financial interests or personal relationships that could have appeared to influence the work reported in this paper.

CRediT authorship contribution statement

Lavern T. Nyamutswa: Conceptualization, Data curation, Formal analysis, Investigation, Methodology, Validation, Visualization, Writing - original draft, Writing - review & editing. **Bo Zhu:** Methodology. **Stephen F. Collins:** Conceptualization, Methodology, Formal analysis, Supervision, Writing - review & editing. **Dimuth Navaratna:** Conceptualization, Methodology, Formal analysis, Supervision, Writing - review & editing. **Mikel C. Duke:** Conceptualization, Methodology, Formal analysis, Funding acquisition, Project administration, Supervision, Resources, Writing - review & editing.

Acknowledgements

This work was supported by the Victoria University International Postgraduate Scholarships (VUIPRS) and the Institute for Sustainable Industries and Liveable Cities (ISILC), Victoria University, Melbourne. The invaluable assistance given by Miroslav Radev and Donald Ermel in setting up the electronics for the UV-LED and workshop fabrication of the stainless steel membrane module, respectively, is greatly appreciated.

Appendix A. Supplementary data

Supplementary data to this article can be found online at https://doi.org/10.1016/j.memsci.2020.118018.

References

[1] H. Vatankhah, C.C. Murray, J.W. Brannum, J. Vanneste, C. Bellona, Effect of pre-ozonation on nanofiltration membrane fouling during water reuse applications, Separ. Purif. Technol. 205 (2018) 203–211.
[2] A. Khalid, A. Abdel-Karim, M. Ali Atieh, S. Javed, G. McKay, PEG-CNTs nanocomposite PSU membranes for wastewater treatment by membrane bioreactor, Separ. Purif. Technol. 190 (2018) 165–176.
[3] A. Merenda, L. Kong, B. Zhu, M.C. Duke, S.R. Gray, L.F. Dumée, Functional nanoporous titanium dioxide for separation applications: synthesis routes and properties to performance analysis, in: M. Pannirselvam, L. Shu, G. Griffin, L. Philip, A. Natarajan, S. Hussain (Eds.), Water Scarcity and Ways to Reduce the Impact: Management Strategies and Technologies for Zero Liquid Discharge and Future Smart Cities, Springer International Publishing, Cham, 2019, pp. 151–186.
[4] R. Zhu, A.J. Diaz, Y. Shen, F. Qi, X. Chang, D.P. Durkin, Y. Sun, S.D. Solares, D. Shuai, Mechanism of humic acid fouling in a photocatalytic membrane system, J. Membr. Sci. 563 (2018) 531–540.
[5] Z. Geng, X. Yang, C. Boo, S. Zhu, Y. Lu, W. Fan, M. Huo, M. Elimelech, X. Yang, Self-cleaning anti-fouling hybrid ultrafiltration membranes via side chain grafting of poly(aryl ether sulfone) and titanium dioxide, J. Membr. Sci. 529 (2017) 1–10.
[6] L. De Angelis, M.M.F. de Cortalezzi, Ceramic membrane filtration of organic compounds: effect of concentration, pH, and mixtures interactions on fouling, Separ. Purif. Technol. 118 (2013) 762–775.
[7] S. Leong, A. Razmjou, K. Wang, K. Hapgood, X. Zhang, H. Wang, TiO2 based photocatalytic membranes: a review, J. Membr. Sci. 472 (2014) 167–184.
[8] S. Banerjee, D.D. Dionysiou, S.C. Pillai, Self-cleaning applications of TiO2 by photo-induced hydrophilicity and photocatalysis, Appl. Catal. B Environ. 176–177 (2015) 396–428.
[9] J. Chen, C.-s. Poon, Photocatalytic construction and building materials: from fundamentals to applications, Build. Environ. 44 (2009) 1899–1906.
[10] G. Matafonova, V. Batoev, Recent advances in application of UV light-emitting diodes for degrading organic pollutants in water through advanced oxidation processes: a review, Water Res. 132 (2018) 177–189.
[11] B.J. Starr, V.V. Tarabara, M. Herrera-Robledo, M. Zhou, S. Roualdès, A. Ayral, Coating porous membranes with a photocatalyst: comparison of LbL self-assembly and plasma-enhanced CVD techniques, J. Membr. Sci. 514 (2016) 340–349.
[12] I. Horovitz, D. Avisar, M.A. Baker, R. Grilli, L. Lozzi, D. Di Camillo, H. Mamane, Carbamazepine degradation using a N-doped TiO2 coated photocatalytic membrane reactor: influence of physical parameters, J. Hazard Mater. 310 (2016) 98–107.
[13] L. Nyamutswa, B. Zhu, D. Navaratna, S. Collins, M. Duke, Proof of concept for light conducting membrane substrate for UV-activated photocatalysis as an alternative to chemical cleaning, Membranes 8 (2018) 122.
[14] Z. Su, T. Liu, W. Yu, X. Li, N.J.D. Graham, Coagulation of surface water: observations on the significance of biopolymers, Water Res. 126 (2017) 144–152.
[15] K. Xiao, X. Wang, X. Huang, T.D. Waite, X. Wen, Analysis of polysaccharide, protein and humic acid retention by microfiltration membranes using Thomas' dynamic adsorption model, J. Membr. Sci. 342 (2009) 22–34.
[16] L. Song, B. Zhu, S. Gray, M. Duke, S. Muthukumaran, Hybrid processes combining photocatalysis and ceramic membrane filtration for degradation of humic acids in saline water, Membranes (Basel) (2016) 6.
[17] G. Plesch, M. Vargová, U.F. Vogt, M. Gorbár, K. Jesenák, Zr doped anatase supported reticulated ceramic foams for photocatalytic water purification, Mater. Res. Bull. 47 (2012) 1680–1686.
[18] M. Optoelectronics, Ultraviolet Emitter MTE3650L2-UV-HP, in, 2016 (Product datasheet).
[19] C. Yang, N. Han, W. Zhang, W. Wang, W. Li, B. Xia, C. Han, Z. Cui, X. Zhang, Adhesive-free in situ synthesis of a coral-like titanium dioxide@poly(phenylene sulfide) microporous membrane for visible-light photocatalysis, Chem. Eng. J. 374 (2019) 1382–1393.
[20] H. Chang, H. Liang, F. Qu, S. Shao, H. Yu, B. Liu, W. Gao, G. Li, Role of backwash water composition in alleviating ultrafiltration membrane fouling by sodium alginate and the effectiveness of salt backwashing, J. Membr. Sci. 499 (2016) 429–441.
[21] M. Cheryan, Ultrafiltration and Microfiltration Handbook, CRC press, 1998.
[22] S. Meng, W. Fan, X. Li, Y. Liu, D. Liang, X. Liu, Intermolecular interactions of polysaccharides in membrane fouling during microfiltration, Water Res. 143 (2018) 38–46.
[23] S.L. Zakharov, Borosilicate microporous glasses for reverse osmosis, Glass Ceram. 61 (2004) 178–179.
[24] W. Yuan, A.L. Zydney, Humic acid fouling during microfiltration, J. Membr. Sci. 157 (1999) 1–12.
[25] C.P. Athanasekou, N.G. Moustakas, S. Morales-Torres, L.M. Pastrana-Martínez, J. L. Figueiredo, J.L. Faria, A.M.T. Silva, J.M. Dona-Rodriguez, G.E. Romanos, P. Falaras, Ceramic photocatalytic membranes for water filtration under UV and visible light, Appl. Catal. B Environ. 178 (2015) 12–19.
[26] M.J. Atlos, R. Liang, M.M. Hatat-Fraile, L.M. Bragg, N.Y. Zhou, M.R. Servos, S. A. Andrews, Photocatalytic decomposition of selected estrogens and their estrogenic activity by UV-LED irradiated TiO2 immobilized on porous titanium sheets via thermal-chemical oxidation, J. Hazard Mater. 318 (2016) 541–550.
[27] W. Han, J. Ren, H. Xuan, L. Ge, Controllable degradation rates, antibacterial, free-standing and highly transparent films based on polylactic acid and chitosan, Colloid. Surface. Physicochem. Eng. Aspect. 541 (2018) 128–136.
[28] G. Pasternak, Y. Yang, B.B. Santos, F. Brunello, M.M. Hanczyc, A. Motta, Regenerated silk fibroin membranes as separators for transparent microbial fuel cells, Bioelectrochemistry 126 (2019) 146–155.
[29] R. Tong, G. Chen, J. Tian, M. He, Highly transparent, weakly hydrophilic and biodegradable cellulose film for flexible electroluminescent devices, Carbohydr. Polym. 227 (2020) 115366.
[30] Z. Li, W. Liu, F. Guan, G. Li, Z. Song, D. Yu, H. Wang, H. Liu, Using cellulose fibers to fabricate transparent paper by microfibrillation, Carbohydr. Polym. 214 (2019) 26–33.
[31] D.B.K. Lim, H. Gong, Highly stretchable and transparent films based on cellulose, Carbohydr. Polym. 201 (2018) 446–453.
[32] H. Bak, S.Y. Cho, Y.S. Yun, H.-J. Jin, Electrically conductive transparent films based on nylon 6 membranes and single-walled carbon nanotubes, Curr. Appl. Phys. 10 (2010) S468–S472.
[33] O. Urper, İ. Çakmak, N. Karatepe, Fabrication of carbon nanotube transparent conductive films by vacuum filtration method, Mater. Lett. 223 (2018) 210–214.
[34] S. Jiang, P.-X. Hou, C. Liu, H.-M. Cheng, High-performance single-wall carbon nanotube transparent conductive films, J. Mater. Sci. Technol. 35 (2019) 2447–2462.
[35] P.K. Narayanam, K. Sundararajan, Organic solvent supported fabrication of transparent free standing graphene oxide membranes, Ceram. Int. 46 (4) (March 2020) 5394–5401.
[36] R. Shang, F. Vuong, J. Hu, S. Li, A.J.B. Kemperman, K. Nijmeijer, E.R. Cornelissen, S.G.J. Heijman, L.C. Rietveld, Hydraulically irreversible fouling on ceramic MF/UF membranes: comparison of fouling indices, foulant composition and irreversible pore narrowing, Separ. Purif. Technol. 147 (2015) 303–310.

[37] K. Katsoufidou, S.G. Yiantsios, A.J. Karabelas, A study of ultrafiltration membrane fouling by humic acids and flux recovery by backwashing: experiments and modeling, J. Membr. Sci. 266 (2005) 40–50.
[38] Z. Xu, T. Wu, J. Shi, K. Teng, W. Wang, M. Ma, J. Li, X. Qian, C. Li, J. Fan, Photocatalytic antifouling PVDF ultrafiltration membranes based on synergy of graphene oxide and TiO2 for water treatment, J. Membr. Sci. 520 (2016) 281–293.
[39] P. dos Santos Araújo, G.B. Belini, G.P. Mambrini, F.M. Yamaji, W.R. Waldman, Thermal degradation of calcium and sodium alginate: a greener synthesis towards calcium oxide micro/nanopartieles, Int. J. Biol. Macromol. 140 (2019) 749–760.
[40] B. Hofs, J. Ogier, D. Vries, E.F. Beerendonk, E.R. Cornelissen, Comparison of ceramic and polymeric membrane permeability and fouling using surface water, Separ. Purif. Technol. 79 (2011) 365–374.
[41] M.T. Alresheedi, B. Barbeau, O.D. Basu, Comparisons of NOM fouling and cleaning of ceramic and polymeric membranes during water treatment, Separ. Purif. Technol. 209 (2019) 452–460.

APPENDIX 3: SUPPLEMENTARY INFORMATION SUBMITTED TO JOURNAL FOR CHAPTER 4

Supplementary information for

Solar activated light conducting photocatalytic membrane for chemical-free fouling control in water treatment

Lavern T. Nyamutswa [a], Bo Zhu [a], Stephen F. Collins [b], Dimuth Navaratna [a, b] and Mikel C. Duke [a, *]

[a] *Institute for Sustainable Industries and Liveable Cities, Victoria University, Melbourne, Australia*

[b] *College of Engineering and Science, Victoria University, Melbourne, Australia*

***** *Corresponding author: Mikel C. Duke (email: mikel.duke@.vu.edu.au)*

[redacted]

The full-text is subject to copyright restrictions, and cannot be included in the online version of the thesis.

APPENDIX 4: SUPPLEMENTARY INFORMATION SUBMITTED TO JOURNAL FOR CHAPTER 5

Supporting information for

Sunlight-transmitting photocatalytic membrane for low energy and low maintenance water and wastewater treatment

Lavern T. Nyamutswa [a], Blair D. Hanson[c], Dimuth Navaratna [a, b], Stephen F. Collins [b], Karl G. Linden[c] and Mikel C. Duke [a, *]

[a] *Institute for Sustainable Industries and Liveable Cities, Victoria University, Melbourne, Australia*

[b] *College of Engineering and Science, Victoria University, Melbourne, Australia*

[c] *Department of Civil, Environmental, and Architectural Engineering, University of Colorado Boulder, 4001 Discovery Drive, Boulder, CO 80303, USA*

***** *Corresponding author: Mikel C. Duke (email: mikel.duke@vu.edu.au)*

[redacted]

The full-text is subject to copyright restrictions, and cannot be included in the online version of the thesis.